JOURNAL OF GEOPHYSICAL RESEARCH

The continuation of

TERRESTRIAL MAGNETISM AND ATMOSPHERIC ELECTRICITY

(1896-1948)

An International Quarterly

VOLUME 58 March, 1953 NUMBER 1

CONTENTS

(Contents concluded on outside back cover)

Address all correspondence to

JOURNAL OF GEOPHYSICAL RESEARCH

5241 BROAD BRANCH ROAD, NORTHWEST

WASHINGTON 15, D.C., U.S.A.

THREE DOLLARS AND FIFTY CENTS A YEAR SINGLE NUMBERS, ONE DOLLAR

PRINTED BY

THE WILLIAM BYRD PRESS, INC.

P. O. Box 2-W—Sherwood Ave. and Durham St., Richmond 5, Virginia

JOURNAL OF GEOPHYSICAL RESEARCH

The continuation of

Terrestrial Magnetism and Atmospheric Electricity

(1896-1948)

An International Quarterly

Founded 1896 by L. A. BAUER *Continued 1928–1948 by* J. A. FLEMING

Fields of Interest

Terrestrial Magnetism
Atmospheric Electricity
The Ionosphere
Solar and Terrestrial Relationships
Aurora, Night Sky, and Zodiacal Light
The Ozone Layer
Meteorology of Highest Atmospheric Levels
The Constitution and Physical States of the Upper Atmosphere
Special Investigations of the Earth's Crust and Interior, including experimental seismic waves, physics of the deep ocean and ocean bottom, physics in geology
And similar topics

This Journal serves the interests of investigators concerned with terrestrial magnetism and electricity, the upper atmosphere, the earth's crust and interior by presenting papers of new analysis and interpretation or new experimental or observational approach, and contributions to international collaboration. It is not in a position to print, primarily for archive purposes, extensive tables of data from observatories or surveys, the significance of which has not been analyzed.

Forward *manuscripts* to one of the Associate Editors, or to the editorial office of the Journal at 5241 Broad Branch Road, Northwest, Washington 15, D. C., U. S. A. It is preferred that manuscripts be submitted in English, but communications in French, German, Italian, or Spanish are also acceptable. A brief abstract, preferably in English, must accompany each manuscript. A *publication charge* of $4 per page will be billed by the Editor to the institution which sponsors the work of any author; private individuals are not assessed page charges. Manuscripts from outside the United States are invited, and should not be withheld or delayed because of currency restrictions or other special difficulties relating to page charges. Costs of publication are roughly twice the total income from page charges and subscriptions, and are met by subsidies from the Carnegie Institution of Washington and international and private sources.

Back issues and *reprints* are handled by the Editorial Office, 5241 Broad Branch Road, N.W., Washington 15, D.C., U.S.A.

Subscriptions are handled by the Editorial Office, 5241 Broad Branch Road, N.W., Washington 15, D.C., U.S.A.

Entered as second-class matter at the Post Office at Richmond, Virginia, under the act of March 3, 1879.

Journal of

GEOPHYSICAL RESEARCH

The continuation of

Terrestrial Magnetism and Atmospheric Electricity

VOLUME 58 MARCH, 1953 No. 1

DIURNAL *Sq*-VARIATION AND OVERHEAD CURRENT-SYSTEM, JULY 1933

BY K. F. WASSERFALL

Magnetisk Byrå, Bergen, Norway

(Received May 3, 1952)

ABSTRACT

In 1937, the author published a paper entitled "Studies on the quiet diurnal variation of magnetic elements" [see 1 of "References" at end of paper], giving results of an analysis based principally on records at Tromsö, Dombås, and Rude Skov, supplemented by data for Sitka and Godhavn. The relation between the magnetic diurnal variation and the *dynamo theory*—first suggested by A. Schuster and later worked out by Sydney Chapman and J. Bartels [2]—was discussed. Analysis based on so few stations could not be satisfactory but the results seemed so promising that an analysis based on data collected during the Second International Polar Year of 1932-33 appeared justified. Dr. la Cour kindly supplied all publications and copies of records for 44 stations situated in the Northern Hemisphere. The analysis, begun in 1939, had to be discontinued during World War II. It was resumed in 1946.

The present paper gives a descriptive study of the solar daily magnetic variation for the month of July 1933. The magnetic field pattern for the Northern Hemisphere, from data obtained at the 44 stations of the Second International Polar Year, is deduced with good coverage in north polar regions. An atmospheric current-system, which would produce the observed field, is derived. Changes in field dependent on Universal Time are neglected.

TABLE 1

No.	Station	St.	Φ	Λ	φ	λ	D	H	Z	I
			°	°	°	°	°	γ	γ	°
1	Thule	Thu	88.0N	0.0E	76.5N	68.9W	80.9W	4565	55695	85.3
2	Godhavn	God	79.8 "	32.5 "	69.2 "	53.5 "	57.3 "	8220	55345	81.6
3	Scoresby Sund	S.S.	75.8 "	81.8 "	70.5 "	22.0 "	34.6 "	10508	51060	78.3
4	Angmagssalik	Ang	74.2 "	52.7 "	65.6 "	37.6 "	39.8 "	10740	51680	78.2
5	Sveagruvan	Svg	73.9 "	130.7 "	77.9 "	16.8E	4.9 "	8330	52525	81.0
6	Chesterfield Inl.	ChI	73.5 "	36.0W	63.3 "	90.7W	12.7 "	3860	60720	86.4
7	Björnöya	Bj.	71.1 "	124.1E	74.5 "	19.2E	1.8 "	9500	55590	80.3
8	Julianehaab	Jul	70.8 "	35.6 "	60.7 "	46.0W	43.7 "	11620	52960	77.6
9	Fort Rae	F.R.	69.0 "	69.1W	62.8 "	116.1 "	37.5E	7740	59950	82.7
10	Tromsö	Tr.	67.1 "	116.7E	69.7 "	18.9E	3.8W	11500	50190	77.1
11	Petsamo	Pet	64.9 "	125.9 "	69.5 "	31.2 "	5.8E	11340	50840	77.4
12	Matotchkin Shar	M.S.	64.8 "	146.5 "	73.9 "	56.4 "	21.6 "	9090	54210	80.5
13	Sodankylä	Sod	63.8 "	120.0 "	67.4 "	26.6 "	3.0 "	12120	49280	76.5
14	Dickson Island	D.I.	63.0 "	161.5 "	73.5 "	80.4 "	28.5 "	6990	57460	83.1
15	Kandalakska	Kan	62.5 "	124.0 "	67.1 "	34.4 "	6.8 "	12310	50120	76.2
16	Lerwick	Ler	62.5 "	88.6 "	60.1 "	1.2W	13.6W	14485	46610	72.7
17	Dombås	Dom	62.3 "	100.0 "	62.1 "	9.1E	8.5 "	14070	47320	73.4
18	Meanook	Mea	61.8 "	59.0W	54.6 "	113.3W	26.3E	12740	59395	77.9
19	Sitka	Sit	60.0 "	84.6 "	57.0 "	135.3 "	30.2 "	15955	55120	73.8
20	Eskdalemuir	Esk	58.5 "	82.9E	55.3 "	3.2 "	14.2W	16560	44890	69.8
21	Lovö	Lov	58.1 "	105.8 "	59.4 "	17.8E	2.5 "	15400	46470	71.7
22	Pavlovsk	Pav	56.0 "	117.0 "	59.7 "	30.5 "	4.4E	15440	47285	71.9
23	Rude Skov	R.S.	55.8 "	98.5 "	55.8 "	12.4 "	5.6W	16850	44840	69.4
24	Agincourt	Agi	55.0 "	13.0W	43.8 "	79.3W	7.6 "	15470	46830	71.7
25	Abinger	Abi	54.0 "	83.3E	51.2 "	0.4 "	11.8 "	18530	42940	66.7
26	De Bilt	D.B.	53.8 "	89.6 "	52.1 "	5.2E	8.9 "	18260	43120	67.0
27	Manhay	Man	52.0 "	84.0 "	50.3 "	5.7 "	8.4 "	19100	42430	65.8
28	Val Joyeux	V.J.	51.3 "	84.5 "	48.8 "	2.0 "	10.4 "	19640	41615	64.7
29	Swider	Sw.	50.6 "	104.6 "	52.1 "	21.2 "	1.6E	18425	43710	67.6
30	Nantes	Nan	50.5 "	80.1 "	47.2 "	1.6W	11.5W	20260	40430	63.4
31	Cheltenham	Ch.	50.1 "	9.5W	38.7 "	75.8 "	7.1 "	18435	54190	71.2
32	Wien Auhof	W.A.	47.9 "	98.1E	48.2 "	16.2 "	3.6 "	20510	41200	63.5
33	Del Ebro	D.E.	43.9 "	79.7 "	40.8 "	0.5E	9.9 "	23425	36630	57.4
34	San Fernando	S.F.	41.0 "	71.3 "	36.5 "	6.2W	12.2 "	25140	33850	53.4
35	Tucson	Tuc	40.4 "	47.8W	32.2 "	110.8 "	13.9E	26320	44965	59.7
36	Toyohara	Toy	36.9 "	156.5 "	47.0 "	142.8E	8.9W	25040	44590	60.7
37	Teoloyucan	Teo	29.6 "	33.0 "	19.7 "	99.2W	9.5E	30970	33380	47.1
38	Helwan	Hel	27.2 "	106.4E	29.9 "	31.3E	0.1W	30190	26900	41.7
39	Honolulu	Hon	21.1 "	93.5W	21.3 "	158.1W	10.1E	28560	23330	39.2
40	Lu Kai Pang	LKP	20.0 "	170.9 "	31.3 "	121.0E	3.6W	33375	33845	45.4
41	Au Tau	A.T.	11.0 "	177.1 "	22.4 "	114.0 "	0.7 "	37540	22150	30.5
42	Alibag	Ali	9.5 "	143.6E	18.6 "	72.9 "	0.2 "	37420	17820	25.5
43	Antipolo	Ant	3.3 "	170.2W	14.6 "	121.2 "	0.3E	38300	10830	15.8
44	Mogadiscio	Mog	2.7S	114.3E	2.0 "	45.4 "	0.3W	33200	9985	16.7

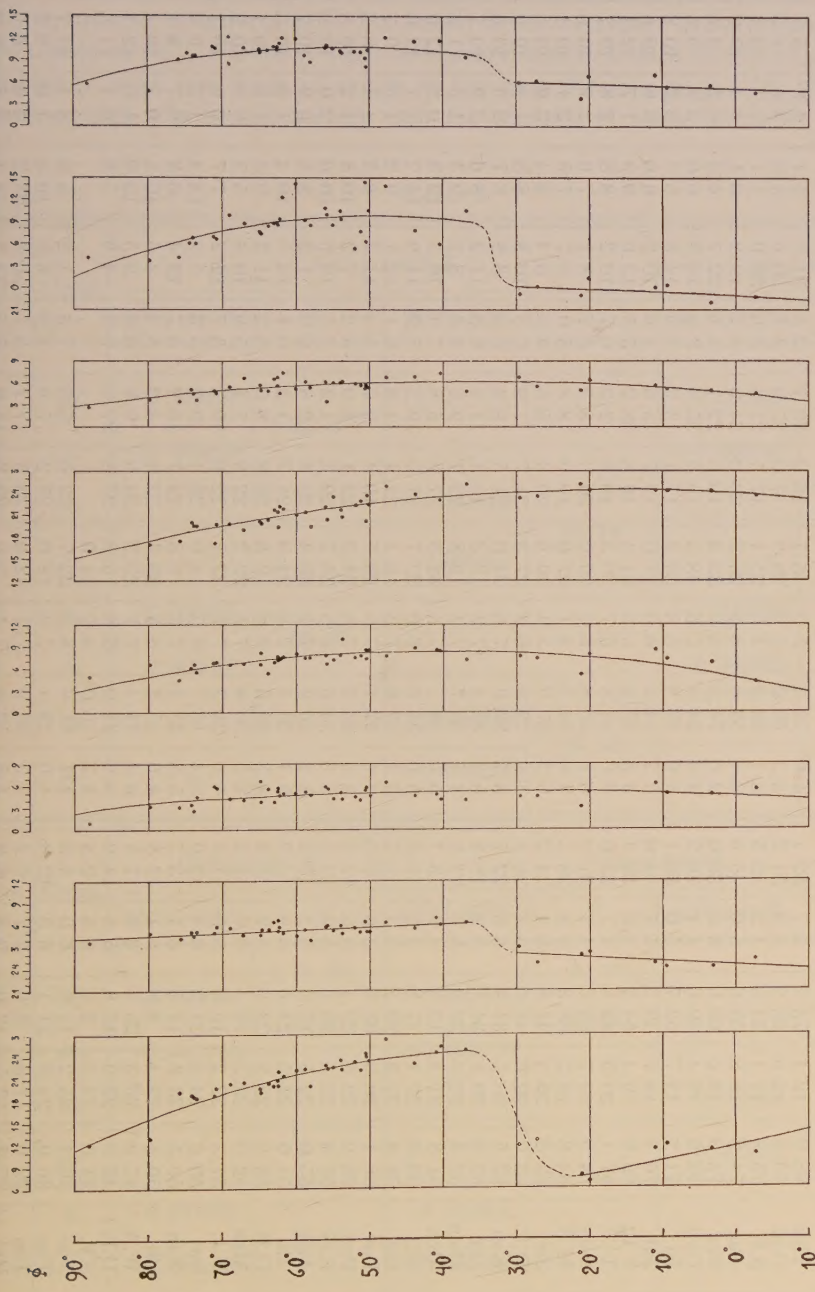

FIG. I—GRAPHS OF HARMONIC CONSTANTS FOR PHASE (T), FOR THE 24-HOUR AND 12-HOUR COMPONENTS OF THE Sq-DATA FOR ΔX, ΔY, ΔZ, AND ΔI AT 44 STATIONS BETWEEN 90° NORTH AND EQUATOR

TABLE 2

No.	Station	Φ	Component X				Component Y				Component Z				Component I			
			24-hour		12-hour		24-hour		12-hour		24-hour		12-hour		24-hour		12-hour	
			T	A	T	A	T	A	T	A	T	A	T	A	T	A	T	A
		°	h	γ	h	γ	h	γ	h	γ	h	γ	h	γ	h	$'$	h	$'$
1	Thu	88.0	12.1	73.9	3.7	52.1	1.0	72.4	5.0	45.1	16.2	39.7	2.8	31.9	4.1	4.8	5.7	2.3
2	God	79.8	12.9	53.9	4.9	51.2	3.2	62.2	6.6	29.9	17.0	27.9	3.7	20.6	3.8	4.6	4.7	1.4
3	S.S.	75.8	19.1	54.9	4.2	42.5	3.1	63.3	4.5	25.1	17.5	21.8	3.6	30.0	4.1	4.7	9.1	1.1
4	Ang	74.2	18.8	53.9	5.0	45.6	3.4	53.8	6.1	25.2	20.0	24.0	5.1	19.9	6.1	4.4	10.0	1.4
5	Svg	73.9	18.6	60.0	3.5	39.0	2.6	74.5	6.7	33.3	19.6	22.1	4.5	22.7	6.6	4.2	9.6	2.4
6	Ch.I.	73.5	18.4	59.0	4.1	46.2	4.4	34.8	5.6	48.6	19.5	35.4	3.9	16.9	6.0	3.8	9.6	2.0
7	Bj.	71.1	18.7	52.7	5.0	38.1	5.9	47.8	6.8	23.9	17.1	13.2	4.9	14.8	6.9	3.2	10.8	2.2
8	Jul	70.8	19.7	49.5	5.7	44.6	5.7	44.4	6.9	27.0	19.7	15.6	4.6	10.2	6.6	3.6	10.6	1.2
9	F.R.	69.0	19.4	54.2	5.6	32.4	4.3	37.8	6.6	31.4	19.8	28.2	5.5	13.0	9.9	1.7	12.1	2.3
10	Tr.	67.1	20.5	43.8	4.7	25.0	4.0	42.8	6.7	20.3	19.8	2.9	6.7	10.2	8.8	2.8	10.7	1.6
11	Pet	64.9	19.7	38.0	4.7	31.9	6.6	39.8	6.6	20.0	20.0	8.3	5.7	8.1	7.6	2.9	10.6	1.8
12	M.S.	64.8	19.2	38.3	5.3	28.3	3.8	54.5	8.1	27.0	19.9	8.8	5.0	9.7	7.5	2.1	10.1	1.8
13	Sod	63.8	20.4	41.8	5.4	24.2	5.5	37.9	5.4	20.6	20.3	5.6	4.9	6.4	8.4	2.0	10.4	1.8
14	D.I.	63.0	20.0	44.0	6.4	26.4	4.9	72.3	6.9	27.3	21.7	7.9	6.5	10.8	8.8	1.9	10.9	1.6
15	Kan	62.5	20.1	34.4	6.6	22.7	5.7	36.0	7.6	24.0	21.5	8.4	5.6	6.8	8.7	2.0	10.6	1.4
16	Ler	62.5	20.8	34.7	5.2	18.8	5.2	37.4	7.2	13.3	19.4	11.5	6.8	11.2	8.6	2.0	10.7	1.0
17	Dom	62.3	22.0	29.2	5.6	21.8	4.7	35.7	7.4	19.8	22.1	9.8	4.6	8.2	9.3	1.9	11.3	1.2
18	Mea	61.8	21.4	15.9	4.9	13.1	5.0	28.7	7.6	32.3	21.9	5.8	7.4	10.3	12.3	0.8	12.0	1.0
19	Sit	60.0	22.1	17.8	4.5	16.8	5.0	31.6	8.0	22.7	21.0	19.2	5.2	11.9	14.2	1.1	12.0	0.7
20	Esk	58.8	22.3	26.2	5.4	16.7	5.1	32.0	7.5	18.1	21.4	11.8	6.1	12.1	9.2	1.6	9.7	0.6
21	Lov	58.1	20.0	33.5	3.8	16.0	4.6	27.1	7.5	23.7	19.4	9.7	5.4	11.3	8.5	1.4	8.8	1.1
22	Pav	56.0	22.8	29.1	5.8	17.8	5.9	33.3	7.8	24.3	22.1	8.9	6.2	7.2	10.8	1.2	10.8	1.2
23	R.S.	55.8	22.6	29.6	5.9	14.8	5.6	34.6	6.6	25.7	20.3	11.3	3.5	12.6	10.0	2.0	10.9	0.7
24	Agi	55.0	22.5	17.5	5.1	17.2	4.2	20.0	7.2	30.4	23.4	2.8	6.0	1.2	8.5	0.9	10.7	0.8
25	Abi	54.0	23.5	24.6	5.9	14.9	5.1	30.4	7.8	24.9	21.7	11.3	6.1	14.1	10.4	1.3	10.3	0.4
26	D.B.	53.8	22.3	23.6	4.9	13.5	4.3	32.0	9.9	19.6	20.8	8.0	6.2	11.3	9.4	1.5	10.1	0.7
27	Man	52.0	23.3	19.4	5.6	11.3	4.5	30.8	7.5	22.2	22.3	7.1	5.9	10.4	5.3	0.9	10.2	0.4
28	V.J.	51.3	22.2	15.0	5.0	11.5	4.0	28.3	7.7	32.2	22.9	10.4	5.7	12.2	7.7	0.9	10.1	0.6
29	Sw.	50.6	24.4	21.2	6.4	12.0	5.4	16.7	8.5	14.0	20.1	9.2	5.3	5.9	14.4	1.2	9.4	0.5
30	Nan	50.5	23.9	14.5	5.1	13.7	5.8	35.4	7.3	18.8	23.7	18.2	5.7	12.4	6.3	0.7	8.1	0.8
31	Ch.	50.1	23.4	8.8	5.1	12.8	4.6	15.2	8.5	28.4	22.4	4.0	5.4	4.6	10.5	0.8	10.4	0.5
32	W.A.	47.9	26.3	23.4	6.3	17.5	6.4	31.4	7.7	25.2	24.9	9.8	6.8	9.5	13.9	1.0	12.1	0.7
33	D.E.	43.9	23.0	13.8	5.5	14.0	4.6	21.0	8.8	15.3	23.8	27.9	6.8	4.0	7.8	0.1	11.6	0.8
34	S.F.	41.0	24.5	3.9	6.8	2.8	4.7	16.0	8.5	14.0	....	....	....	....	....	....	....	....
35	Tuc	40.4	25.2	11.8	6.0	4.3	4.1	11.6	8.5	22.7	23.0	8.3	7.3	1.2	5.9	1.1	11.7	0.5
36	Toy	36.9	24.8	21.1	6.3	12.6	4.0	28.4	7.2	18.0	25.2	7.6	4.9	6.9	10.5	1.0	9.5	0.7
37	Teo	29.6	11.8	8.6	2.7	6.2	4.5	20.9	7.7	12.9	23.3	7.1	6.7	6.8	23.2	1.0	6.0	0.8
38	Hel	27.2	12.5	13.0	0.8	8.9	4.5	12.6	7.4	9.6	23.6	15.6	5.5	13.2	24.1	1.5	6.2	1.5
39	Hon	21.1	7.8	8.4	1.9	9.0	3.1	16.2	5.1	17.1	25.1	10.3	5.0	14.4	22.9	1.6	3.8	1.4
40	LKP	20.0	6.9	4.4	2.1	11.0	5.3	31.6	7.9	22.1	24.3	11.2	6.4	9.0	25.3	0.8	6.8	0.8

Material and methods

It was planned originally to collect mean diurnal *Sq*-data for *D*, *H*, *Z*, and *I* for the three summer months of 1933, but finally it was necessary to limit the discussion to the month of July 1933 only. The stations and essential data are listed in Table 1. Preliminary work was done to arrive at the best possible graphs for the diurnal *Sq*-curves; this was comparatively easy for stations in lower latitudes, but very

TABLE 3

Wave	Const.	Component *X*				Component *Y*	
		90°N–37°N	*T*	22°N–10°S	*T*	90°N–10°S	*T*
			h m		*h m*		*h m*
24	α_1	−0.139595		.....		−0.026246	
			23 23		.. ..		05 02
24	β_1	−0.003982		.....		−0.000724	
24	α_2	.....		−0.160895		.....	
			.. ..		02 10		.. ..
24	β_2	.....		0.000537		.....	
12	α_1	−0.039508		.....		−0.042704	
			05 38		.. ..		08 14
12	β_1	0.000047		.....		−0.002262	
12	α_2	.....		0.035986		.....	
			.. ..		02 52		.. ..
12	β_2	.....		−0.000275		.....	

Wave	Const.	Component *Z*		Component *I*			
		90°N–10°S	*T*	90°N–30°N	*T*	30°N–10°S	*T*
			h m		*h m*		*h m*
24	α_1	−0.116594		−0.005751		.....	
			22 31		08 59		.. ..
24	β_1	−0.001740		−0.005108		.....	
24	α_2	.....		.....		0.013009	
			.. ..		.. ..		24 35
24	β_2	.....		.....		−0.000412	
12	α_1	−0.031802		0.020394		.....	
			06 03		10 47		.. ..
12	β_1	−0.001232		−0.003753		.....	
12	α_2	.....		.....		0.009438	
			.. ..		.. ..		06 21
12	β_2	.....		.....		−0.000248	

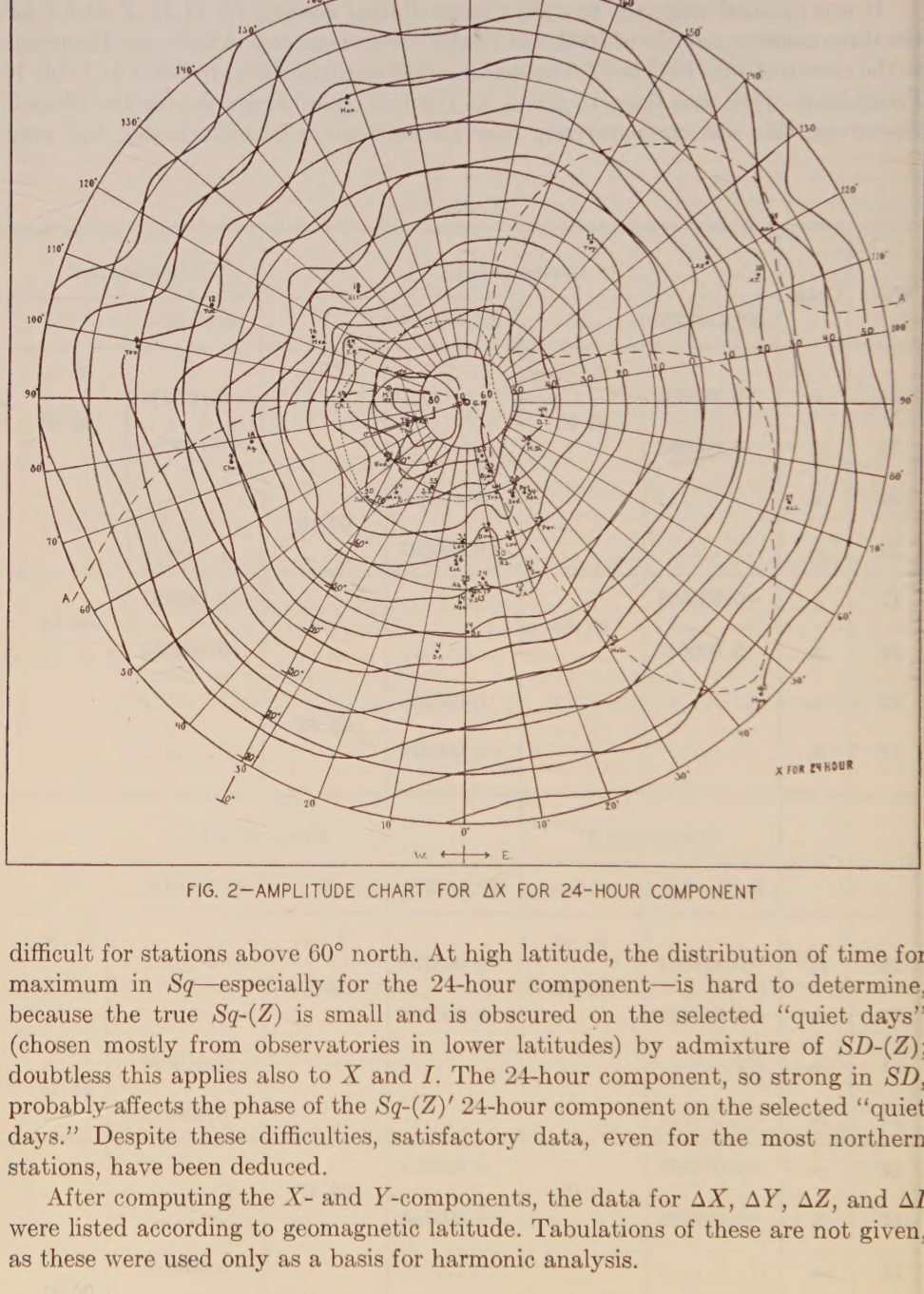

FIG. 2—AMPLITUDE CHART FOR ΔX FOR 24-HOUR COMPONENT

difficult for stations above 60° north. At high latitude, the distribution of time for maximum in *Sq*—especially for the 24-hour component—is hard to determine, because the true *Sq*-(*Z*) is small and is obscured on the selected "quiet days" (chosen mostly from observatories in lower latitudes) by admixture of *SD*-(*Z*); doubtless this applies also to *X* and *I*. The 24-hour component, so strong in *SD*, probably affects the phase of the *Sq*-(*Z*)′ 24-hour component on the selected "quiet days." Despite these difficulties, satisfactory data, even for the most northern stations, have been deduced.

After computing the *X*- and *Y*-components, the data for ΔX, ΔY, ΔZ, and ΔI were listed according to geomagnetic latitude. Tabulations of these are not given, as these were used only as a basis for harmonic analysis.

Harmonic phase constant (*T*)

The results of discussions for the harmonic constants for phase (*T*) and ampli-

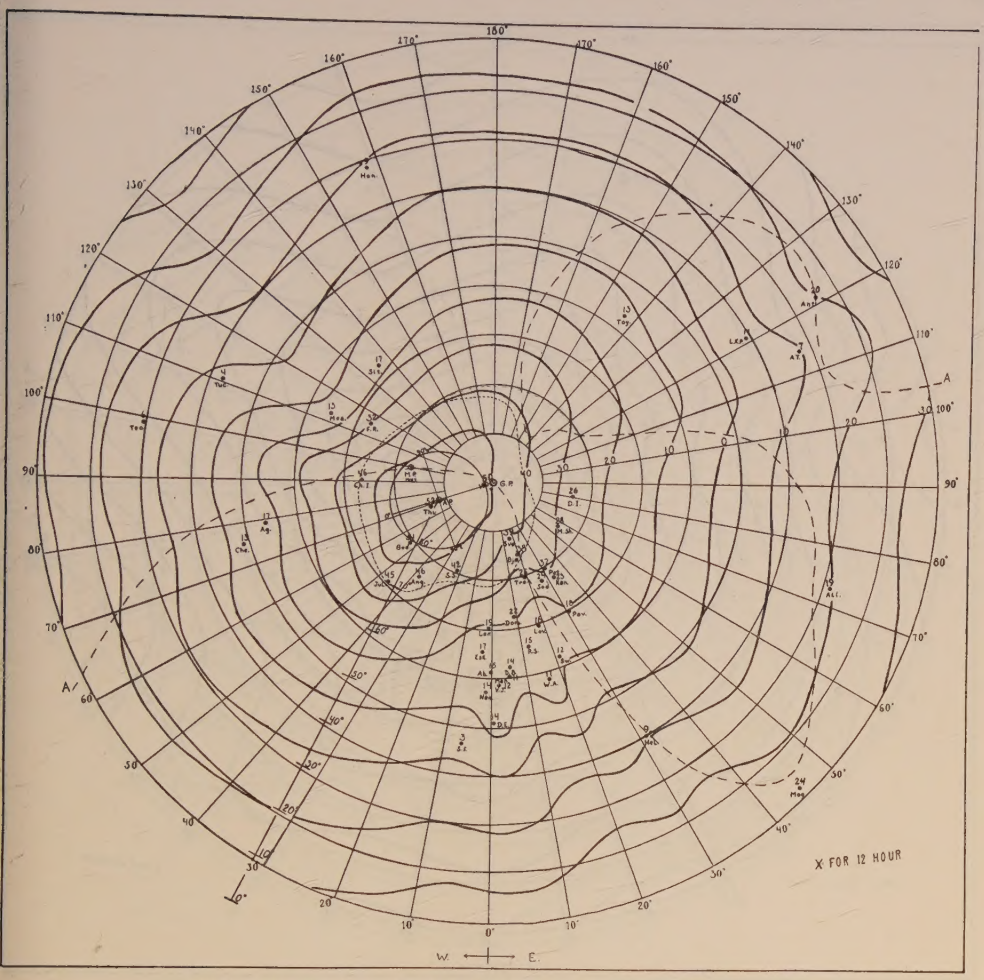

FIG. 3—AMPLITUDE CHART FOR ΔX FOR 12-HOUR COMPONENT

tude (A) are given in Table 2, which shows the data for the 24-hour and 12-hour components ΔX, ΔY, ΔZ, and ΔI. Graphs for maximum local mean times of the 24-hour and 12-hour components, based on the harmonic constants for phase, are plotted in Figure 1 for the 44 stations for values of T using Table 2.

The graphs of Figure 1 show that maximum for ΔX at 90° north occurs at about 11 o'clock, and the phase constant gradually increases to about one o'clock the next day at 37° north. Between 37° north and 22° north, there is a phase change of about 17 hours. A similar change also appears in the 12-hour component for ΔX, but is comparatively small—about four hours. The components ΔY and ΔZ show no such change in phase before the Equator is passed. For component ΔI, there is again a small change in the phase, both for the 24-hour and the 12-hour components, at about the same latitude as for ΔX.

The reality of the spread of points for individual stations may be questioned. For a theoretical study, however, we may draw a mean line through the points from

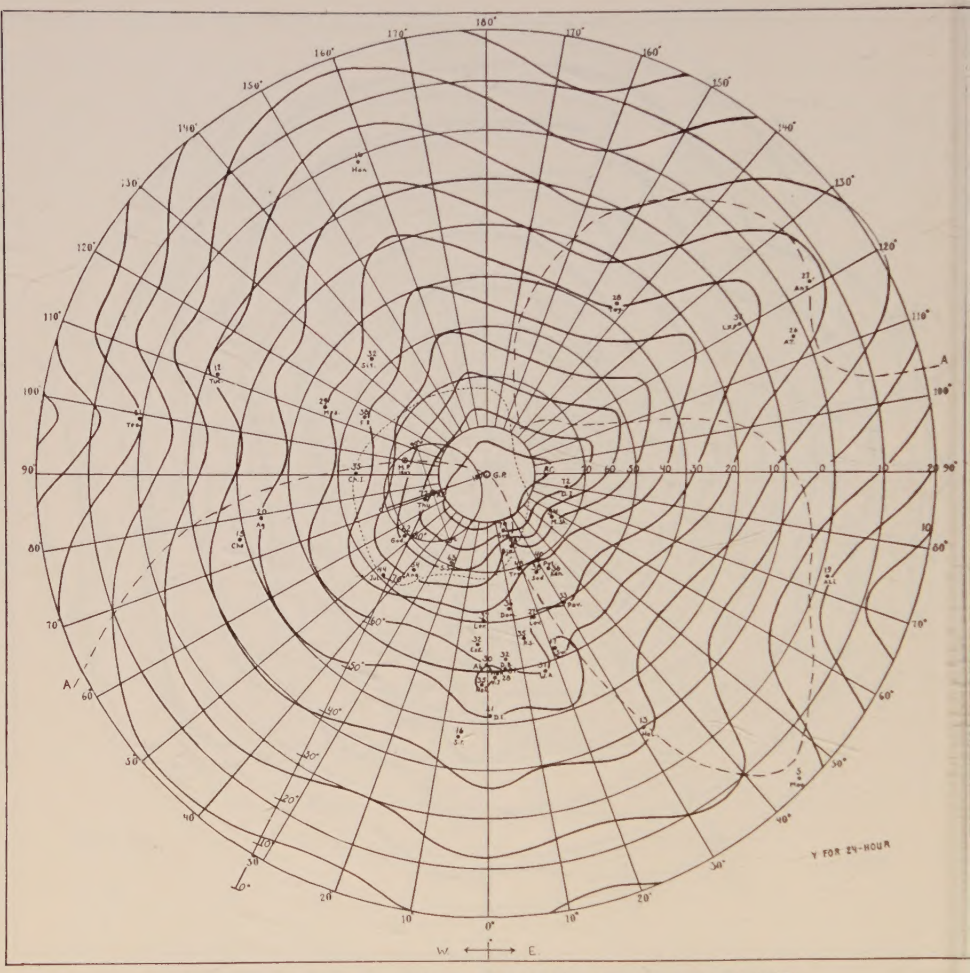

FIG. 4—AMPLITUDE CHART FOR ΔY FOR 24-HOUR COMPONENT

90° north to the Equator. The graphs were determined by the method of least squares. The general formula used is given in equation (1)

$$T_0 = g + \Delta\Phi\alpha + \Delta\Phi^2\beta \quad \text{.....(1)}$$

where T stands for time and Φ for geomagnetic latitude. Adopting the notations

$$a = \Sigma\Delta\Phi \qquad c = \Sigma\Delta\Phi^3 \qquad e = \Sigma T\Delta\Phi \qquad g = \Sigma T$$

$$b = \Sigma\Delta\Phi^2 \qquad d = \Sigma\Delta\Phi^4 \qquad f = \Sigma T\Delta\Phi^2 \qquad n = \text{number of data}$$

the following three equations may be developed:

$$\text{(I)} \quad e - aT_0 - b\alpha - e\beta = 0$$

$$\text{(II)} \quad f - bT_0 - c\alpha - d\beta = 0$$

$$\text{(III)} \quad g - nT_0 - a\alpha - b\beta = 0$$

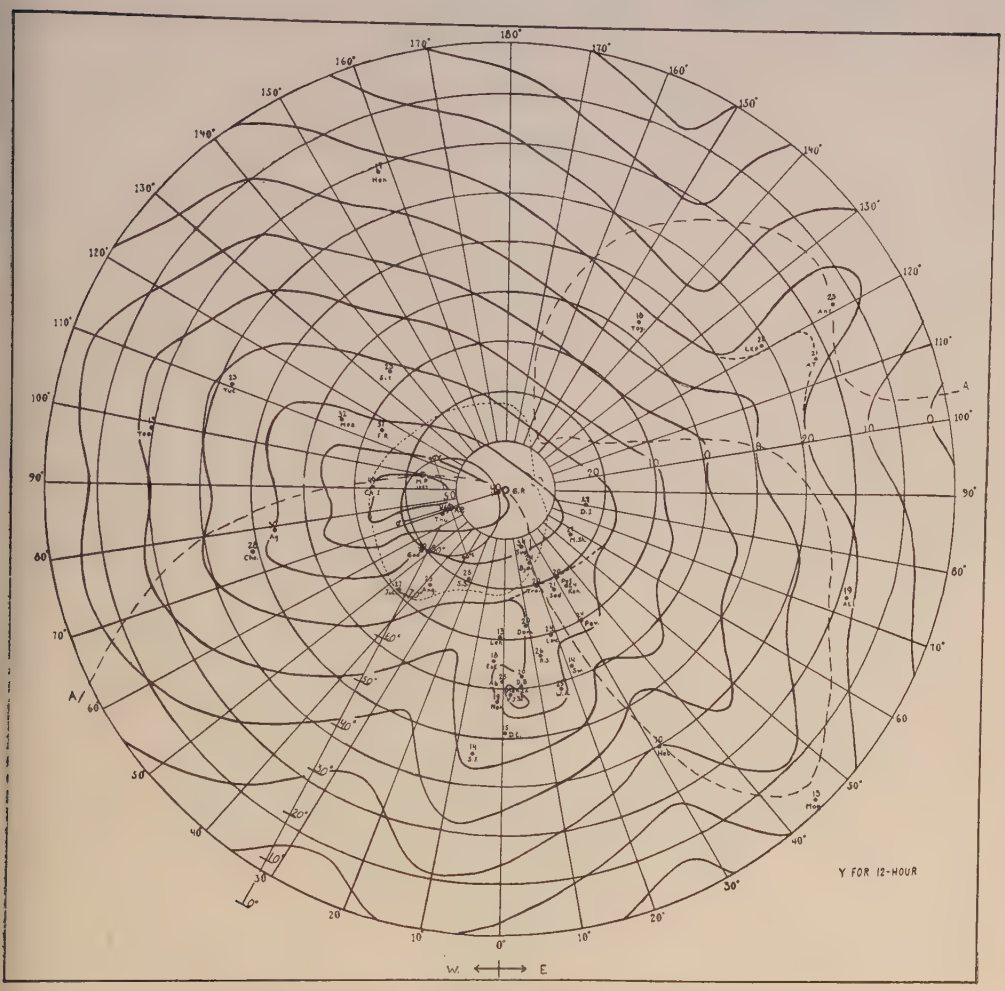

FIG. 5—AMPLITUDE CHART FOR ΔY FOR 12-HOUR COMPONENT

These involve three unknowns, α, β, and T_0, for which the equations in (2) are derived, as follows:

$$\left.\begin{aligned} \alpha &= \frac{(ag - en) + (cn - ab)\beta}{a^2 - bn} \\ \beta &= \frac{abe + acg - cen - a^2f - b^2g + bfn}{2abc - c^2n - b^3 - a^2d + bdn} \\ T_0 &= \frac{g - a\alpha - b\beta}{n} \end{aligned}\right\} \quad \ldots\ldots\ldots\ldots (2)$$

Table 3 lists the results for α, β, and T_0. Where phase changes occur in ΔX and ΔI, it is necessary to make two least-square analyses, based on the two parts of the graph, before and after the phase change.

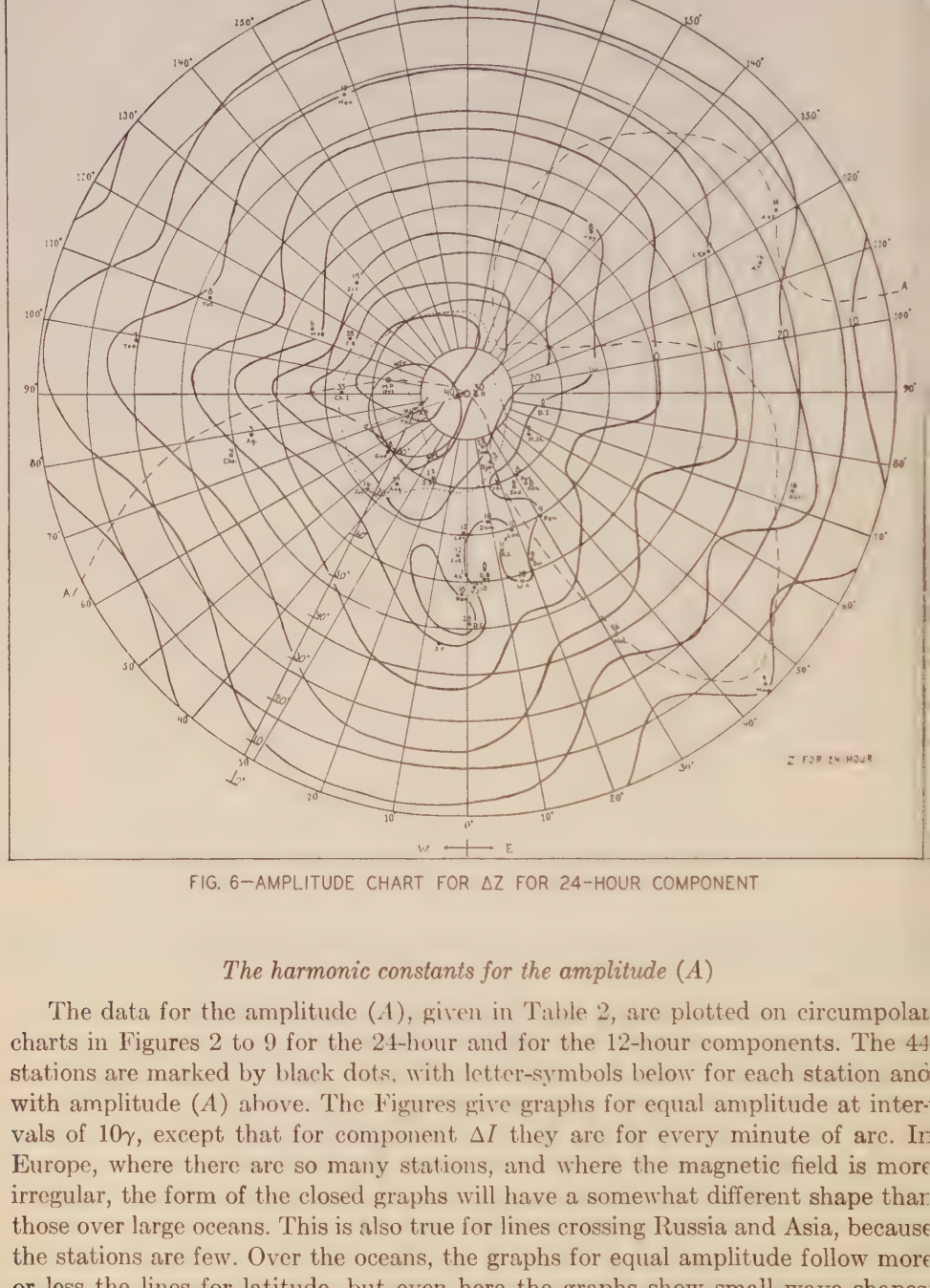

FIG. 6—AMPLITUDE CHART FOR ΔZ FOR 24-HOUR COMPONENT

The harmonic constants for the amplitude (A)

The data for the amplitude (A), given in Table 2, are plotted on circumpolar charts in Figures 2 to 9 for the 24-hour and for the 12-hour components. The 44 stations are marked by black dots, with letter-symbols below for each station and with amplitude (A) above. The Figures give graphs for equal amplitude at intervals of 10γ, except that for component ΔI they are for every minute of arc. In Europe, where there are so many stations, and where the magnetic field is more irregular, the form of the closed graphs will have a somewhat different shape than those over large oceans. This is also true for lines crossing Russia and Asia, because the stations are few. Over the oceans, the graphs for equal amplitude follow more or less the lines for latitude, but even here the graphs show small wave shapes which it is assumed are real.

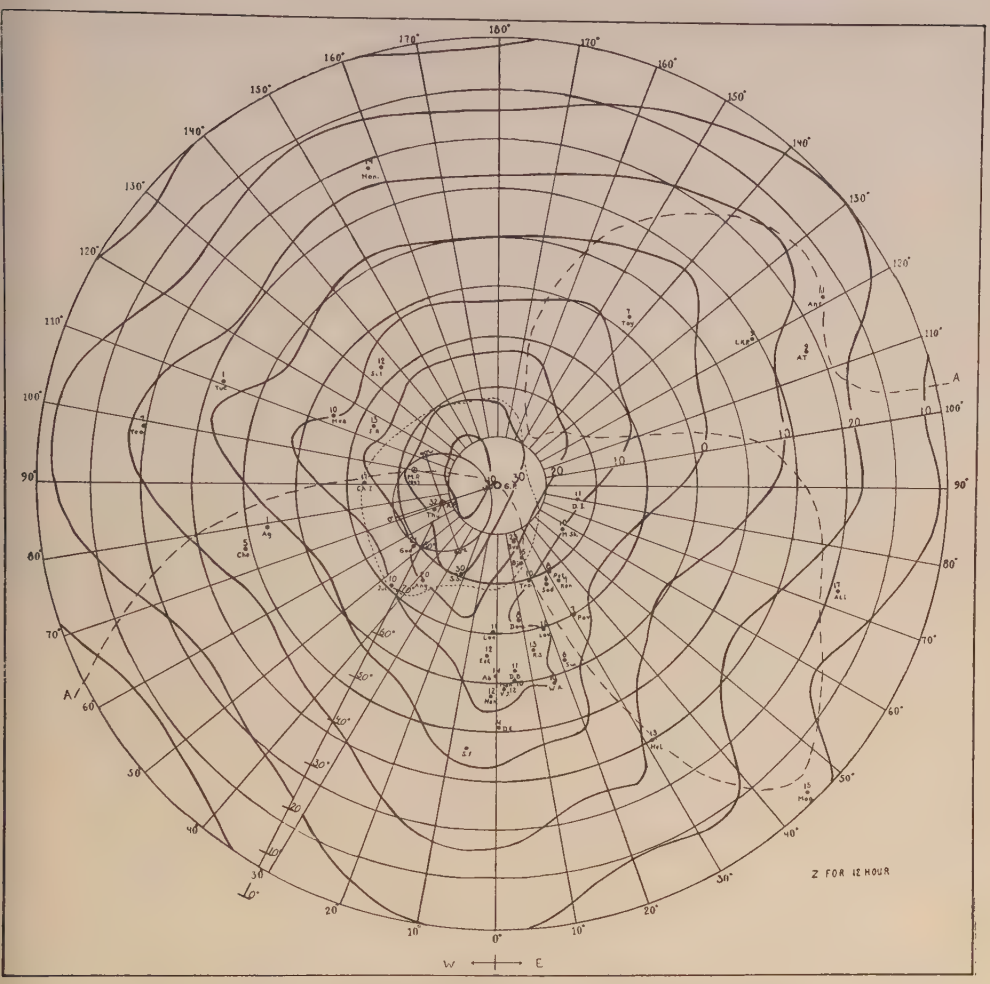

FIG. 7—AMPLITUDE CHART FOR ΔZ FOR 12-HOUR COMPONENT

The harmonic curves of diurnal Sq for ΔX, ΔY, ΔZ, and ΔI

From the mean graphs in Figure 1, the times for the maximum points for every five degrees of latitude between 90° north and the Equator, and the corresponding amplitudes A, can be derived from the charts of Figures 2 to 9. Theoretically, the results for the A-data should be the same for whichever section between the Pole and the Equator, but this is not quite the case. In choosing our section, it is necessary to consider which gives the best average; it seems that a section along the 45° east geomagnetic meridian should be comparatively favorable. The A-values from this section for the four elements and corresponding T-values are listed for the 24-hour and for the 12-hour components in Table 4. Based on these data, Figure 10 shows the harmonic curves for diurnal variation for the four elements. The early data for such harmonic curves can be calculated when the two harmonic constants are known, that is, phase and amplitude.

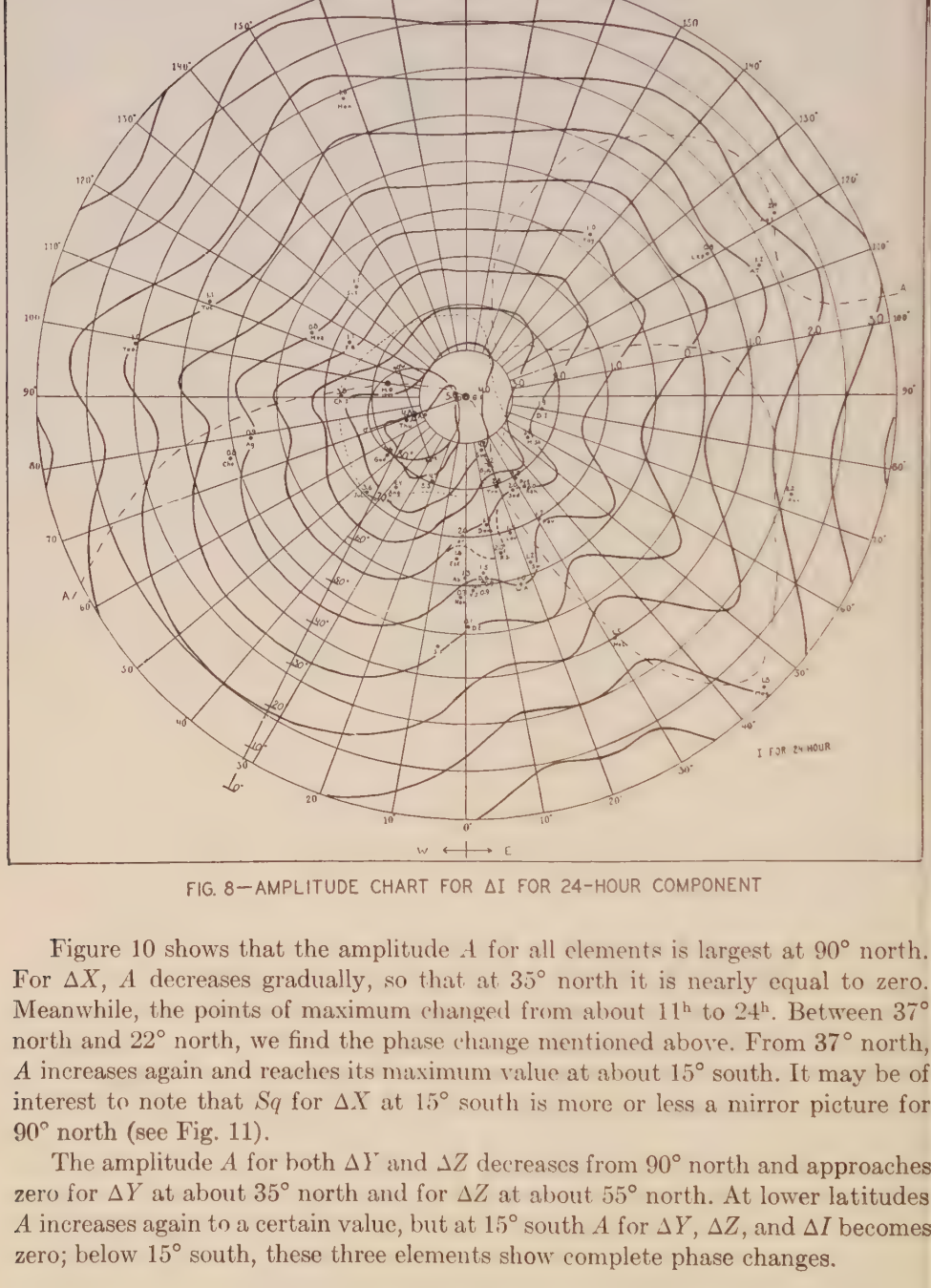

FIG. 8—AMPLITUDE CHART FOR ΔI FOR 24-HOUR COMPONENT

Figure 10 shows that the amplitude A for all elements is largest at 90° north. For ΔX, A decreases gradually, so that at 35° north it is nearly equal to zero. Meanwhile, the points of maximum changed from about 11^h to 24^h. Between 37° north and 22° north, we find the phase change mentioned above. From 37° north, A increases again and reaches its maximum value at about 15° south. It may be of interest to note that Sq for ΔX at 15° south is more or less a mirror picture for 90° north (see Fig. 11).

The amplitude A for both ΔY and ΔZ decreases from 90° north and approaches zero for ΔY at about 35° north and for ΔZ at about 55° north. At lower latitudes A increases again to a certain value, but at 15° south A for ΔY, ΔZ, and ΔI becomes zero; below 15° south, these three elements show complete phase changes.

Overhead electric magnetic current-system

The dynamo theory of Schuster was taken up by Chapman and Bartels—the

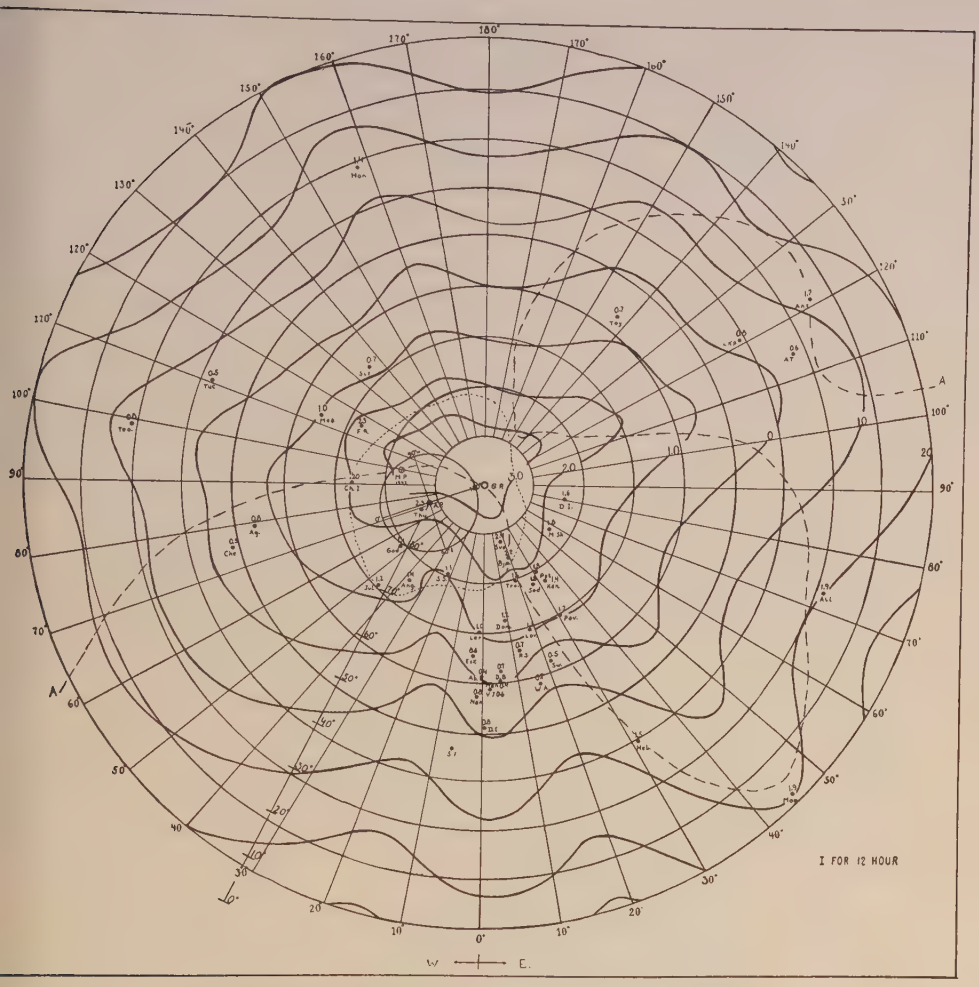

FIG. 9—AMPLITUDE CHART FOR ΔI FOR 12-HOUR COMPONENT

esult of their work is given in reference [2]. In Chapters XVII and XX of that eference (pp. 606 and 686), a description is given of a spherical harmonic analysis vhich leads to the determination of the intensity and distribution of the system of iorizontal electric currents in the upper atmosphere that could produce the *Sq*-field.

In the present investigation, the *Sq*-curves for ΔX, ΔY, ΔZ, and ΔI, as based on all magnetic data between 90° north and the Equator for the Northern Hemisphere, represent the magnetic *Sq*-field as of July 1933. Based on this field—especially on the graphs for ΔX and ΔY—it is possible to work in the opposite manner to that developed by Chapman (see [2], p. 228) and thus to determine the shape of the electric current-system in the upper atmosphere from what we know about the magnetic *Sq*-field, represented by the graphs of Figure 12. The method used is the one introduced by Chapman (see [2], p. 232).

The current-system is assumed to be stationary in relation to the sun and;

Table 4

Φ	Component X				Component Y				Component Z				Component I			
	24-hour		12-hour		24-hour		12-hour		24-hour		12-hour		24-hour		12-hour	
	Ampl.	Time	Ampl.	Time	Ampl.	Time	Ampl.	Time	Ampl.	Time	Ampl.	Time	Ampl.	Time	Ampl.	Time
°	γ	h	γ	h	γ	h	γ	h	γ	h	γ	h	′	h	′	h
90	80	11.4	53	4.1	37	2.2	24	2.8	42	15.1	33	2.8	4.7	1.4	2.6	5.6
85	67	13.5	52	4.3	36	3.0	21	3.9	36	16.3	29	3.4	5.2	3.4	1.9	6.9
80	58	15.5	51	4.5	31	3.6	15	4.8	30	17.4	24	4.0	4.8	5.0	1.7	8.1
75	55	17.4	50	4.7	27	4.0	13	5.7	23	18.5	19	4.5	4.3	6.4	1.4	9.1
70	50	18.9	44	4.9	22	4.2	12	6.5	17	19.5	11	5.0	3.7	7.7	1.1	9.7
65	43	20.3	37	5.0	18	4.5	11	7.1	12	20.4	7	5.3	3.3	8.5	0.7	10.2
60	34	21.5	27	5.2	14	4.7	8	7.6	7	21.2	3	5.5	2.6	9.2	0.3	10.5
55	27	22.5	21	5.4	12	4.9	6	8.0	4	21.9	0	5.9	2.0	9.6	0.1	10.7
50	19	23.4	15	5.6	9	5.0	4	8.2	1	22.5	4	6.0	1.5	9.8	0.4	10.7
45	13	24.0	10	5.8	7	5.1	2	8.2	3	23.1	7	6.1	1.1	9.7	0.8	10.6
40	6	24.5	6	6.0	5	5.1	0	8.2	6	23.5	10	6.1	0.7	9.4	1.2	10.2
35	0	24.3	2	5.8	3	5.2	2	8.2	8	23.9	13	6.1	0.2	8.6	1.6	9.5
30	6	15.5	2	2.0	1	5.2	4	8.1	10	24.1	16	6.1	0.1	24.2	1.9	6.1
25	12	8.3	6	1.7	0	5.2	6	7.9	13	24.2	18	6.0	0.5	23.9	2.2	5.9
20	17	7.7	10	1.4	2	5.1	8	7.5	16	24.3	21	5.9	0.9	23.7	2.5	5.8
15	22	8.6	13	1.2	3	5.0	8	7.0	18	24.4	24	5.5	1.2	23.5	2.8	5.7
10	26	9.6	18	0.9	5	4.9	8	6.4	19	24.4	27	5.3	1.7	23.4	3.1	5.5
5	30	10.6	21	0.6	7	4.7	7	5.6	15	24.2	29	5.0	2.0	23.2	3.5	5.4
0	36	11.5	25	0.4	9	4.6	6	4.7	12	24.0	31	4.5	2.3	22.9	3.8	5.3

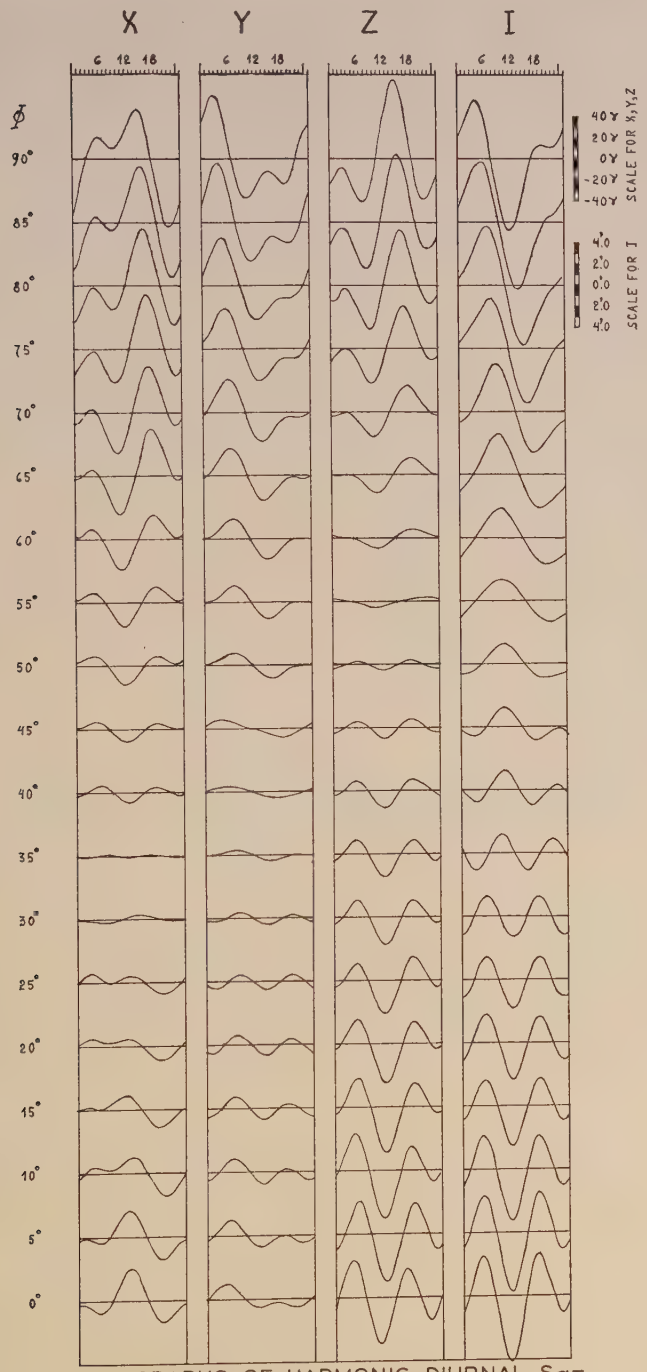

FIG. 10—GRAPHS OF HARMONIC DIURNAL Sq-CURVES FOR EVERY FIVE DEGREES OF GEOMAGNETIC LATITUDE BETWEEN 90° NORTH AND EQUATOR

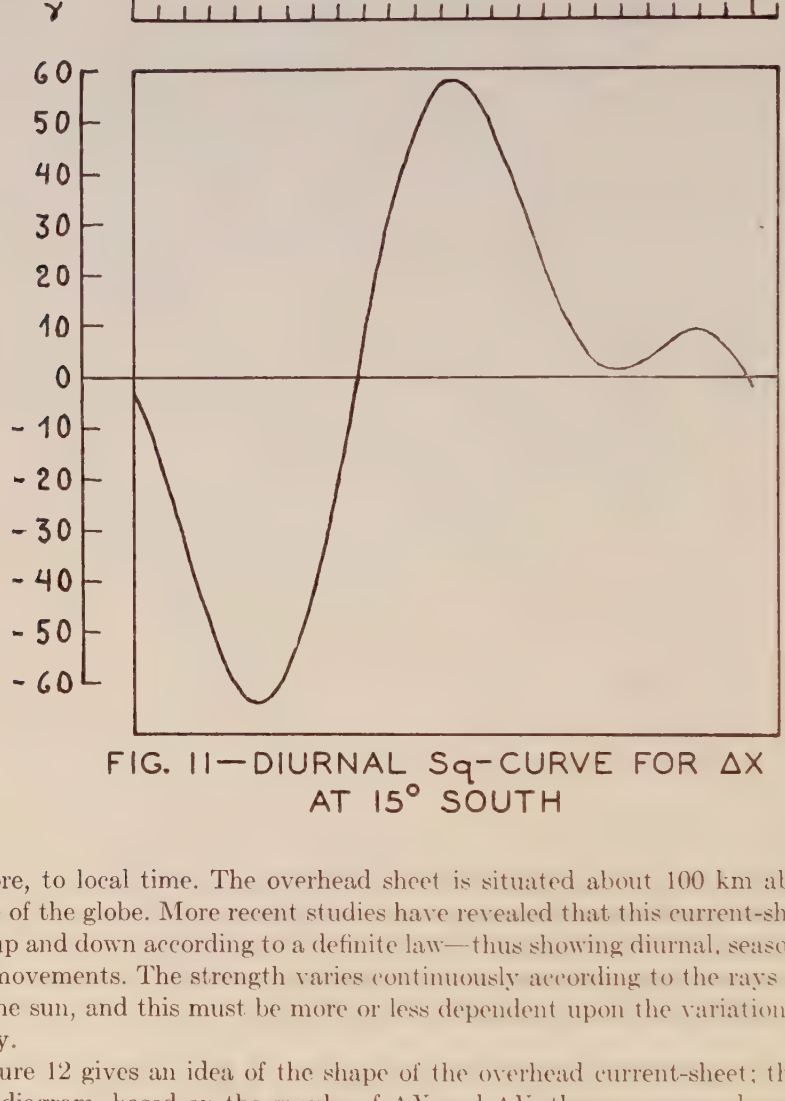

FIG. 11—DIURNAL Sq-CURVE FOR ΔX AT 15° SOUTH

therefore, to local time. The overhead sheet is situated about 100 km above the surface of the globe. More recent studies have revealed that this current-sheet may move up and down according to a definite law—thus showing diurnal, seasonal, and other movements. The strength varies continuously according to the rays received from the sun, and this must be more or less dependent upon the variation in solar activity.

Figure 12 gives an idea of the shape of the overhead current-sheet; through a vector-diagram, based on the graphs of ΔX and ΔY, the arrows are drawn for 2-hours for every five degrees of latitude between 90° north and the Equator. As only the direction of the arrows is of interest, they are all of the same length. To show the general tendency of the distribution of the direction-arrows, the graphs are plotted between them at convenient intervals. Figure 12 shows clearly the centers of the various circuits. The center of the main current-system is at latitude about 33° north, at about 11 o'clock; all the arrows are there directed towards a point which is denoted by C_0. The magnetic force in the horizontal plane must be zero because there it has no definite direction. At about 2 o'clock in 8° north latitude another center is exhibited, where the arrows point in all directions and issue from the center, denoted as C', and where the horizontal force must be zero.

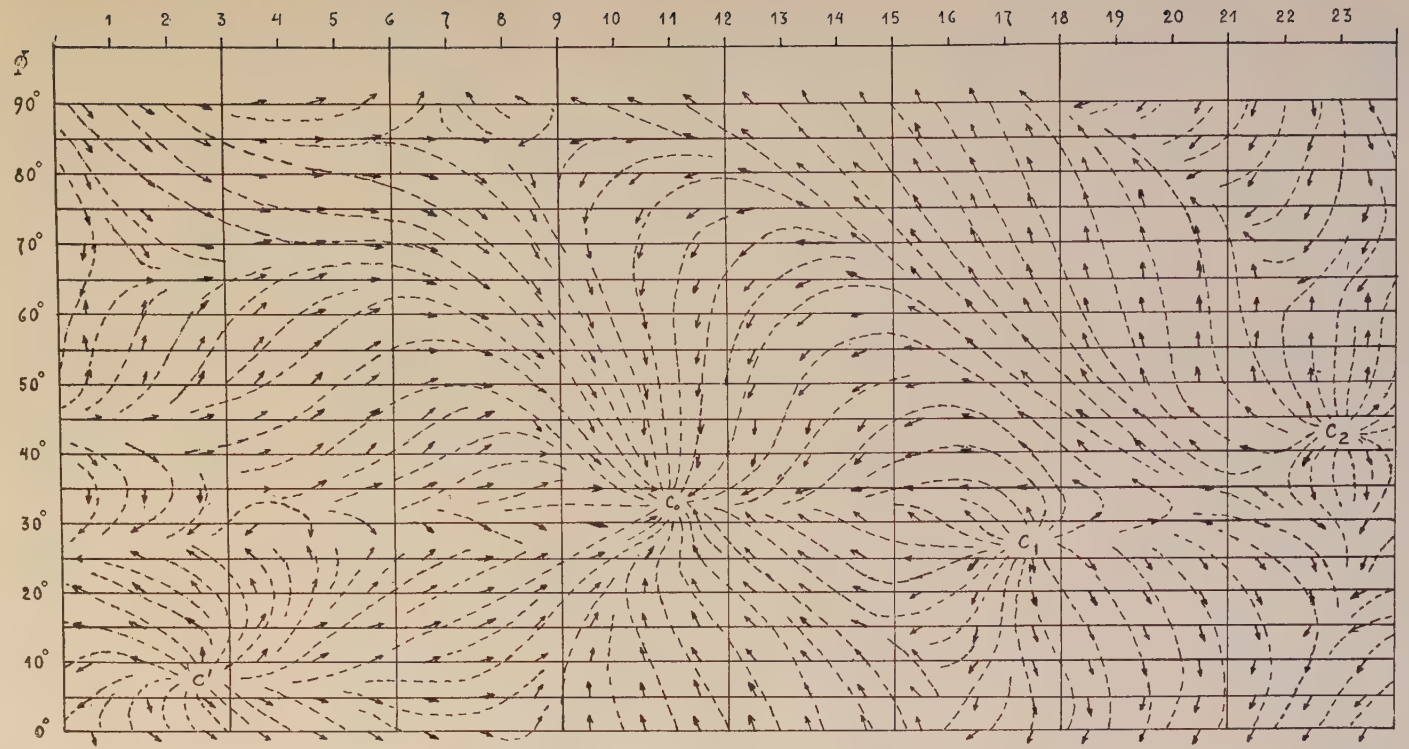

FIG. 12—DIAGRAM OF DIRECTION OF Sq-VARIATION DURING DAY FOR EVERY FIVE DEGREES OF LATITUDE ACCORDING TO THE GRAPHS OF ΔX AND ΔY BETWEEN 90° NORTH AND EQUATOR (DIRECTIONS GIVEN IN FIGURE 10)

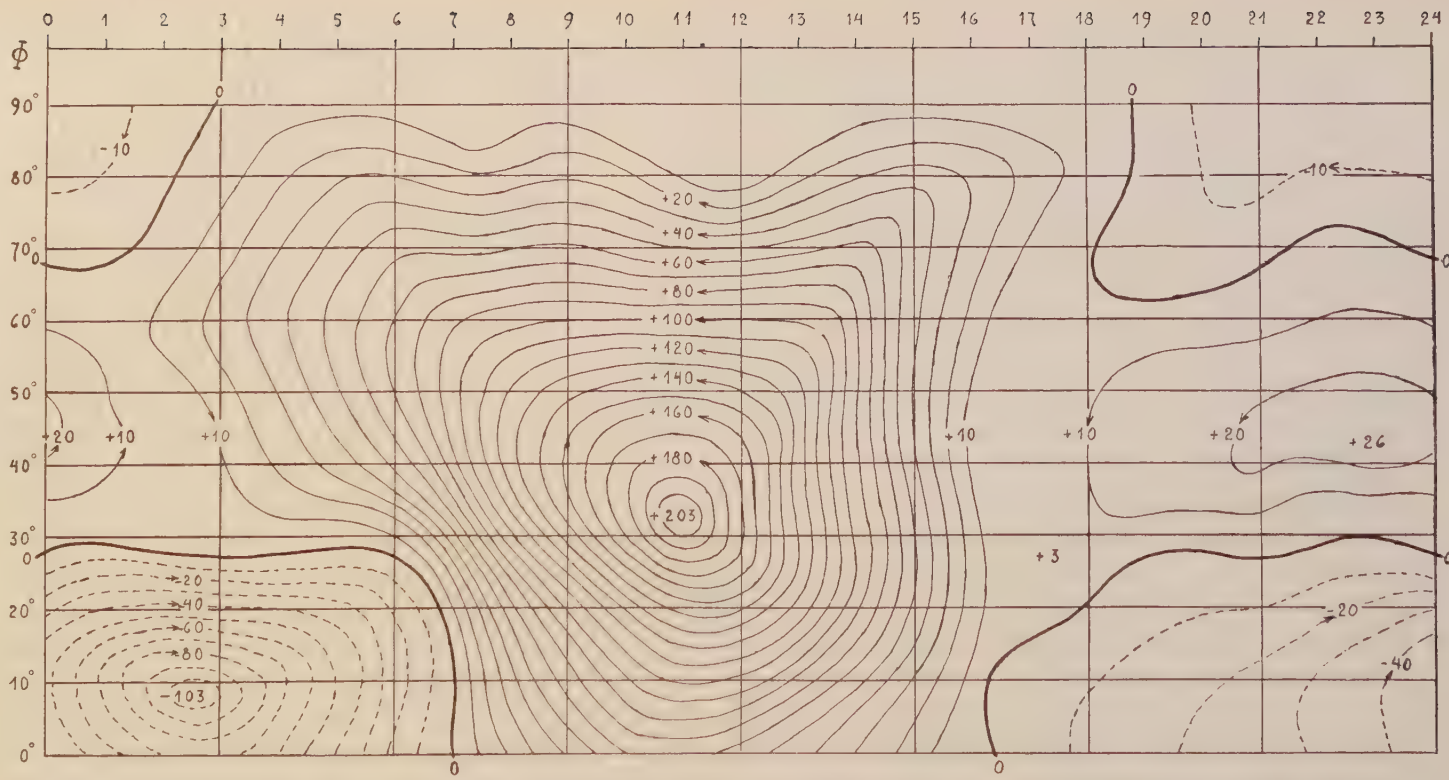

FIG. 13—GRAPH OF OVERHEAD CURRENT-SYSTEM APPROXIMATELY SATISFYING Sq-CURVES OF FIGURE 12 (THE 10,000 AMPERES FLOW IN DIRECTION OF ARROWS BETWEEN THE CONSECUTIVE STREAM-LINES)

In addition to these two main centers, there are two secondary ones at $17^h\ 30^m$ and at $23^h\ 30^m$, which are designated as C_1 and C_2 . The spherical sheet-current distribution may be derived from magnetic observations by a rather complicated mathematical process of spherical harmonic analysis. Fortunately, it is possible to determine also approximately the current-intensity and the total current of the various circuits using a simpler method introduced by Chapman (see reference [2], p. 316).

Denoting current-intensity by i, the horizontal magnetic force at C_0 will be $2\pi i$ northward. This is not, however, the observed magnetic intensity ΔX at C_0 , because ΔX includes a contribution due to a secondary current-system flowing *within* the earth. The existence of this system is definitely established by spherical harmonic analysis of the *Sq*-field; the fraction of ΔX arising from the atmospheric current-system is approximately 0.6. Thus, equating the fraction f of the observed ΔX-variation at C_0 to the magnetic force $2\pi i_0$, we have

$$\left.\begin{aligned} f\Delta X_0 &= 2\pi i_0 \text{ , or} \\ i_0 &= \frac{f\Delta X_0}{2\pi} \text{ emu/cm} \\ &= \frac{10 f\Delta X_0}{2\pi} \text{amp/cm} \end{aligned}\right\} \quad \ldots\ldots\ldots\ldots\ldots\ldots\ldots (3)$$

Taking ΔX as 58γ (derived from the maximum positive amplitude from the *Sq*-curve for 15° south, as in Fig. 11), $i_0 = 5.54 \times 10^{-4}$ amp/km = 55.4 or 60.9 amp per 10°-range in latitude.

To get the total current (I_{day}) flowing around the daytime current-circuit, it is necessary to know the mean current-intensity $\bar{i}$ between the center of the circuit at latitude 33° north and 15° south—an interval of about 50°. Chapman shows that the mean value of $\bar{i}$ between these two latitudes is about $2/3(i_0)$; hence $\bar{I}_{day} = 2/3 \times 5.54 \times 50 = 183{,}000$ amperes, or as derived from spherical harmonic analysis 202,000 amperes.

The value for the point C_0' , using the principal minimum of the *Sq*-curve for ΔX at 15° south is 102,000 amperes.

Figure 13 is the graph for the current-system approximately satisfying the *Sq*-curves of Figure 12. The stream-lines are drawn perpendicular to the general direction of the arrows, and the flow direction about the center C_0 is opposite to that of C_0' .

The corresponding figures for the two centers C_1 and C_2 , derived from the secondary maximum and minimum in the *Sq*-curve for ΔX at 15° south, are 26,000 and 3,000 amperes; direction of the stream-lines is the same as for the main current-system about C_0 . There is no zero line between the main current-system and that about C_2 .

Between the Pole and 70° north, from 19 o'clock until 3 o'clock the next day, there must also be a current-system, the center of which is somewhat difficult to place. The stream-line direction is probably sometime about 23^h—the same as for C_0' .

Acknowledgments

The author takes this opportunity to thank Dr. J. A. Fleming, Chairman of the Committee on the Agenda of the International Polar Year of 1932–33, and its Executive Officer, V. Laursen, for a grant-in-aid for the services of an able assistant and for other help at the Danish Meteorological Institute. The author also thanks Dr. Chapman for the interest he has shown in this investigation and for the suggestions he has made.

References

[1] B. Trumpy and K. F. Wasserfall, Studies on the quiet diurnal variation of magnetic elements, Trondheim, kgl. Vid. selsk. Skr., Nr. 3 (1937).

[2] S. Chapman and J. Bartels, Geomagnetism, Oxford, Clarendon Press, Volumes I and II (1940).

THE FIELDS OF AN ELECTRIC DIPOLE IN A SEMI-INFINITE CONDUCTING MEDIUM*

BY JAMES R. WAIT AND L. LORNE CAMPBELL

Radio Physics Laboratory, Defense Research Board, Ottawa, Canada

(Received July 16, 1952)

ABSTRACT

The behaviour of an electric dipole situated above a semi-infinite conductor is investigated. Expressions for the electric and magnetic fields within the conductor are derived for the case that significant distances are much less than a free space wave-length. Curves are plotted which show the dependence on conductivity, frequency, and position of the observer. The application of the results to propagation in sea-water is indicated.

Introduction

The theory of propagation of electromagnetic waves in a conducting medium has received little attention. Although the fields are solutions of Maxwell's equations, explicit and useful results are difficult to obtain if the proper conditions at the boundaries in the medium are met.

The theory of the propagation of plane waves in a conducting medium of infinite extent is well summarized by Stratton [see 1 of "References" at end of paper]. The radiation from a dipole source in an infinite medium has been considered by Tai [2]. Wait [3,4] has investigated the electric and magnetic fields in the medium due to both steady state and transient dipole sources.

In this paper, the vertical electric dipole situated in the air and just above the surface of a semi-infinite conducting half space will be investigated. Expressions in terms of tabulated functions will be derived for the electric and magnetic fields at all points within the conductor. The fields of the dipole in the insulator above the surface have been given adequately by Norton [5] and others, and hence need not be of further concern here.

Derivation of the fields

A current element of length ds carrying a current equal to the real part of $I \exp(i\omega t)$ is situated at the origin of a cylindrical polar coordinate system (ρ,φ,z) and is oriented in the z direction. A homogeneous semi-infinite medium of conductivity σ and dielectric constant ϵ occupies the space corresponding to negative values of z. The insulator has a dielectric constant ϵ_0. The situation is shown in Figure 1. The magnetic permeability is μ and is the same throughout the entire space.

*This work was carried out under Radio Physics Laboratory Project No. 19.

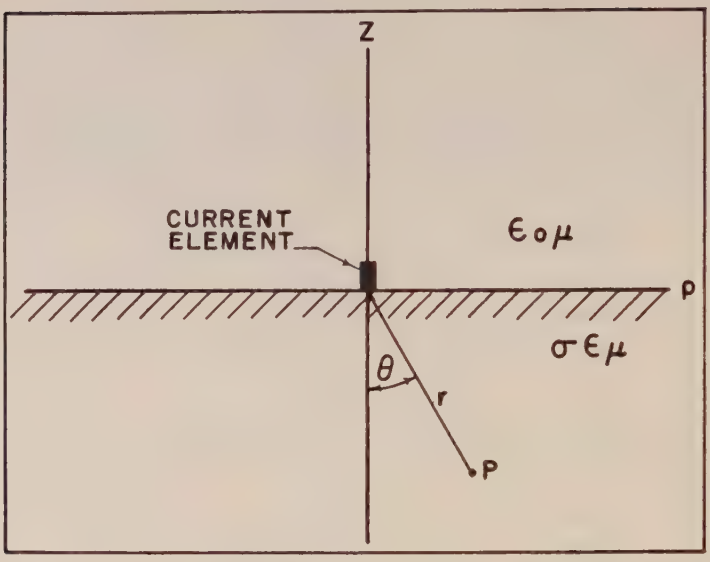

FIG. 1—THE COORDINATE SYSTEM FOR THE ELECTRIC CURRENT ELEMENT ON THE SURFACE OF THE CONDUCTOR

Sommerfeld [6] has derived formal expressions for the fields in the insulator and the conductor. He has shown that the fields can be represented everywhere in terms of a Hertz vector with only a z component. The value of Π_z in the conductor is

$$\Pi_z = \frac{i\mu\omega\, I\, ds}{2\pi} \int_0^\infty \frac{J_0(\lambda\rho)e^{uz}\lambda\, d\lambda}{\gamma^2 u_0 + \gamma_0^2 u} \quad \ldots\ldots(1)$$

where

$$\gamma^2 = i\sigma\mu\omega - \epsilon\mu\omega^2, \qquad \gamma_0^2 = -\epsilon_0\mu\omega^2$$

$$u_0 = (\lambda^2 + \gamma^2)^{1/2} \qquad \text{and} \qquad u_0 = (\lambda^2 + \gamma_0^2)^{1/2}$$

The fields in the conductor are then given by

$$E_z = -\gamma^2\Pi_z + \frac{\partial^2\Pi_z}{\partial z^2} \quad \ldots\ldots(2)$$

$$E_\rho = \frac{\partial^2\Pi_z}{\partial\rho\,\partial z} \quad \ldots\ldots(3)$$

$$H_\varphi = -\frac{\gamma^2}{i\mu\omega}\frac{\partial\Pi}{\partial\rho} \quad \ldots\ldots(4)$$

and

$$E_\varphi = H_\rho = H_z = 0 \quad \ldots\ldots(5)$$

To evaluate these fields for points in the conducting medium, a simplification will be made which is justified for cases of practical interest. The approximation is that all displacement currents in the air are neglected. This is effected by setting $\gamma_0 = 0$. Actually, this implies that the fields are a solution of Laplace's equation in the air. This is a good approximation if the fields are observed at distances much

less than a free space wave-length. Foster [7] has made this same approximation in connection with mutual impedance of grounded wires.

The Hertz vector now is

$$\Pi_z = \frac{I\,ds}{2\pi(\sigma + i\omega\epsilon)} \int_0^\infty J_0(\lambda\rho)e^{uz}\,d\lambda \quad \ldots\ldots(6)$$

The following integral given by Foster [7] is now introduced

$$\int_0^\infty J_0(\lambda\rho)e^{uz}/u\,d\lambda = I_0\left[\frac{\gamma}{2}(r+z)\right]K_0\left[\frac{\gamma}{2}(r-z)\right] \quad \ldots\ldots(7)$$

where

$$r = (\rho^2 + z^2)^{1/2}$$

and I_0 and K_0 are modified Bessel functions of zero order of the first and third type, respectively. Employing this result, the function Π_z is given by

$$\Pi_z = \frac{I\,ds}{2\pi(\sigma + i\omega\epsilon)} \frac{\partial}{\partial z} I_0K_0 \quad \ldots\ldots(8)$$

where the arguments of the Bessel functions have been omitted.

The expressions for the fields are then obtained by carrying out the operations indicated by equations (2), (3), and (4), so that

$$E_z = \frac{I\,ds\,U}{2\pi(\sigma + i\omega\epsilon)r^3} \quad \ldots\ldots(9)$$

$$E_\rho = \frac{I\,ds\,V}{2\pi(\sigma + i\omega\epsilon)r^3} \quad \ldots\ldots(10)$$

and

$$H_\varphi = \frac{-I\,ds\,W}{2\pi r^2} \quad \ldots\ldots(11)$$

where

$$U = r^3\left(\frac{\partial^3}{\partial z^3} - \gamma^2\frac{\partial}{\partial z}\right)I_0K_0 \quad \ldots\ldots(12)$$

$$V = r^3\frac{\partial^3}{\partial\rho\,\partial z^2}I_0K_0 \quad \ldots\ldots(13)$$

and

$$W = r^2\frac{\partial^2}{\partial\rho\,\partial z}I_0K_0 \quad \ldots\ldots(14)$$

The derivatives of I_0 and K_0 can be reduced to expressions containing only zero-order and first-order Bessel functions by employing the following recurrence relations given by Watson [8, p. 79].

$$sI_n'(s) = sI_{n-1}(s) - nI_n(s) \quad \ldots\ldots(15)$$

and

$$sK_n'(s) = -sK_{n-1}(s) - nI_n(s) \quad \ldots\ldots(16)$$

where the prime indicates a derivative with respect to the argument s of the Bessel function of order n.

The differentiations are carried out to give

$$U = \tfrac{1}{2}[-\alpha^2 \cos\theta(1 - 3\cos^2\theta)I_0K_0 - \alpha[\alpha^2 \sin^2\theta \cos\theta + (1 - 3\cos^2\theta)(1 + \cos\theta)]I_0K_1 + \alpha[\alpha^2 \sin^2\theta \cos\theta - (1 - 3\cos^2\theta)(1 - \cos\theta)]I_1K_0 + 3\alpha^2 \sin^2\theta \cos\theta\, I_1K_1] \quad \ldots\ldots(17)$$

$$V = -\frac{\sin\theta}{2}[3\alpha^2 \cos^2\theta\, I_0K_0 + \alpha[3\cos\theta(1 - \cos\theta) - \alpha^2\cos^2\theta]I_1K_0 + \alpha[3\cos\theta(1 + \cos\theta) + \alpha^2\cos^2\theta]I_0K_1 + \alpha^2(2 - 3\cos^2\theta)I_1K_1] \quad \ldots\ldots(18)$$

and

$$W = \frac{\sin\theta}{2}[-\alpha^2 \cos\theta\, I_0K_0 - \alpha(1 + \cos\theta)I_0K_1 - \alpha(1 - \cos\theta)I_1K_0 + \alpha^2 \cos\theta\, I_1K_1] \quad \ldots\ldots(19)$$

where

$$\theta = -\tan^{-1}\rho/z$$

and

$$\alpha = \gamma r$$

The argument of the I_0 and I_1 functions is $\gamma(r + z)\ 2$ and of the K_0 and K_1 functions is $\gamma(r - z)/2$. These expressions are exact to the extent that displacement currents in the air are neglected. If the displacement currents in the ground are also negligible, then the propagation constant γ is given by

$$\gamma \approx (i\sigma\mu\omega)^{1/2}$$

where it has been assumed that $\sigma/\epsilon\omega \gg 1$. This will always be true for frequencies less than 100 kc/sec in normal soil or sea-water. The Bessel functions, then, all have an argument proportional to $(i)^{1/2}$, and can be expressed in terms of the well-known Thomson's functions which are tabulated and defined by McLachlan [9]. The connecting relations are

$$I_0(i^{1/2}g) = \mathrm{ber}\, g + i\,\mathrm{bei}\, g \quad \ldots\ldots(20)$$

$$I_1(i^{1/2}g) = i^{-1/2}[\mathrm{ber}'\, g + i\,\mathrm{bei}'\, g] \quad \ldots\ldots(21)$$

$$K_0(i^{1/2}g) = \mathrm{ker}\, g + i\,\mathrm{kei}\, g \quad \ldots\ldots(22)$$

$$K_1(i^{1/2}g) = -i^{-1/2}[\mathrm{ker}'\, g + i\,\mathrm{kei}'\, g] \quad \ldots\ldots(23)$$

where g is real.

The magnitude of the functions U, V, and W are plotted in Figures 2, 3, and 4, respectively. The abscissa is the magnitude of the parameter α given by

$$|\alpha| = (\sigma\mu\omega)^{1/2}r$$

and is proportional to the radial distance down into the conductor as measured from the source dipole. Several values of the angle θ measured from the normal are chosen.

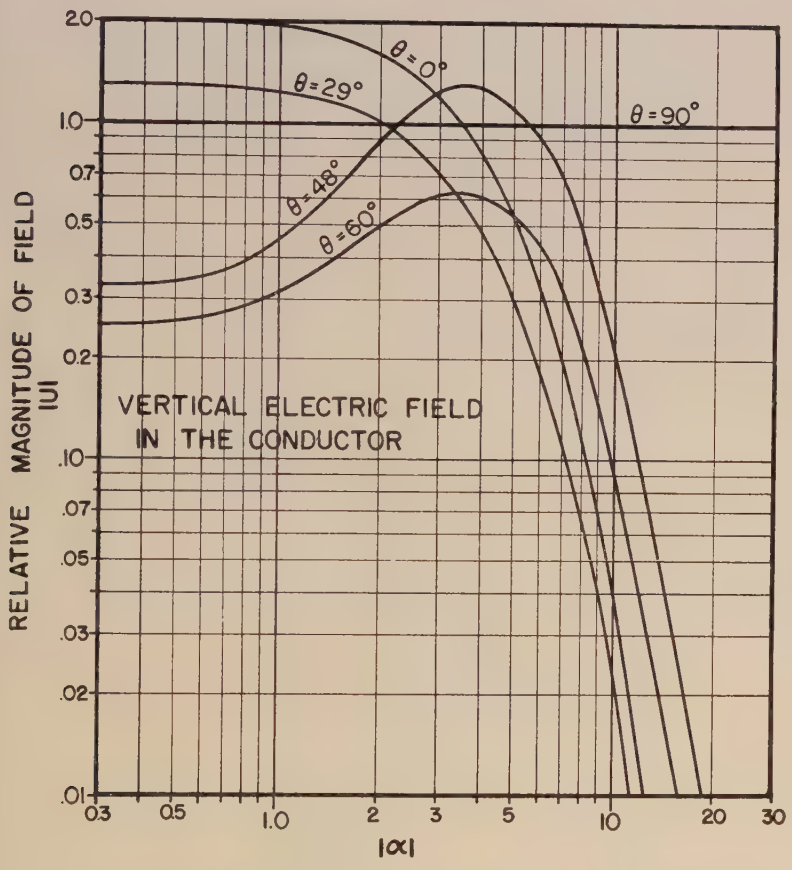

FIG. 2—THE BEHAVIOUR OF THE VERTICAL ELECTRIC FIELD WITHIN THE CONDUCTOR

Discussion of result

As seen in Figure 2, the vertical electric field in the conductor approaches

$$E_z = I\,ds/2\pi\sigma r^3 \quad \ldots\ldots\ldots\ldots\ldots\ldots\ldots\ldots\ldots\ldots (24)$$

as the angle θ tends to 90°. The current density normal to the surface is then given by

$$J_z = I\,ds/2\pi r^3 \quad \ldots\ldots\ldots\ldots\ldots\ldots\ldots\ldots\ldots\ldots\ldots (25)$$

Since this current is continuous across the interface, the electric field E_{0z} in the insulator just above the interface is

$$E_{0z} = I\,ds/2\pi i\omega\epsilon_0 r^3 \quad \ldots\ldots\ldots\ldots\ldots\ldots\ldots\ldots (26)$$

which agrees with an expression given by Norton [5] for the electric field in the insulator when r is much less than a free space wave-length; that is,

$$\sqrt{\epsilon_0\mu}\,\omega r \ll 1$$

In the conductor, the field behaves quite differently with respect to the distance r. When the parameter α has a magnitude greater than 10, the fields are all attenuated exponentially, as shown by the lines of constant slope in Figure 2. For small values of $|\alpha|$, the fields approach values corresponding to the electrostatic case; that is, the fields are those as predicted by direct current theory. In the intermediate range of α, the behaviour is quite complicated.

The electric field E_ρ is shown in Figure 3. The curve corresponding to $\theta = 90°$ is quite interesting. It shows that the tangential electric field on the surface becomes

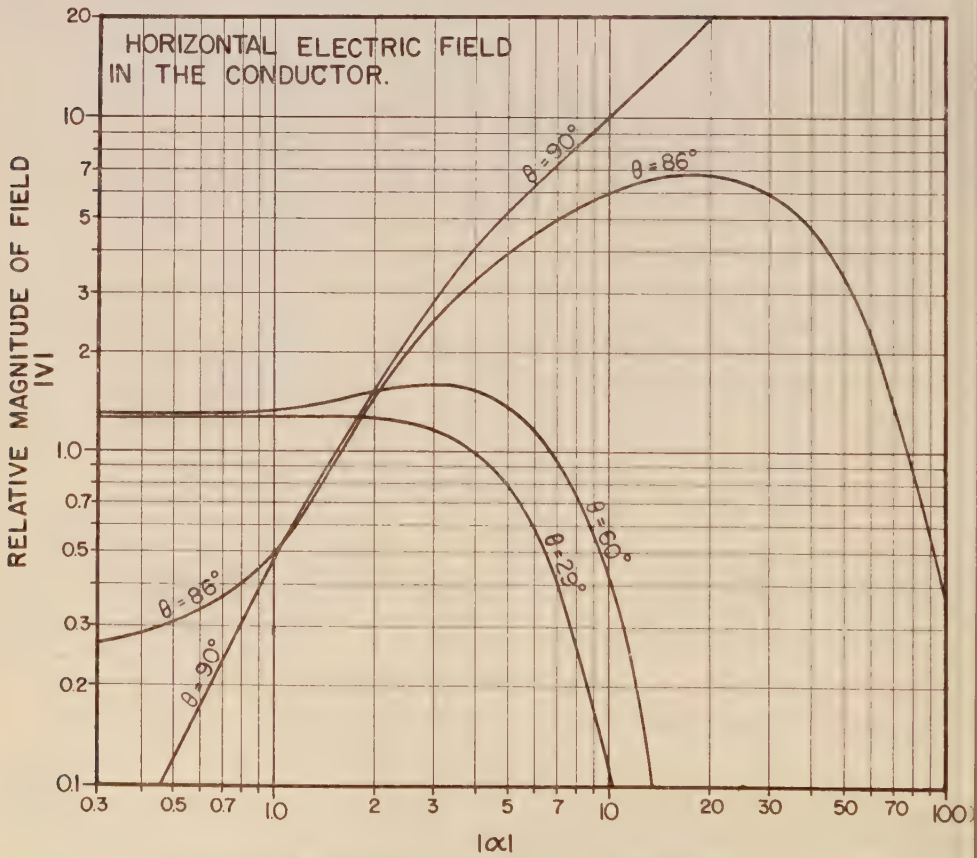

FIG. 3—THE BEHAVIOUR OF THE HORIZONTAL ELECTRIC FIELD WITHIN THE CONDUCTOR

quite large relative to the vertical electric field within the conductor. It varies inversely as the square of the distance for values of $|\alpha|$ greater than 10. Corresponding curves for other angles are also shown on Figure 3, where it can be seen that the fields behave quite differently within the conductor. For angles less than 90°, the fields are attenuated exponentially for large values of the parameter $|\alpha|$. Again at small values of $|\alpha|$, the fields are governed by direct current theory.

The magnetic field which has only a φ component is shown in Figure 4. These fields have similar characteristics to the electric fields in the conductor.

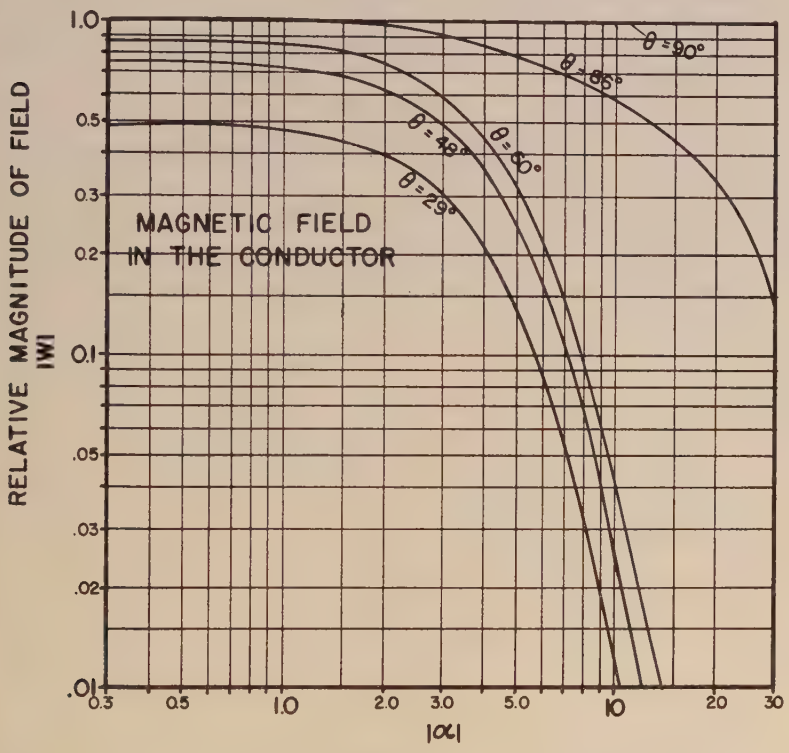

FIG. 4—THE BEHAVIOUR OF THE MAGNETIC FIELD WITHIN THE CONDUCTOR

The following typical values might be employed if the conducting medium was sea-water with an operating frequency of 30 kc:

$$\sigma = 4 \text{ mhos per metre}$$

$$\mu = 4\pi \times 10^{-7} \text{ henries per metre}$$

$$\omega = 2\pi \times 30{,}000 \text{ radians per sec}$$

then

$$r \approx |\alpha| \text{ metres}$$

That is, the abscissa in Figures 2, 3, and 4 is read directly in metres for this particular example. It can be seen that for angles less than 60°, the fields have been attenu-

ated at least 20 decibels for a distance of 30 metres relative to the field on the surface.

Higher frequencies will of course be attenuated a great deal more rapidly.

References

[1] J. A. Stratton, Electromagnetic theory, New York, McGraw-Hill Book Co., Inc., p. 276 (1941).
[2] C. T. Tai, Hertzian dipole immersed in a dissipative medium, Cruft Laboratory, Report No. 21 (1948).
[3] J. R. Wait, Transient electromagnetic propagation in a conducting medium, Geophysics **16**, 213-221 (1951).
[4] J. R. Wait, Magnetic dipole antenna in a conducting medium, Proc. Inst. Radio Engs. **40**, 1244-1245 (1952).
[5] K. A. Norton, Propagation of radio waves over the surface of the earth and in the upper atmosphere, Proc. Inst. Radio Eng., **25**, 1203-1236 (1937).
[6] A. Sommerfeld, Über die Ausbreitung der Wellen in der drahtlosen Telegraphie, Ann. Physik, **81**, 1135-1153 (1926).
[7] R. M. Foster, Mutual impedance of grounded wires lying on the surface of the earth, Bell System Tech. J., **10**, 408-419 (1931).
[8] G. N. Watson, Theory of Bessel functions, Cambridge, University Press, 2nd ed. (1944).
[9] N. W. McLachlan, Bessel functions for engineers, London, Oxford University Press (1946).

MAGNETO-IONIC MULTIPLE SPLITTING DETERMINED WITH THE METHOD OF PHASE INTEGRATION

BY WOLFGANG PFISTER

Geophysics Research Directorate,
Air Force Cambridge Research Center,
230 Albany Street, Cambridge, Mass.

(Received July 28, 1952)

ABSTRACT

The method used is a first-order W.K.B. approximation with an integration path in the complex height plane. The refractive index *versus* height is represented on a Riemann surface with four sheets corresponding to upgoing and downcoming waves and ordinary and extraordinary types of polarization. The branch points connecting the sheets are characterized as reflection points or as coupling points. Suitable paths of integration in the Riemann surface determine the reflection coefficient for the various magneto-ionic components. Five possible fundamental components have been found, and an infinite number of additional components due mainly to multiple reflections between the different reflection points.

Numerical computations have been carried out for one ionospheric model with a Chapman distribution of electrons and an exponential decrease of collision frequency located in a moderate magnetic latitude. The results are represented in a sweep frequency picture of virtual height and absorption for five fundamental modes of propagation.

INTRODUCTION

A signal transmitted vertically upwards toward the ionosphere is split into two magneto-ionic components at the entry into the ionized region. Now, according to the ray treatment, both components are propagated independently from each other in the ionosphere, and the medium is assumed to be slowly varying so that partial reflections can be neglected [see 1 of "References" at end of paper]. If the maximum electron concentration is high enough, each of the components reaches a point where the refractive index becomes zero and the component is totally reflected. When leaving the ionosphere, generally both components are separated in time, which shows up as magneto-ionic splitting on an ionospheric record. Phase path, group path, and absorption for each of the components can easily be determined from the phase integral $\int k \, dz$, where $k = \mu\omega/c$ is the propagation constant of the component concerned. k is a function of the height z. The integral has to be taken over the entire path up to the reflection point and back.

It is obvious that a treatment like that has limits. So it is hard to define the

point of reflection if the number of collisions is appreciable and no easy way can be seen to deal with a phenomenon like the third or z trace. Difficulties of this kind are avoided by using the concept of a *complex plane for the height coordinate* [2,3]. The propagation constant can be represented as a single valued function of height on a Riemann surface with four sheets. The phase integral has to be taken along a suitable path in the Riemann surface, otherwise the method is the same as in the conventional ray treatment.

ISOTROPIC MEDIUM

As illustration of the method, first an isotropic medium may be assumed. The wave equation to be used is

$$\partial^2\pi/\partial x^2 + k^2\pi = 0$$

The medium shall be stratified in the x direction. π as well as k are functions of x, generally complex ones. A formal analytical continuation can be made by using the complex coordinate $z = x + jy$. Now an approximate solution of the wave equation is the well-known W.K.B. solution.

$$\pi = k^{-1/2}(Ae^{-iW} + Be^{+iW})$$

with the phase integral $W = \int k\,dz$. It can easily be verified that the solution is good as long as $\mid \partial k/\partial x \mid \ll \mid k^2 \mid$, which is the condition for the slowly varying medium. Assuming a time factor $e^{i\omega t}$, the A term represents an upgoing wave traveling in the x direction. In the neighborhood of the reflection or turning point, the approximate solution breaks down and the upgoing wave is transformed in a downcoming wave represented by the B term. A connection formula has been derived [4] which allows to compute the reflection coefficient.

Now let us take a different viewpoint. Since, for an isotropic stratified medium, the propagation constant can be written in the form

$$k^2(z) = (\omega/c)^2[1 - f(z)]$$

k is double valued and can be represented as a single valued function of z on a Riemann surface with two sheets. The branch point may be called in this case reflection point (z_r) or turning point, and is defined by $f(z) = 1$. The cut line between the two sheets may be made conveniently along $Re[k] = 0$. Now the W.K.B. approximation may be restricted to the expression

$$\pi = k^{-1/2} \exp\left\{-j \int k\,dz\right\}$$

The sheet defined by a positive real part of k contains the upgoing wave, the other one the downcoming wave. Both waves can be connected with each other by using a phase integral path around the reflection point. Since the W.K.B. solution is restricted to the slowly varying medium, obviously it cannot be used in the neighborhood of a branch point. But if it is possible to find a good path around the branch point, such that everywhere the condition $\mid k' \mid \ll \mid k^2 \mid$ is fulfilled, the solution is useful and the reflection coefficient can be expressed by

$$R = \sqrt{-1} \exp\left\{-j2 \int^{z_r} k\,dz\right\}$$

We note that the branch point should be encircled counter-clockwise to obtain the right phase in agreement with the usual connection formula.

For a simple ionospheric layer, two reflection points are formed, one on each side of the layer maximum. Consequently, an infinite number of phase integrals and reflection coefficients may be defined due to the possibility of multiple reflections between the two reflection points [5]. It is justified to talk of different reflected components, for in regard to pulse transmissions these components can be, at least theoretically, separated in time. In *praxis*, we will find all but the first component suppressed by absorption.

MAGNETO-IONIC MEDIUM

The basic wave equations for the magneto-ionic medium are

$$\partial^2\pi^o/\partial x^2 + (k^{o^2} + \psi^2)\pi^o = -j\pi^x\partial\psi/\partial x - j2\psi\partial\pi^x/\partial x$$

$$\partial^2\pi^x/\partial x^2 + (k^{x^2} + \psi^2)\pi^x = j\pi^o\partial\psi/\partial x + j2\psi\partial\pi^o/\partial x$$

The indices o and x for π and k refer to the ordinary and extraordinary types of propagation. The coupling term ψ is defined by

$$\psi = \frac{1}{1 - P^2}\frac{\partial P}{\partial x}$$

where P is the polarization vector of the wave. The same type of W.K.B. approximation as before may be used provided several conditions are satisfied. Of course, again a path has to be found where the medium is slowly varying or $| k' | \ll | k^2 |$. Additionally, the coupling term has to be small or $| \psi^2 | \ll | k^2 |$, and the right side of the equation is allowed to have only a negligible effect. With respect to that, it is hard to make a guess unless the solution is already known. Anyhow, if π^o and π^x are of the same order of magnitude, it is estimated that the right side can be neglected, provided the coupling term is small and provided $| \psi | \ll | k^o - k^x |$. The latter condition is necessary to exclude a path outside of the ionosphere. Here the medium is isotropic and homogeneous, and a formal distinction between ordinary and extraordinary component could be made only on the basis of sufficient coupling [6].

Four types of waves have to be taken into account in a magneto-ionic medium, as follows: The ordinary and the extraordinary upgoing types and the two downcoming types. Correspondingly, the propagation constant k can be represented on a Riemann surface with four sheets in accordance with the four solutions of the Appleton-Hartree formula. Branch points connecting upgoing and downcoming waves (reflection points) are defined by $k(z) = 0$ or by $k(z) = \infty$. Branch points connecting ordinary and extraordinary waves (coupling points) are defined by $k_o = k_x$. The polarization vector at these points is ± 1, and consequently the coupling term ψ goes to infinity at the coupling point. It is clear that a good path for the phase integral in the four sheet Riemann surface has to avoid the neighborhood of any of the branch points. However, if the existence of any good path can be taken for granted, it is convenient for computations to use a path right over the branch points.

It is instructive to locate the branch points and the cut lines in the Riemann surface. Figure 1 shows an example of the situation for a Chapman-type layer with

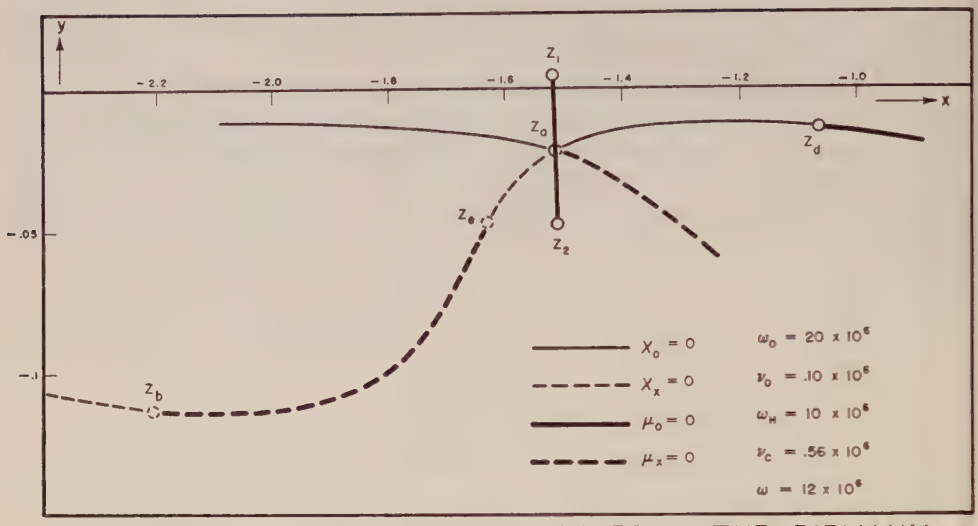

FIG. 1—BRANCH POINTS AND CUT LINES IN THE RIEMANN SURFACE

exponentially decreasing collision frequency. We distinguish "ordinary" and "extraordinary" sheets defined by a positive or negative imaginary part of the polarization vector ($P = r + js$), respectively. The two sheets are connected crosswise along a line of linear polarization which ends at the two coupling points z_1 and z_2 given by $1 - \omega_N^2/\omega^2 - j\nu/\omega = \pm j\nu_c/\omega$. This line and each of the two coupling points exist twice, that is, in the "upgoing" and "downgoing" sheets.

"Upgoing" and "downgoing" sheets of each polarization are connected along lines where the real part of the refractive index $(\mu + j\chi) =$ zero. These lines end at reflection points or at infinity.

Reflection point z_a is determined by $1 - \omega_N^2/\omega^2 - j\nu/\omega = 0$. It is the normal reflection point of the ordinary wave. It is situated on the cut line between the two coupling points on that part of the Riemann surface which connects the upper (ordinary) sheet at low plasma frequencies with the lower (extraordinary) sheet at high plasma frequencies. Waves of either type of polarization can be reflected at that level. Reflection point z_b is determined by $1 - \omega_N^2/\omega^2 - j\nu/\omega = +\omega_H/\omega$. It is the normal reflection point of the extraordinary wave. It is situated in the lower sheet and cannot exist at frequencies below the gyrofrequency. A third reflection point z_d is determined by $1 - \omega_N^2/\omega^2 - j\nu/\omega = -\omega_H/\omega$ and belongs in the upper sheet. While the refractive index is zero at these reflection points, it is infinite at the fourth reflection point z_e given by

$$\frac{\omega_N^2}{\omega^2} = \frac{\omega_H^2(1 - j\nu/\omega) - \omega^2(1 - j\nu/\omega)^3}{\omega_L^2 - \omega^2(1 - j\nu/\omega)^2}$$

This point is situated in the lower sheet. It disappears together with z_b as ω approaches the gyrofrequency. However, for frequencies below ω_L (the longitudinal component of the gyrofrequency), it is present again and terminates the cut line starting from z_a.

For that part of the ionosphere where the plasma frequency increases with the x axis, all the reflection points and the coupling point z_2 are below the real axis. The coupling point z_1 is above the real axis only if ν_c , the critical collision frequency, is larger than ν_a , the collision frequency at the a level.

A suitable path for the phase integral has to start on the left-hand side of the real axis, to go around at least one reflection point, and to come back taking care of the cut line between the coupling points. A number of different phase integrals is possible corresponding to a number of magneto-ionic components. In fact, if multiple reflections between the branch points are considered, this number is infinite.

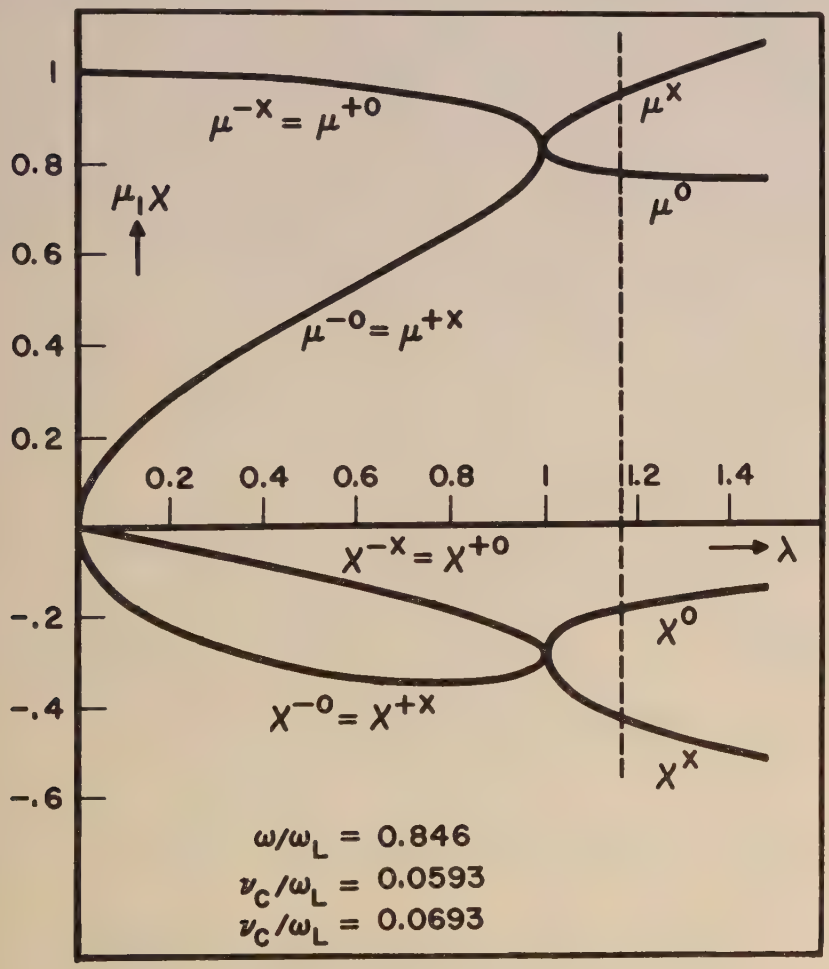

FIG. 2—REFRACTIVE INDEX ALONG THE CUT LINE OF LINEAR POLARIZATION AND THE CONTINUING LINE OF CIRCULAR POLARIZATION (LEFT- AND RIGHT-HAND SIDES OF THE CUT ARE CHARACTERIZED BY THE MINUS AND PLUS SIGN, RESPECTIVELY)

Instead of using the conventional *o* and *x* component only, a second letter (*a*, *b*, *d*, or *e*) may be used to indicate the reflection point considered. Thus, in this terminology, the *z* component may be called *odo* component, while the normal *o* component would be the *oao* component. The components are called fundamental if the integration path encircles one reflection point only and if it ends with the same polarization as it started. A formal application of the phase integral method leads to eight fundamental components. However, as numerical computation would show, the *obo* and *oeo* components violate the condition upon which the approximation is based and the *xex* component is always highly absorbed. The remaining five fundamental components are indicated shortly by *oa*, *od*, *xb*, *xa*, and *xd*. Of major importance are also the *xao*, *oax*, *xdo*, and *odx* components.

NUMERICAL COMPUTATION

The numerical computation of the phase integrals is only slightly more complicated by extending them into the complex plane. In almost all cases of practical interest, the branch points are not far off from the real axis. The integration is carried out along the real axis up to the points $x = a$, b, or d, defined by $1 = \omega_N^2(x)\ \omega^2 = 0$ $= +\omega_H/\omega$ or $= -\omega_H/\omega$. The point $x = a$ is in one line with z_a and with z_1. Introducing a new real variable λ, this line is defined by

$$1 - \frac{\omega_N^2(z)}{\omega^2} - j\frac{\nu(z)}{\omega} = -j\lambda\frac{\nu_c}{\omega}$$

At the reflection point $\lambda = 0$, at the coupling point $\lambda = 1$, and at point a $\lambda = \nu_a$ ν (Fig. 2).

The Appleton-Hartree formula will be reduced to

$$\mu^2 = \frac{1 \pm \sqrt{1-\lambda^2} + \lambda^2\nu_c/\omega_L}{1 \pm \sqrt{1-\lambda^2} + \lambda(j + \nu(z)/\omega)\omega/\omega_L}$$

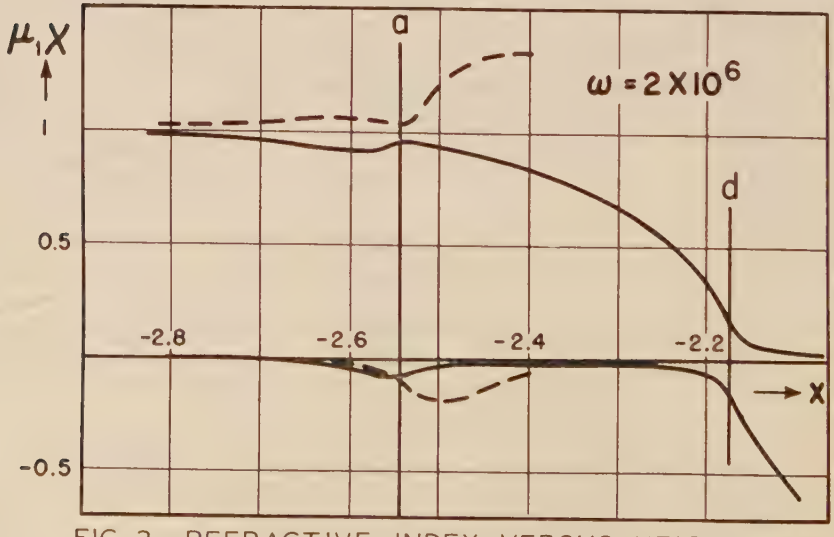

FIG. 3—REFRACTIVE INDEX VERSUS HEIGHT FOR QUASI-LONGITUDINAL PROPAGATION

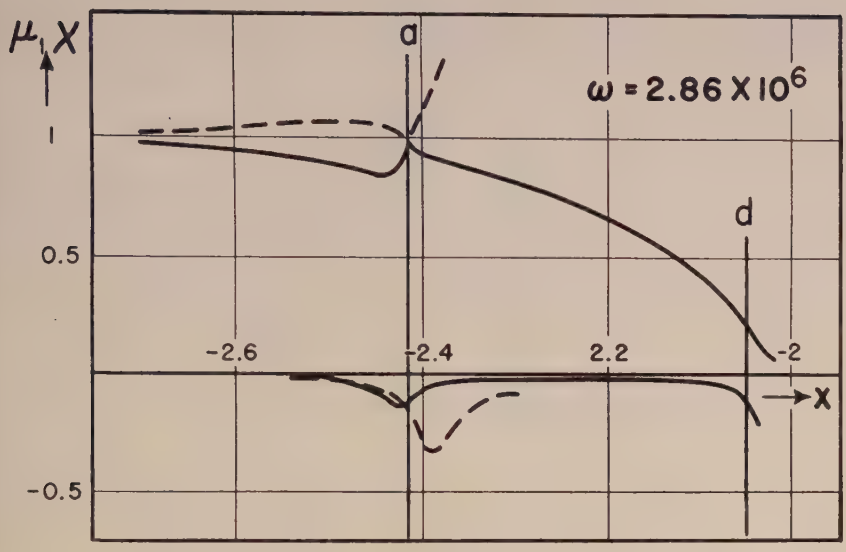

FIG. 4—REFRACTIVE INDEX VERSUS HEIGHT WITH THE COUPLING POINT ON THE REAL AXIS

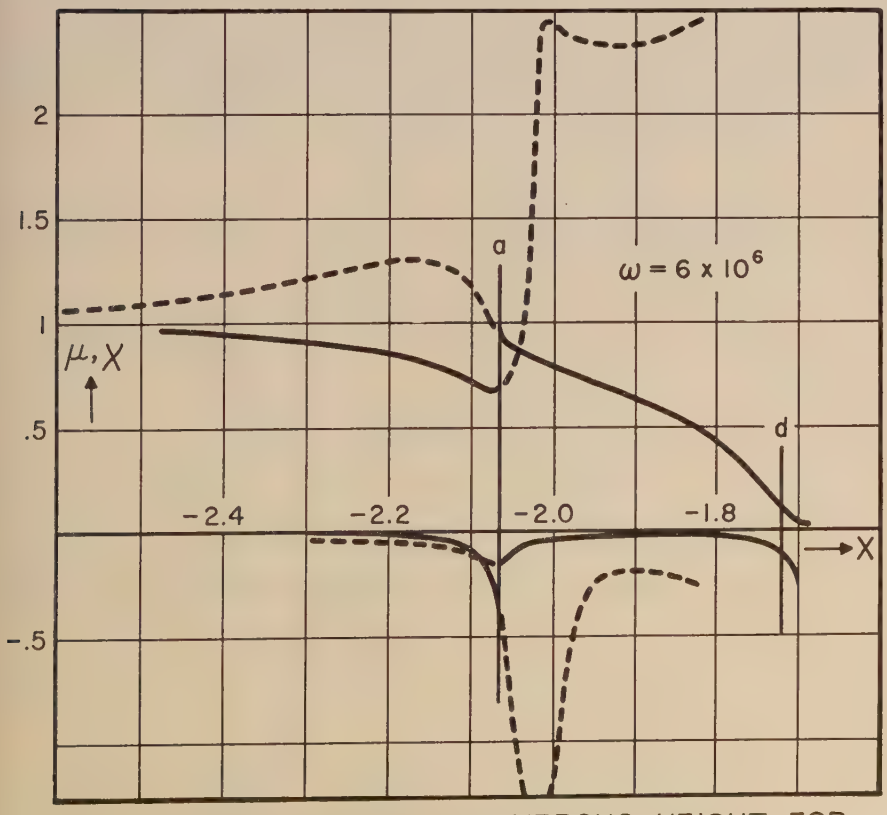

FIG. 5—REFRACTIVE INDEX VERSUS HEIGHT FOR QUASI-TRANSVERSE PROPAGATION

Since the branch points are close to the x axis, $\nu(z)$ can safely be replaced by ν_a, the value of ν at the point $x = a$. Furthermore, dz may be expressed by $d\lambda$ using

$$d\lambda = \frac{\omega}{\nu_c}\left[-j\frac{\partial\omega_N^2}{\omega^2\partial x} + \frac{\partial\nu}{\omega\partial x}\right]dz$$

where the derivatives of ω_N^2 and ν can be taken at point $x = a$. Thus, it is really no problem to compute the phase integrals from a to z_a or to z_1 by numerical or graphical methods. No manipulation with complex values of ω_N^2 or ν is necessary. It is sufficient to know ω_N^2 and ν, and functions of x and their first derivatives. An analog method may be used for the phase integrals from b to z_b and from d to z_d.

An example of the phase integral method as outlined above has been worked out in computing a theoretical sweep frequency picture for a given *model of the ionosphere*. The model chosen is an ideal Chapman-type layer with exponentially decreasing collision frequency, as follows: $\omega_o = 20 \times 10^6$ rad/sec, $\nu_o = 0.05 \times 10^6$ sec, $\omega_H = 10 \times 10^6$ rad/sec, and $\nu_c = 0.56 \times 10^6$/sec, corresponding to a magnetic dip angle of 19°. A series of Figures shows the behavior of the refractive index along the real height. The curves with positive ordinates represent the real part of the refractive index. Full lines belong in the ordinary sheet, broken lines in the extraordinary sheet. The lowest frequency $\omega = 2$ Megaradians per second (Fig. 3) shows curves characteristic for quasi-longitudinal propagation. Although the reflection level at a shows up slightly, the curves are fairly smooth up to the marked reflection level at d. At 2.86 Megaradians (Fig. 4), the coupling point happens to fall on the real axis. The connection between the two polarizations is apparent. At higher fre-

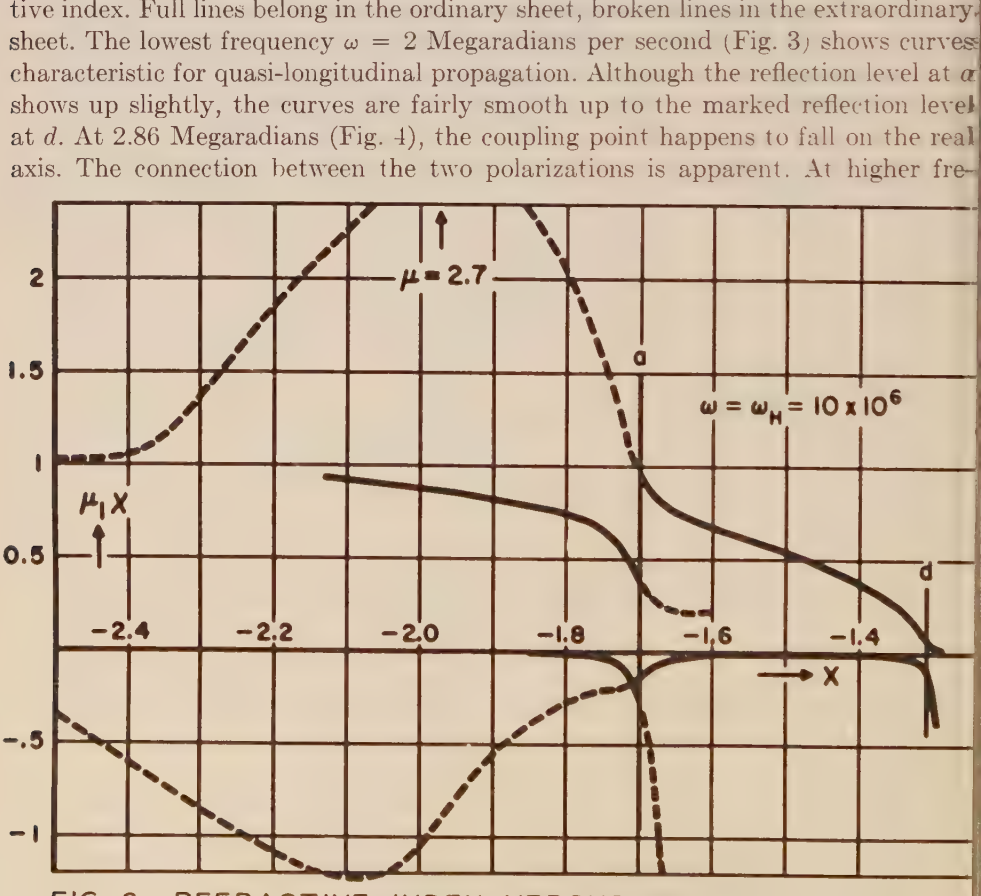

FIG. 6—REFRACTIVE INDEX VERSUS HEIGHT AT THE GYROFREQUENCY

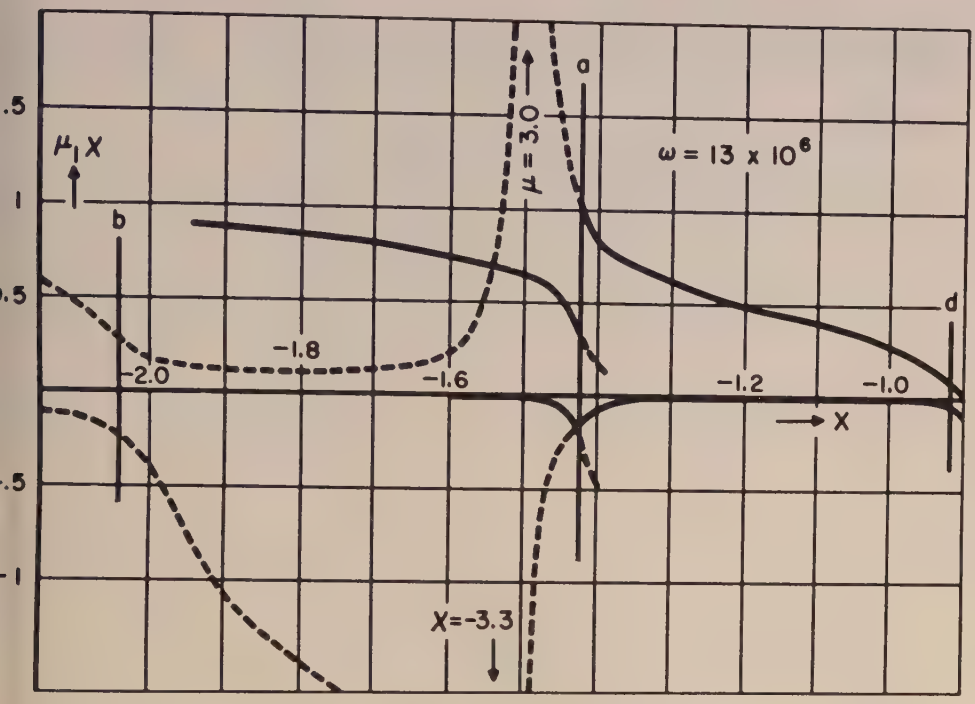

FIG. 7—REFRACTIVE INDEX VERSUS HEIGHT FOR A FREQUENCY ABOVE THE GYROFREQUENCY

quencies (Fig. 5), the curves pass through the cut line, where they change the polarization. The two ordinary branches could be linked together by a short path in the complex plane. This Figure is also a good example for the influence of the fourth reflection point shortly above the *a* level which shows up in the peak of the μ and χ curves. For frequencies above the gyrofrequency (Fig. 7), the *b* reflection level comes into action. Any extraordinary component going up to the *a* or *d* levels would be highly absorbed.

The final result is plotted on two graphs showing the absorption (Fig. 8) and the group height (Fig. 9) for five different magneto-ionic components. The scale of the absorption $ln\rho$ is based on an atmospheric scale height of 10 km. Two ordinary components (*oa* and *od*) are plotted. They are known as the quasi-transversal and the quasi-longitudinal or *z* component. They differ in height over the entire frequency range, and vary in relative amplitude from a predominant *od* component at low frequencies to a predominant *oa* component at high frequencies. The frequency of equal amplitude happens to be higher than $\omega = 2.86$ Mc/sec, the frequency where the coupling point passes the real axis. Both components are expected to appear as split echoes around $\omega = 5$ Mc/sec. It may reasonably be concluded that the *z* component is not restricted to high latitudes, that it represents the normal type of propagation at low frequencies, and that the transition from the quasi-transversal to the quasi-longitudinal type of propagation occurs in form of split echoes. The frequency range of this transition depends entirely on the proper ionospheric model and on the magnetic latitude. Split echoes observed at moderate

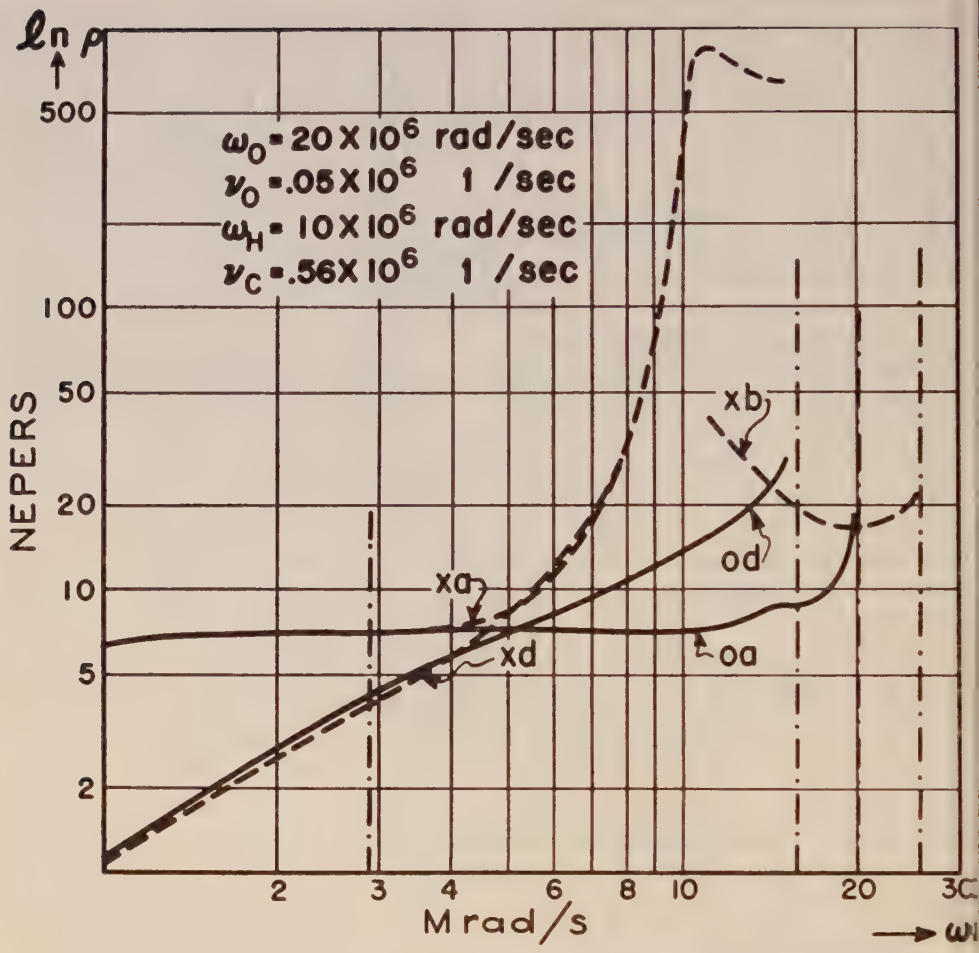

FIG. 8—SWEEP FREQUENCY PICTURE OF ABSORPTION FOR VARIOUS MAGNETO-IONIC COMPONENTS

latitudes in the frequency range from 100 to 400 kc/sec are very likely due to that transition. Even a greater number of equally spaced traces is expected, caused by multiple reflections between the *a* and *d* levels. Their polarization would be ordinary. But, according to the graph, also weaker extraordinary traces *xa* and *xd* are expected in that frequency range. Not shown in the graph are the *xao* and *oax* traces. They would appear between the *oa* and *xa* traces and, since they are not separated, would combine to a mixed polarization. The situation is similar for the *xdo* and *odx* traces. It is interesting to note that in the lowest frequency range the ordinary and extraordinary traces join each other in a single trace. This is reasonable, insofar as the effect of the magnetic field should disappear when the reflection occurs at a level of high enough collisions. The graph shows high absorption of all extraordinary traces around the gyrofrequency. As already mentioned, the conditions of the simple phase integral method are not given in that case, and therefore

he group height traces of *xa* and *xd* have been omitted in the graph around the yrofrequency.

FINAL REMARKS

It should be kept in mind that the phase integral method as outlined above is n approximation based on the existence of a "good" path around the branch points. n the numerical example shown, the quality of the different paths has not been ully examined. This should be done especially in the lower frequency range. More erious is the fact that a merely formal application of the method can lead to entirely vrong results in spite of an apparently good path. It is believed that certain paths re "forbidden" like the clockwise going path in the isotropic case mentioned above. A more rigorous mathematical proof for the applicability of the method is certainly eeded.

Nevertheless, the method is much more powerful than ray theory and is cer-

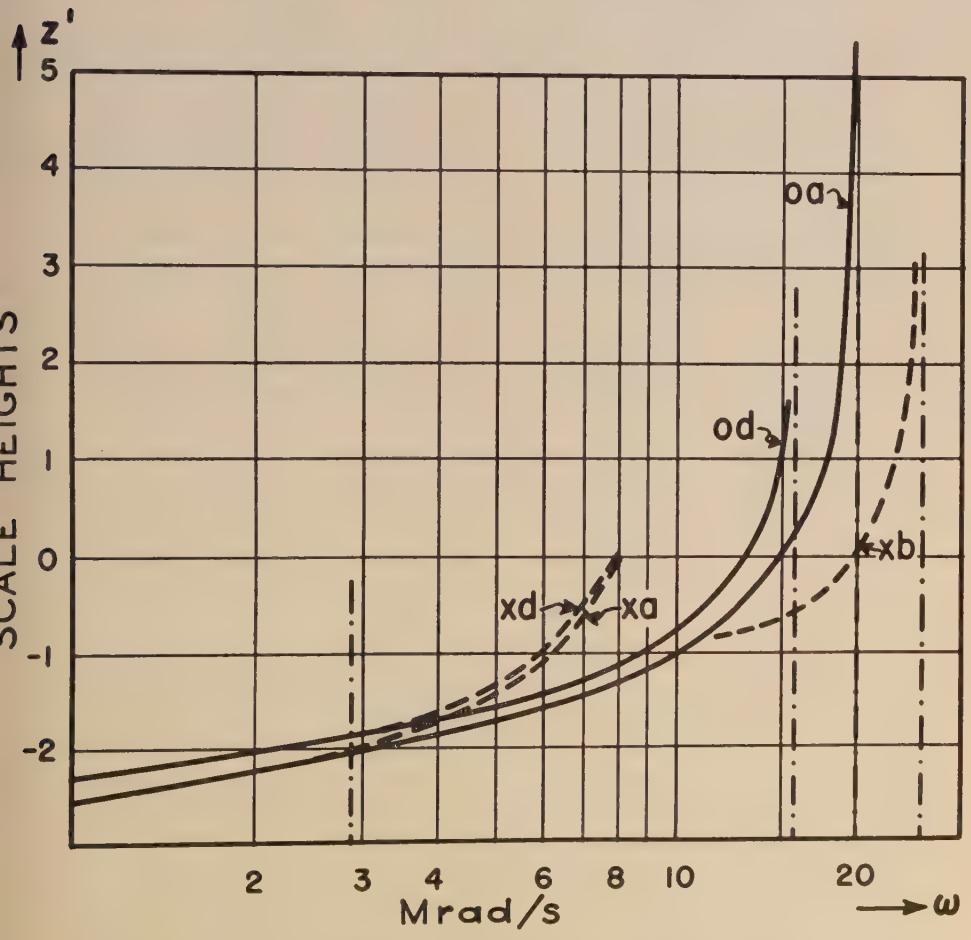

FIG. 9—SWEEP FREQUENCY PICTURE OF GROUP HEIGHT FOR VARIOUS MAGNETO-IONIC COMPONENTS

tainly very useful in a wide range of the lower frequencies. The method does nc need to be restricted to vertical incidence. It would work just as well for obliqu incidence by representing Booker's q term on a sheet Riemann surface.

References

[1] H. G. Booker, Oblique propagation of electromagnetic waves in a slowly-varying non isotropic medium, Proc. R. Soc., A, **155**, 235-257 (1936).

[2] T. L. Eckersley, Coupling of the ordinary and extraordinary rays in the ionosphere, Proc Phys. Soc., B, **63**, 49-58 (1950).

[3] O. E. H. Rydbeck, The theory of magneto-ionic triple splitting, Trans. Chalmers Univ No. **101**, 1-38 (1951); and Com. Pure and Appl. Math., **4**, 129-160 (1951).

[4] W. H. Furry, Two notes on phase integral methods, Phys. Rev., **71**, 360-371 (1947).

[5] O. E. H. Rydbeck, On the propagation of waves in an inhomogeneous medium, Trans Chalmers Univ., No. 74, 1-33 (1948).

[6] K. G. Budden, The theory of the limiting polarization of radio waves reflected from th ionosphere, Proc. R. Soc., A, **215**, 215-233 (1952).

ON THE COMPARATIVE INCREASES OF THE $F1$ AND $F2$ IONIZATIONS FROM SUNSPOT MINIMUM TO SUNSPOT MAXIMUM

By (Miss) Mrinmayee Ghosh

Institute of Radio Physics and Electronics,
University of Calcutta, Calcutta 9, India

(Received August 11, 1952)

ABSTRACT

Ionospheric records show that between the epochs of sunspot minimum and sunspot maximum the ionization of the $F2$ region increases by a much larger factor than the ionizations of the E and $F1$ regions (by a factor of about 3 for $F2$ maximum and a factor of about 1.6 for the $F1$ maximum). This anomaly can be explained on a proper consideration of the current hypothesis of the formation of the composite F region. According to this hypothesis, there is only one ionizing radiation (ionizing atomic oxygen) for the composite F region. $F1$ is formed, at a height where the rate of ion production is maximum, by the usual Chapman process, and another bank of ionization with greater ionization density appears at a greater height, as a result of rising temperature and falling (effective) recombination coefficient above $F1$ maximum. In the present paper, the ionization distribution of the composite F region with height is calculated with the help of the formulae derived recently by A. P. Mitra in a paper in which this hypothesis has been discussed. It is found that a comparatively small increase in $F1$ ionization (due to an increase in the ionizing radiation) leads to a much larger increase in the $F2$ ionization. The increase of $F2$ ionization from sunspot minimum to sunspot maximum, as calculated, is found to agree well with that as observed.

1. INTRODUCTION

The ionizations of the different ionospheric regions are known to vary not only with the hour of the day and the season of the year, but also with the phase of the unspot activity. Although there is no obvious short-term parallelism between the ariations of the observed ionization density and the sunspot number, yet a close ong-term parallelism has been found to exist between the 12-month running verages of the critical frequencies of the different ionospheric regions and 12-month unning averages of the sunspot numbers. In fact, the former varies in an approximately linear fashion with the latter [see 1 and 2 of "References" at end of paper], hough, as has been pointed out by Phillips [2], the existence of such relations seems urprising in view of the arbitrary manner in which sunspot number is defined. It s, however, natural to expect that there should be some functional relation between he averages of the relative sunspot numbers and those of the critical frequencies,

because it has been found that the intensity of the solar ultraviolet radiation near the wave-length 3200 Å, close to the edge of the ozone absorption limit, varies with the 11-year sunspot cycle [3]. Hence, one may suppose that the intensities of the solar ultraviolet radiations as cause ionizations of the different ionospheric layers, also vary with the sunspot number.

A rather remarkable feature of the variation of the ionization with the sunspot cycle is that the proportionate increase of ionization, from the epoch of sunspot minimum to that of sunspot maximum, is not the same for the different ionospheric regions. An inspection of Table 1 shows that, while the average proportionate increase of ionization of the $F1$ region is about 1.6 times, that of the $F2$ region is about 3.0 times.

Table 1

Location	Latitude	Ratios of maximum ionization densities at sunspot maximum and sunspot minimum		Mean ratio for $F1$	Mean ratio for $F2$
		$F1$	$F2$		
	°				
Slough	51.5N	1.70	3.21		
Washington	39 N	1.45	3.00		
Huancayo	12 S	1.34	2.65	1.62	2.91
Brisbane	28 S	1.96	2.72		
Watheroo	64 S	1.65	2.95		

One way of explaining this higher increase is to suppose that the ionizing radiation which produces the $F2$ region is of different solar origin (coronal, instead of photospheric or chromospheric [4]), and that its intensity increases by a much larger factor from sunspot minimum to sunspot maximum than the intensities of the (photospheric or chromospheric) radiations which produce the lower E and the $F1$ regions. This, though not improbable, seems rather unlikely. There is, however, a way out of this difficulty if one considers the current theory regarding the origin of the $F2$ region.

According to current ideas, there is only one ionizing radiation for the composite F region [5,6]. This is $\lambda < 910$ Å which ionizes atomic oxygen. This radiation produces, according to the Chapman process, only one ionization maximum, namely, that of the $F1$. However, as there is a rising temperature above the $F1$ maximum, the ionization extends to great heights. Further, in the higher regions the recombination coefficient (effective) decreases rapidly with height, as a result of which the dip in ionization with increasing height above the $F1$ maximum is checked beyond a certain height, and there is again a rise in ionization density. This bank of increasing ionization is called the $F2$ region. This view has recently been closely examined by A. P. Mitra [7]. By making reasonable assumptions regarding the rates of decrease in (effective) recombination coefficient and of in

crease in temperature with height, he has obtained, for the composite $F1$-$F2$ region, curves of the height variation of ionization, the shapes of which resemble closely the shapes as deduced from ionospheric sounding.

In the present paper, the analysis of A. P. Mitra will be utilised to show that a comparatively small rise in the $F1$ ionization, from the epoch of sunspot minimum to that of the sunspot maximum (as observed), results in a much larger increase in the ionization of the $F2$ region between the same epochs. The calculated comparative increase is found to agree well with the mean observed increase.

2. CALCULATION OF THE HEIGHT DISTRIBUTION OF $F2$ IONIZATION—SUNSPOT MINIMUM AND SUNSPOT MAXIMUM

The method of estimating the height distribution of $F2$ ionization for the epochs of sunspot minimum and sunspot maximum, starting with the observed midday mean value of $F1$ ionization (N_0), is as follows:

First, from the equilibrium relation

$$\frac{dN_0}{dt} = q - \alpha N_0^2 = 0 \quad \ldots\ldots\ldots\ldots\ldots\ldots\ldots\ldots (1)$$

the midday rate of ion production, $q/\text{sec}\cdot\text{cm}^3$, in the region of $F1$ maximum is calculated from the known value of the recombination coefficient α in this region.

Next, the number of ionizing solar quanta, Q, reaching the $F1$ maximum level per cm^2 per sec is calculated from the relation

$$q = An_0Q \ldots\ldots\ldots\ldots\ldots\ldots\ldots\ldots\ldots\ldots (2)$$

where A is the absorption cross-section of the active constituent (oxygen atom) and n_0 is the concentration of the same at the $F1$ maximum level.

The number of ionizing solar quanta Q_0 reaching the top of the atmosphere, corresponding to the value of Q at the $F1_{max}$ level, is now calculated. For this purpose, reasonable assumptions, based on observational data, are made regarding the gradient of the rising scale height (H). The expression for Q(for vertical incidence) is now obtained from the Chapman expression (for constant H), suitably modified to take account of a rising H. Q is related to Q_0 by

$$Q = Q_0 \exp\left[-n_0AH_0\left(1 + \frac{a}{H_0}\cdot h\right)^{-1/a}\right] \quad \ldots\ldots\ldots\ldots\ldots (3)$$

where a is the gradient of the scale height and H_0 is the scale height at $F1$ maximum.

The height distribution of ionization, above the $F1$ maximum level is now calculated. For this purpose, the analysis of A. P. Mitra [7], in which account is taken of the effect, not only of a rising H, but also that of a decreasing α with height, is utilised. N, at a height h above $F1_{max}$, is given by

$$N^2 = \frac{An_0Q_0\left(1 + \frac{a}{H_0}\cdot h\right)^{-(1+1/a)} \exp\left[-n_0AH_0\left(1 + \frac{a}{H_0}\cdot h\right)^{-1/a}\right]}{\alpha} \ldots\ldots (4)$$

where α is, in general, a function of T, N, and particle concentration n, and varies with the height h [8].

An important correction, however, has to be introduced in order that the expression may yield acceptable results. In deducing the expression, it had been assumed at the start that, at midday, equilibrium condition exists; that is, $dN/dt = 0$. This, however, is not correct. In the attenuated $F2$ region, where the value of α is low, equilibrium condition is not attained even in the noon time. Hence the calculated height distribution of N from equation (4) tends to rise monotonously without showing any definite $F2$ maximum. If, however, a correction factor to take account of the fact that $dN/dt \neq 0$ is introduced, a definite maximum is obtained, both for the sunspot minimum and for the sunspot maximum condition.

For numerical calculations, we start with the observed data of $F1_{max}$ ionization density (electron concentration) during epochs of sunspot minimum and sunspot maximum. The mean values as adopted from the recorded ionospheric data are as follows:

Sunspot minimum	$2.5 \times 10^5/cm^3$
Sunspot maximum	$4.0 \times 10^5/cm^3$

For the recombination coefficient α at $F1_{max}$ level, we adopt the value 4.0×10^{-4} cm^3/sec, as the mean deduced from $F1$ region observations [9]. For the absorption cross-section (A) of the active gas oxygen, we take the value 4.5×10^{-18} cm^2 [10].

Besides these, we require the upper atmospheric data of temperature and pressure at the level of $F1_{max}$ and the temperature gradient above the same. For this we shall use three different representative sets of values taken from the data on the "model" ionosphere or atmosphere as conceived by three different authors, namely, [*i*] Ken-ichi Maeda [11], [*ii*] Bates and Massey [8,12], [*iii*] Gerson [13].

We give below the various steps of the calculation for one of the representative sets of values, namely, that of Ken-ichi Maeda.

(*i*) *Calculations with the data for the model ionosphere of Ken-ichi Maeda* [11]:

Active gas (atomic oxygen) concentration at the $F1_{max}$ level	4×10^{10} cm^3
Height of $F1_{max}$	200 km
Height of $F2_{max}$	250-300 km
Temperature, T_0, at $F1_{max}$	800°K
Height gradient of temperature above $F1_{max}$	4°/km

These data are assumed to correspond to the epoch of sunspot minimum. They are also (except the temperature gradient) assumed to remain unaltered for the epoch of sunspot maximum. dT/dh for sunspot maximum is taken to be 5°/km.

From the equilibrium relation in equation (1) and from the $F1_{max}$ ionization value given earlier, we obtain for the rates of ion production at the $F1_{max}$ level

For sunspot minimum	$250/cm^3 \cdot sec$
For sunspot maximum	$640/cm^3 \cdot sec$

Using these values of q in equation (2), we readily obtain the value of Q, the number of quanta of the ionizing radiation reaching the $F1_{max}$ level per cm^2 per sec.

Q, for sunspot minimum	$1.39 \times 10^9/cm^2 \cdot sec$
Q, for sunspot maximum	$3.55 \times 10^9/cm^2 \cdot sec$

Q_0 , the number of quanta of the ionizing radiation incident (normally) on the top of the atmosphere per cm^2 per sec, is now calculated with the help of equation (3).

Q_0 , for sunspot minimum . . . . $2.38 \times 10^9/cm^2 \cdot sec$
Q_0 , for sunspot maximum . . . . $6.09 \times 10^9/cm^2 \cdot sec$

[It may be noted that for a "black" sun, the number of quanta available for the ionization of the $F1$ region ($\lambda < 910$ Å) is $9.3 \times 10^8/cm^2 \cdot sec$ only.]

The height distribution of ionization density above $F1_{max}$ is now calculated with the help of equation (4). The term, the value of which is most uncertain in this equation, is α, the effective recombination coefficient. It always varies with the temperature and, also, especially when the pressure is low (as in the $F2$ region), with the pressure and with electron concentration [8]. Two expressions for α have been suggested by the previous workers for the two regions $F1$ and $F2$ based on the general expression for the rate of decay of electrons, and we shall utilise these expressions in our numerical calculations.

For the $F1$ region, α varies only with the temperature and we write [7]

$$\alpha = \alpha_0\left(1 + \frac{a}{H_0} \cdot h\right)^{-1} \quad \ldots\ldots\ldots\ldots\ldots\ldots\ldots\ldots (5)$$

For the $F2$ region, the dependence of α on N and T is given, after A. P. Mitra [7] by

$$\alpha = \frac{\eta n}{TN} \quad \ldots\ldots\ldots\ldots\ldots\ldots\ldots\ldots\ldots\ldots (6)$$

where $\eta = 1.5 \times 10^{-11}$ degree cm^3/sec.

Calculation with equation (5) shows that for small heights above $F1$ maximum up to about 30 km—heights which may be regarded as lying within the $F1$ region proper—α changes very little with height. No serious error is therefore committed if, for calculating the $F1$ ionization, α is taken as constant.

For calculating $F2$ ionization (beyond 30 km, above $F1$ region proper), we substitute the expression for α from equation (6) into equation (4), which now becomes

$$N = \frac{AQ_0T \exp\left[-n_0AH_0\left(1 + \frac{a}{H_0} \cdot h\right)^{-1/a}\right]}{\eta} \quad \ldots\ldots\ldots\ldots\ldots (7)$$

The results of calculation of the variation of ionization density N with height, for the composite $F1$-$F2$ region, are shown in curves (*a*) and (*b*) of Figure 1, for the epochs of sunspot minimum and sunspot maximum, respectively. It will be noticed that, as already explained, the ionization in the $F2$ region, instead of passing through a maximum, tends to increase indefinitely with height. We now apply corrections to the calculated ionization values, after A. P. Mitra, to take account of the unjustified assumption that an equilibrium condition of ionization has been established in the $F2$ region.

We have now, unlike equation (1), $dN/dt = q - \alpha N^2$, *not* equal to zero. dN/dt is evidently a function of height, and, as shown by A. P. Mitra, it can be put approximately equal to lN, where l is a constant. Now, if account is taken of the

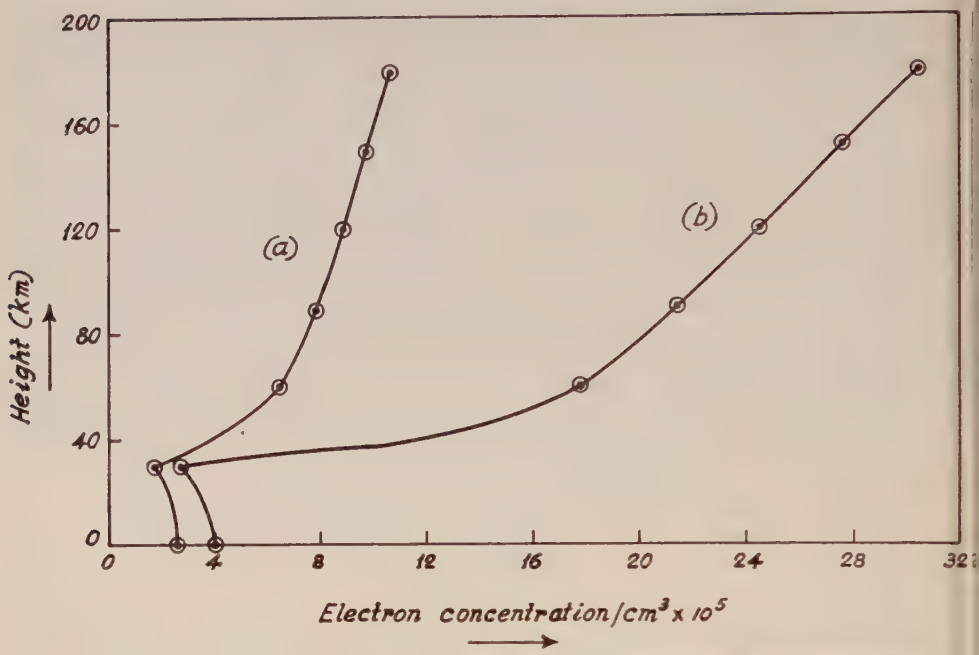

FIG. 1—ALTITUDE DISTRIBUTION OF ELECTRON CONCENTRATION IN THE F REGION: (a) FOR SUNSPOT MINIMUM, (b) FOR SUNSPOT MAXIMUM. IT IS ASSUMED THAT A STEADY STATE EXISTS IN THE F REGION ($dN/dt = 0$). THE VALUES OF PARTICLE CONCENTRATION AND TEMPERATURE AT, AND TEMPERATURE GRADIENT ABOVE, THE $F1_{MAX}$ LEVEL ARE TAKEN FROM KEN-ICHI MAEDA'S MODEL IONOSPHERE. HEIGHT IS MEASURED FROM $F1_{MAX}$ LEVEL.

variations of temperature and particle concentration with height according to equation (6), then the value of α for any height h is given by

$$\alpha = \frac{\eta n_0}{T_0 N}\left(1 + \frac{a}{H_0}\cdot h\right)^{-(2+1/a)} \qquad \ldots\ldots(8)$$

The actual ratio of N/N_0 is, thus, related to the steady state ratio $(N/N_0)_s$ by the relation

$$\frac{N}{N_0} = \frac{(N/N_0)_s}{1 + \frac{lT_0}{\eta n_0}(1+P)^{(2+1/a)}} \qquad \ldots\ldots(9)$$

where

$$P = \frac{\frac{a}{H_0}(h - h_0)}{1 + \frac{a}{H_0}\cdot h},$$

h_0 being the height of $F1_{max}$. The value of the quantity $lT_0/\eta n_0 = B$ (say) is of the order of 10^{-2} and is nearly a constant. A. P. Mitra has carried out calculations by

assuming different typical values (0.01 and 0.005) of B. For the case under consideration, we take B to be equal to 0.01 for the sunspot minimum and 0.005 for the sunspot maximum. Curves (*a*) and (*b*) in Figure 2 depict the corrected variations of ionization with height. It will be seen that there are now well-defined $F2$ maxima. Further, the $F2_{max}$ ionization density is found to have increased by a factor of 3.0 from sunspot minimum to sunspot maximum, whereas the $F1_{max}$ increase (as assumed at the start) is only 1.6 times. The increase in the $F2_{max}$ ionization is of the same order as observed.

(*ii*) *Calculations with data from the model ionosphere of Bates and Massey* [8,12]:

Particle concentration (total) at the $F1_{max}$ level.... $1 \times 10^{11}/cm^3$
Hence, concentration of the active gas (atomic oxygen) is taken to be..... $4 \times 10^{10}/cm^3$
Height of $F1_{max}$ ..... 220 km
Height of $F2_{max}$ ..... 300 km
T_0 at $F1_{max}$ ..... 1000°K
Height gradient of T ..... 12°/km

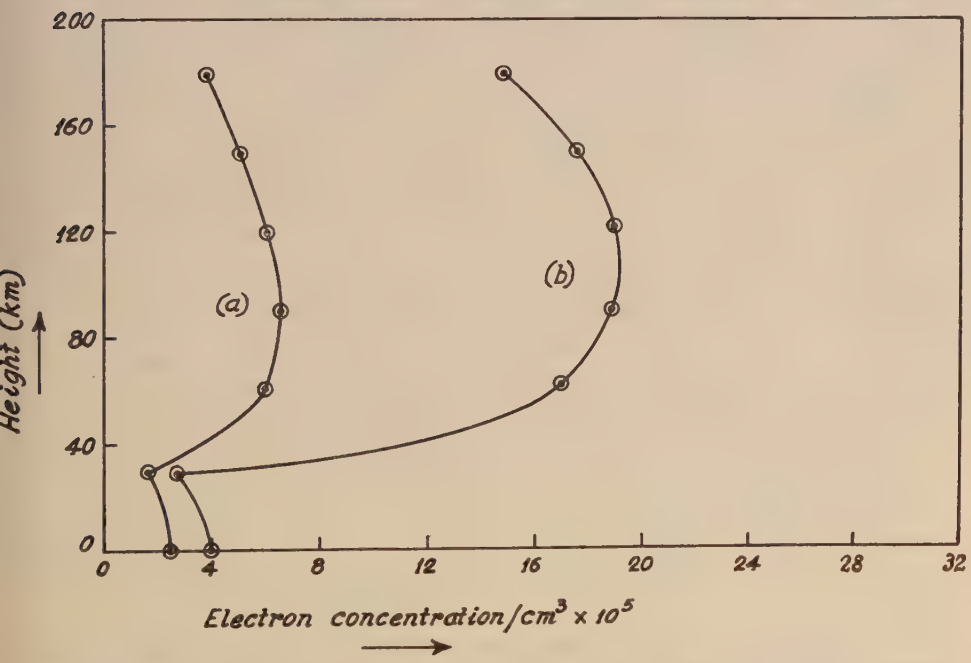

FIG. 2—ALTITUDE DISTRIBUTION OF ELECTRON CONCENTRATION IN THE F REGION: (a) FOR SUNSPOT MINIMUM, (b) FOR SUNSPOT MAXIMUM. THE CURVES ARE DRAWN FROM FIGURE 1 (a) AND (b), INTRODUCING CORRECTIONS TO TAKE ACCOUNT OF THE FACT THAT STEADY CONDITION IS NOT ATTAINED IN THE GREAT HEIGHTS OF THE F2 REGION. NOTE THAT WHILE F1 IONIZATION MAXIMUM HAS INCREASED BY A FACTOR OF 1.6, F2 MAXIMUM IONIZATION HAS INCREASED BY A FACTOR OF 3.0 FROM SUNSPOT MINIMUM TO SUNSPOT MAXIMUM.

All the above data, except for T_0, are assumed to remain unaltered from sunspot minimum to sunspot maximum. T_0 is assumed to increase to the value 1120°K during sunspot maximum.

The value of B in equation (9) for the corrections to be applied is taken as 0.01 for sunspot minimum and as 0.005 for sunspot maximum.

The ionization distribution curves, as obtained after the application of the corrections, are depicted in Figure 3(*a*) and (*b*) for sunspot minimum and sunspot maximum, respectively. It will be noticed the $F2_{max}$ ionization has increased by a factor 3.2 from minimum to maximum.

(*iii*) *Calculations with data from the model atmosphere of Gerson* [13]:

Particle concentration at $F1_{max}$ level (200 km) calculated from the data given for the 100-km level ..... $5.4 \times 10^{10}/cm^3$
T_0 at $F1_{max}$ ..... 1300°K
Height gradient of T ..... 10°/km

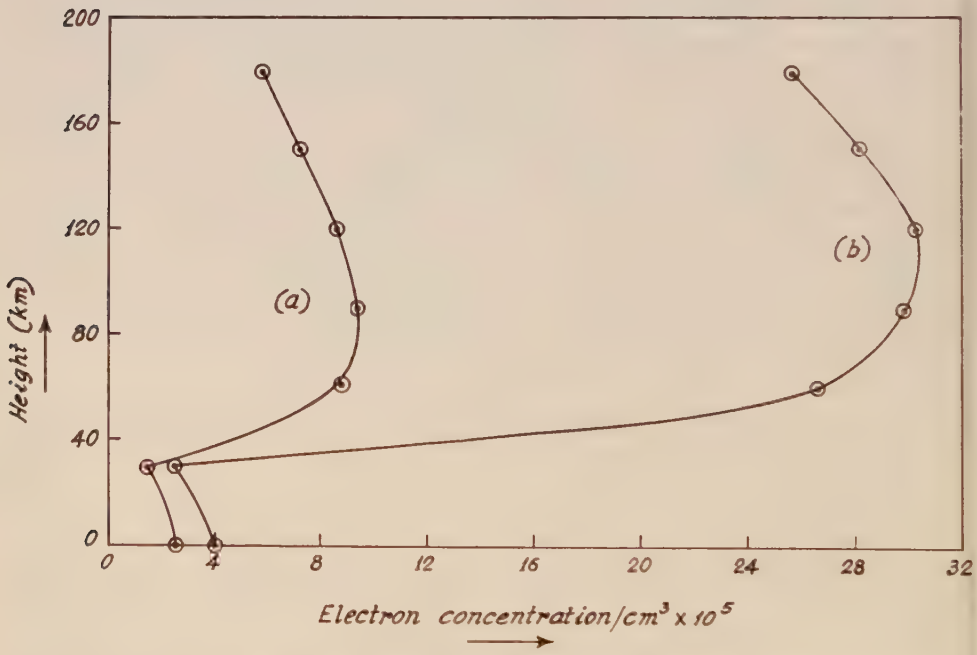

FIG. 3—ALTITUDE DISTRIBUTION OF ELECTRON CONCENTRATION IN THE F REGION: (a) FOR SUNSPOT MINIMUM, (b) FOR SUNSPOT MAXIMUM. CORRECTIONS FOR ($dN/dt \neq 0$) HAVE BEEN INTRODUCED. THE VALUES OF PARTICLE CONCENTRATION AND TEMPERATURE AT, AND THE TEMPERATURE GRADIENT ABOVE, $F1_{MAX}$ LEVEL ARE TAKEN FROM BATES AND MASSEY'S MODEL IONOSPHERE. $F2_{MAX}$ HAS INCREASED BY A FACTOR OF 3.2 FROM SUNSPOT MINIMUM TO SUNSPOT MAXIMUM. THE INCREASE OF $F1_{MAX}$ IS THE SAME AS IN FIGURE 2.

The particle concentration and the height gradient of temperature are assumed
) remain the same from sunspot minimum to sunspot maximum. T_0, however, is
ssumed to increase to the value 1400°K during sunspot maximum. The values of
in the correction expression of equation (9) are taken, as in the above cases, 0.01
nd 0.005 for sunspot minimum and sunspot maximum, respectively.

The corrected ionization distribution curves are shown in Figure 4 (*a*) and (*b*).
he $F2_{max}$ ionization has increased by a factor 3.1 from sunspot minimum to sunspot
aximum.

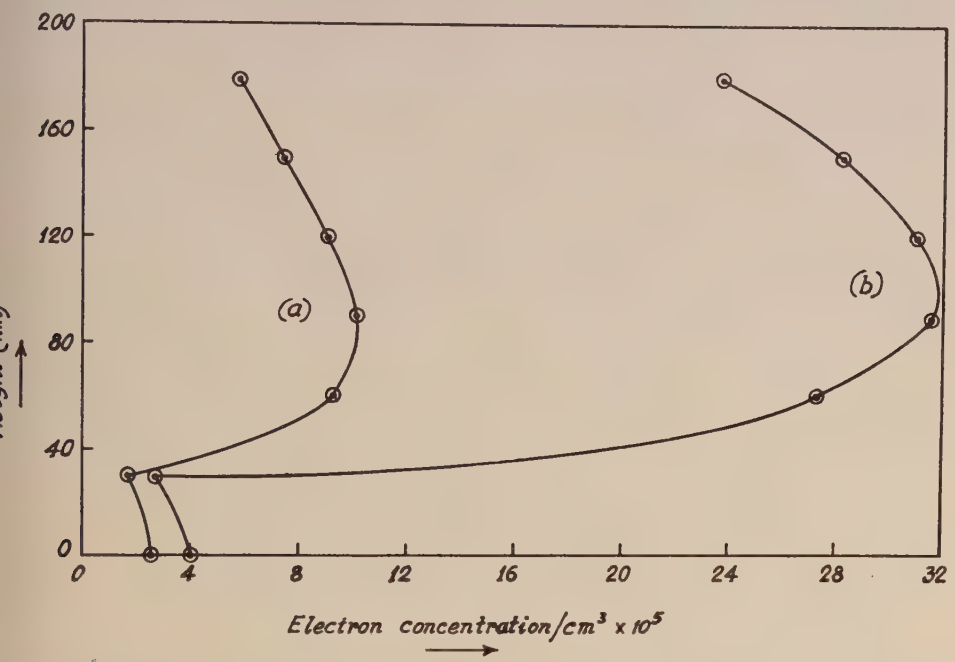

IG. 4—ALTITUDE DISTRIBUTION OF ELECTRON CONCENTRA-
ION IN THE F REGION: (a) FOR SUNSPOT MINIMUM, (b) FOR
UNSPOT MAXIMUM. CORRECTIONS FOR $(dN/dt \neq 0)$ HAVE
EEN INTRODUCED. THE VALUES OF PARTICLE CONCENTRA-
ION AND TEMPERATURE AT, AND THE TEMPERATURE GRA-
IENT ABOVE, $F1_{MAX}$ LEVEL ARE TAKEN FROM THE DATA
IVEN BY GERSON. $F2_{MAX}$ HAS INCREASED BY A FACTOR OF
.1 FROM SUNSPOT MINIMUM TO SUNSPOT MAXIMUM, CORRE-
PONDING TO AN INCREASE IN THE $F1_{MAX}$ AS IN FIGURES 2
AND 3.

3. DISCUSSION

A comparison of the curves in Figures 2, 3, and 4 shows that the effect of assum-
g higher temperatures at the $F1$ maximum level is to increase the ionization
ensity in the $F2$ region. However, the ratio between the $F2$ maximum ionizations
sunspot maxima and sunspot minima remains nearly the same, namely, about
times. Inspection of Table 1 shows that this calculated increase agrees well with
e observed increase.

The agreement might seem a little surprising and criticism might be made on the ground that this has been a result of the deliberate choice of the numerical values of the parameters involved. It may, however, be pointed out that, insofar as the $F1_{max}$ parameters during sunspot minimum are concerned, these have been taken from models as adopted by independent workers and thus avoid any personal bias. However, the increased values as assumed for dT/dh in case (*i*) and for T_0 in cases (*ii*) and (*iii*) during the epoch of sunspot maximum may be open to objection as having been arbitrarily chosen. But, it is to be remembered that both dT/dh and T_0 are expected to increase from sunspot minimum to sunspot maximum on account of the increased intensity of the ionizing radiation. Hence, the sense at least (that is, increase), in which the values have been modified is justified. Criticism of arbitrary choice may also be made in respect to the assumed values of B in the calculations of the corrections according to equation (9). But, as has been shown by A. P. Mitra, the possible values of B, for all reasonable values of the parameters involved, lie within these narrow limits. One may also object that the particle concentration at the $F1_{max}$ level has been assumed to remain the same from sunspot minimum to sunspot maximum, though the temperature is expected to increase. Trial calculations have been made by assuming that the particle concentration is altered (within reasonable limits) between sunspot minimum and sunspot maximum, but that the values of dT/dh, T_0 , and B remain the same. The calculations show that the main effect of such modification is to alter somewhat the height of the $F2$ maximum. The ratio of the $F2$ ionization densities (sunspot maximum and sunspot minimum) is also altered; but it remains substantially higher than the corresponding $F1$ ratio.

The results of calculations in the preceding section thus show that for explaining the larger increase in the $F2$ ionization, as compared to a much smaller increase in the $F1$ ionization, from the epoch of sunspot minimum to that of sunspot maximum, one need not invoke the aid of solar radiation from two different sources, one for $F1$ (photospheric or chromospheric) and another for $F2$ (coronal). Satisfactory explanation is provided on the basis of the current theory of the composite F region (produced by ionization of atomic oxygen) if account is taken of the effects of reasonable increase of temperature with height and decrease of the effective recombination coefficient with the same. The agreement of the calculated with the observed increase also shows that the method of calculation of the height distribution of ionization in the composite F region, as adopted by A. P. Mitra, is substantially correct.

ACKNOWLEDGMENT

The investigations described in the paper were carried out with the help of grants received from the Council of Scientific and Industrial Research, Government of India, and form part of the programme of the Radio Research Committee.

The author is indebted to Professor S. K. Mitra for constant guidance during the progress of the work.

References

[1] C. W. Allen, Terr. Mag., 51, 1 (1946).
[2] M. L. Phillips, Terr. Mag., 52, 321 (1947).
[3] E. Pettit, Astroph. J., 75, 185 (1932).

[4] R. v. d. R. Woolley, Mixed Commission on Ionosphere, U.R.S.I., Bruxelles, p. 85 (1949).
[5] F. L. Mohler, J. Res., Nation. Bur. Stand., **25**, 507 (1940).
[6] N. E. Bradbury, Terr. Mag., **43**, 55 (1938).
[7] A. P. Mitra, Indian J. Phys., **26**, 79 (1952).
[8] D. R. Bates and H. S. W. Massey, Proc. R. Soc., A, **187**, 261 (1946).
[9] S. K. Mitra, The upper atmosphere, The Royal Asiatic Society of Bengal, Calcutta, 2nd ed., p. 311 (1952).
[10] M. Nicolet, Mixed Commission on Ionosphere, U.R.S.I., Bruxelles, p. 44 (1949).
[11] K. Maeda, Mixed Commission on Ionosphere, U.R.S.I., Bruxelles, p. 217 (1950).
[12] D. R. Bates and H. S. W. Massey, Proc. R. Soc., A, **192**, 1 (1947).
[13] N. C. Gerson, Mixed Commission on Ionosphere, U.R.S.I., Bruxelles, p. 98 (1950).

RADIO MEASUREMENTS AND AURORAL ELECTRON DENSITIES

By P. A. Forsyth*

Physics Department, University of Saskatchewan, Saskatoon, Canada

(Received August 20, 1952)

ABSTRACT

Radar echoes from aurora have been recorded simultaneously at frequencies of 56 and 106.5 Mc/sec. The ratio of the echo amplitudes at the two frequencies varies between wide limits. An attempt is made to reconcile the experimental evidence with (*i*) partial reflections from the surfaces of large ionized regions in the aurora, (*ii*) scattering from inhomogeneities in the auroral ionization, and (*iii*) critical reflections from small volumes of intense ionization. It is concluded that (*iii*) is responsible for the typical auroral echoes which are observed at Saskatoon, although (*ii*) may be responsible for echoes of small amplitude which are often observed in the early stages of an auroral display. If these conclusions are correct, the occasional existence is indicated of electron densities of 10^8 per cm^3 in small volumes of the aurora.

I—INTRODUCTION

Radio reflections from aurora were first observed at high frequencies by Harang and Stoffregan in 1938 [see 1 of "References" at end of paper]. More recently, radio observations have been made at a number of frequencies between 30 and 150 Mc/sec [2,3,4,5,6,7]. Two different experimental methods have been used. In each case, the radio apparatus consists of one or more transmitters and receivers. In the first method, the transmitter is caused to emit radiation continuously (continuous wave method), whereas in the second short pulses of radiation are emitted (radar method). The continuous wave method requires the use of several stations in order to determine the location of the reflecting region. On the other hand, only one station is required for the radar method, since range is measured directly. In either case, it is necessary to supplement the radio data with photographic or visual observations in order to identify instances in which the reflections are associated with visible aurora. In the course of the experiment described below, radio reflections, arising apparently in the lower ionosphere, were detected in the absence of aurora; however, this paper is concerned only with radio reflections of the type which are known to be associated with visible aurora.

Starting in 1948, an extensive study of auroral radio reflections was undertaken at Saskatoon, Canada (52°.1 north, 106°.6 west). Up to the present time, a search

*The author is a member of the professional staff of the Radio Physics Laboratory, Defense Research Board, Ottawa, Canada. His services were made available to the University of Saskatchewan for the work described in this paper.

for echoes has been made at frequencies of 3,000, 106 and 56 Mc/sec. Reflections have not been observed at 3,000 Mc/sec, but are observed frequently at the two lower frequencies. The progress made in this investigation will be reported in a separate paper which is now in preparation. The purpose of the present paper is to discuss auroral echoes observed simultaneously at frequencies of 56 and 106 Mc/sec in order to throw some light on the reflection mechanism.

Three different processes have been suggested by which auroral echoes may arise, as follows: Partial reflection from relatively sharp boundaries of the ionized regions associated with auroral structures; scattering from inhomogeneities in the auroral ionization; and critical reflection. The first process is suggested by the physical appearance of aurora, but should lead to observable echoes only when the radio wave is incident normally upon an auroral surface. The second may be regarded as somewhat unlikely from the appearance of a fully-developed auroral display. The third process requires an unusually high degree of ionization in order to be effective at the frequencies under consideration.

The possibility that radar echoes from aurora are due to a partial reflection mechanism was first pointed out by Herlofson [8]. According to this suggestion, if the ionized region were large and the boundary sharp, the free electron density within the aurora need be no greater than that of the daytime E-region in order to produce the observed effects. The second suggested mechanism is an outgrowth of the theory of tropospheric scattering developed by Booker and Gordon [9]. This theory recently has been applied to scattering from irregularities in the normal ionosphere [10]. In the absence of detailed knowledge of the fine structure and extent of auroral ionization, it may be postulated that a similar scattering process operates in an auroral display. The third suggestion implies that the electron density, within at least part of the auroral display, is larger than the critical value for reflection of the wavelengths employed. This process is analogous to that responsible for reflection of radio waves from the ionosphere. The electron density required to reflect three-metre waves is greater than 10^8 electrons per cm^3, a value far in excess of that existing in the non-auroral ionosphere.

II—APPARATUS AND EXPERIMENTAL PROCEDURES

The relevant characteristics of the radar equipment are as follows:

Frequency (Mc/sec)	56	106.5
Wavelength (metres)	5.35	2.82
Elevation angle of first maximum in radiation pattern (degrees)	6.0	6.0
Aerial gain (relative to a Hertzian dipole)	16	48
Transmitted power (Kw)	50	25
Pulse width (duration in micro-seconds)	16	35
Pulse recurrence frequency (cycles/second)	~57	~57
Threshold pulse sensitivity of receiving equipment including recording apparatus (watts)	5×10^{-13}	1.3×10^{-12}

The two aerial arrays were mounted on a single rotating tower so that the two beams were directed toward the same part of the sky. The auroral echoes were

resented on separate traces of a conventional range-amplitude display and photo-raphed. Individual components of the echoes exhibit a high frequency fading hich probably follows a Rayleigh distribution. Due to the integrating effect of he photographic process, the recorded amplitude approximates the most probable mplitude of the fading signal. The aerial tower was motor driven and executed a weep through an azimuth sector of 180° once every two minutes. The rate of sweep as constant and equal to 135° per minute. The camera was exposed during the erial sweep at the discretion of the operator, but only those records were retained or which the camera shutter had been opened before the appearance of echoes and losed after the echoes had disappeared. This procedure was designed to ensure that he recorded amplitudes of both the 3-metre and 5-metre echoes were those ob-ained when the axis of the beam was directed toward the reflecting region. The orizontal width of the 5-metre beam was nearly twice that of the 3-metre beam. f the duration of an echo was short compared with the time taken for the aerial o rotate through one beam width, the echo might appear to have an erroneously mall amplitude at the higher frequency. Experience has shown that this is a rare vent, but, in any case, the exposures were such that short-lived echoes did not ppear on the photographic record. Echoes of comparable amplitude appearing

TABLE 1—*Frequency of occurrence of amplitudes*

Amplitude interval	Number of occurrences	
	56 Mc/sec	106 Mc/sec
1.1– 2.0	440	157
2.1– 3.0	314	
3.1– 4.0	164	87
4.1– 5.0	100	
5.1– 6.0	65	32
6.1– 7.0	37	
7.1– 8.0	33	6
8.1– 9.0	12	
9.1–10.0	10	0
10.1–11.0	1	
11.1–12.0	5	
Total	1,181	282

simultaneously at different bearings and the same range may also lead to some error in the observed amplitude ratio. These instances may be detected by comparing the amplitude records with simultaneous range-azimuth records. The amplitude records used for the following analysis contain at most a negligible number of such occurrences.

In analyzing the records, the total range displayed on the record (1,000 km) was divided into 20 km intervals, corresponding to about four times the equivalent range of the longer transmitter pulse. The maximum amplitude of any echo occurring within each range interval was measured for each frequency and treated as a separate occurrence. The unit of amplitude was an arbitrary level which approximates the mean noise amplitude. This level corresponds to the receiver threshold sensitivity given in the table of constants for the equipment.

III—DATA

Selected records obtained in one month of operation (23 February to 22 March, 1952) were analyzed. The analysis was confined to records taken on nights during

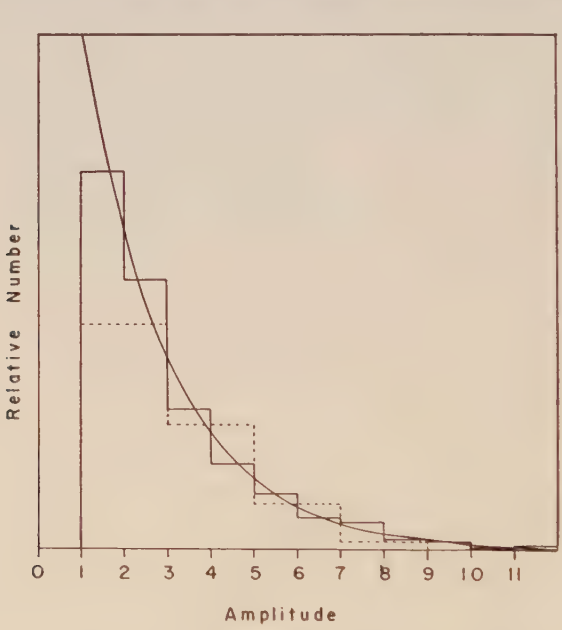

FIG. 1—FREQUENCY DISTRIBUTION OF AMPLITUDES FOR 56 MC/SEC (SOLID-LINE HISTOGRAM) AND 106 MC/SEC (BROKEN-LINE HISTOGRAM); THE CURVE IS THE PROBABILITY CURVE OF EQUATION (1)

which echoes were observed at 106 Mc/sec. This selection of the records reduced greatly the work involved in analysis and, at the same time, ensured that all the 3-metre echoes and an adequate sample of the 5-metre echoes were measured. In

ll, 282 occurrences at 106 Mc/sec were measured and 1,181 at 56 Mc/sec, including 59 simultaneous occurrences at both frequencies.

The symbols A_5 and A_3 will be used to indicate the measured amplitudes of choes observed at 56 and 106 Mc/sec, respectively (the subscript refers to the ravelength). The symbol R will indicate the ratio A_5/A_3 for echoes occurring imultaneously at the two frequencies.

The frequency distribution of amplitudes for each of the two wavelengths is iven in Table 1, and the corresponding histograms are shown in Figure 1. The istogram for A_5 (solid line) is approximated very closely by the probability curve

$$P(A)\,dA = \tfrac{1}{2}\exp(-A/2)\,dA \quad \ldots\ldots\ldots\ldots\ldots\ldots (1)$$

The histogram for A_3 (broken line) is derived from a much smaller number of occurrences, but nevertheless is represented adequately by the same probability urve. The 259 simultaneous occurrences are shown separately in Figure 2, where

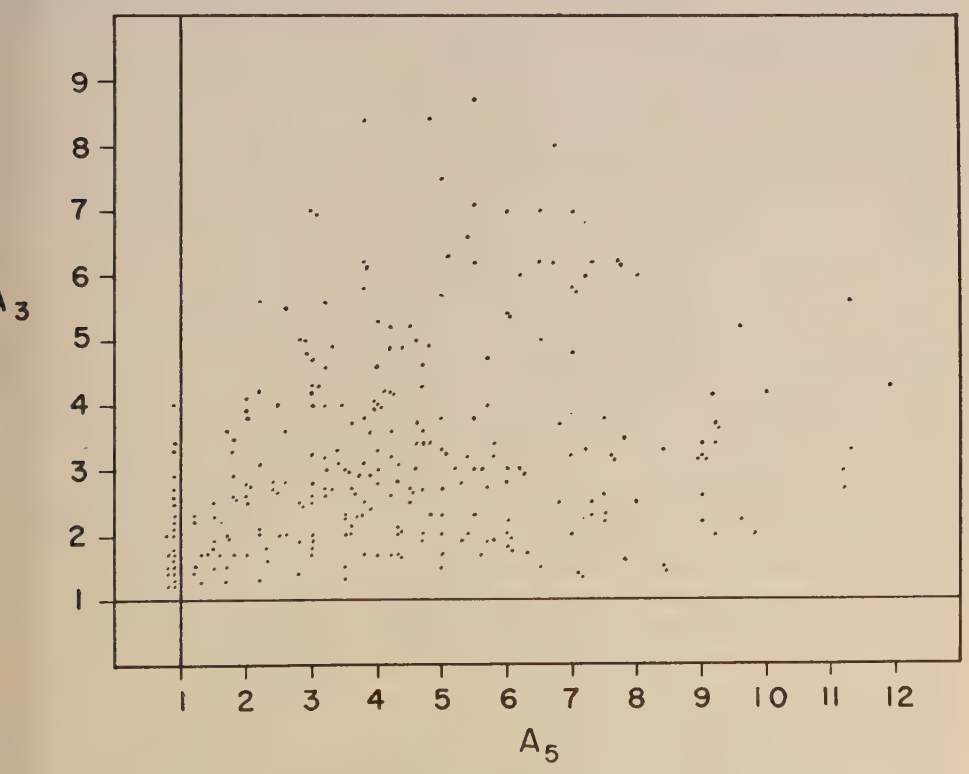

FIG. 2—RELATIVE AMPLITUDES OF ECHOES OBTAINED SIMULTANEOUSLY AT FREQUENCIES OF 56 MC/SEC (A_5) AND 106 MC/SEC (A_3); THE MINIMUM OBSERVABLE AMPLITUDE IS UNITY IN EACH CASE; THE POINTS PLOTTED TO THE LEFT OF $A_5=1$ REPRESENT ECHOES OBSERVED AT 106 MC/SEC FOR WHICH NO CORRESPONDING ECHOES WERE OBSERVED AT 56 MC/SEC

A_3 is plotted against A_5 for each occurrence. It is clear from this Figure that there is no simple law relating A_3 and A_5. If the two quantities are completely unrelated, it is possible to calculate the probability of occurrence of an amplitude ratio R, lying between R and $R + dR$, assuming that the probability distribution of amplitude for each wavelength is given independently by the expression (1). Since occurrences are observed only when both amplitudes are greater than unity, the appropriate expression is, for $R > 1$,

$$P(R)\,dR = \frac{1}{1+R}\exp\left(-\frac{1+R}{2}\right) - \frac{1}{1+R+dR}\exp\left(-\frac{1+R+dR}{2}\right)$$

and for $R < 1$

$$P(R)\,dR = \frac{R+dR}{1+R+dR}\exp\left(-\frac{1+R+dR}{2R+2dR}\right) - \frac{R}{1+R}\exp\left(-\frac{1+R}{2R}\right)$$

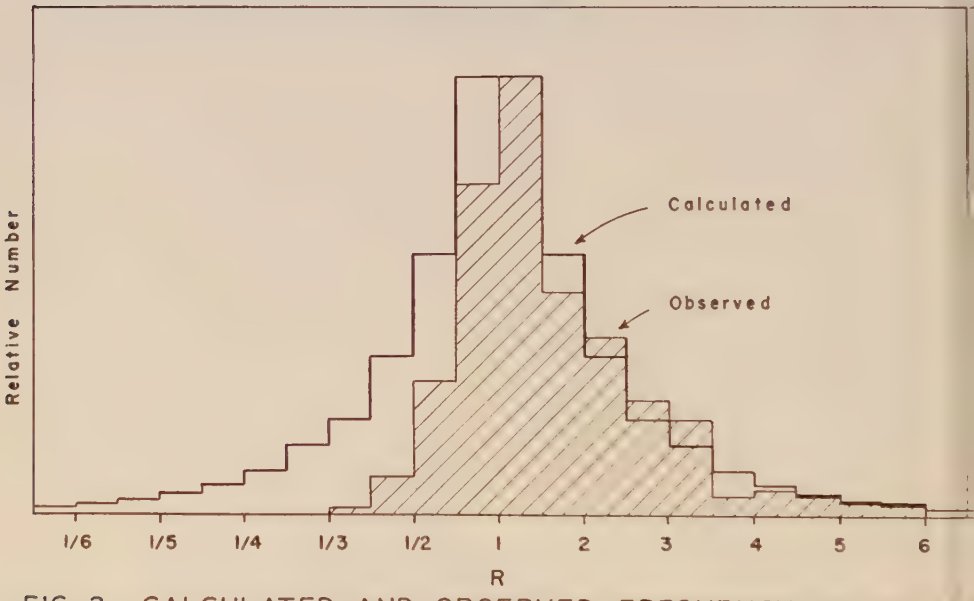

FIG. 3—CALCULATED AND OBSERVED FREQUENCY DISTRIBUTIONS OF AMPLITUDE RATIOS

This result is shown as the unshaded histogram in Figure 3. The experimentally observed frequency distribution is given in Table 2 and is shown as the shaded histogram in Figure 3. The agreement is good for values of R greater than unity but the experimental values fall rapidly below the calculated values for R less than unity. Apparently, the two amplitudes are relatively independent for the larger but not for the smaller values of R. This means that for a given value of A_5 there is an upper limit to the corresponding value of A_3, although all smaller values of A_3 are possible. This conclusion is borne out by the very large number of 5-metre echoes (922) for which there were no corresponding 3-metre echoes. Only 23 echoes were observed at the 3-metre wavelength for which there were no corresponding

TABLE 2—*Frequency of occurrence of amplitude ratios*

Ratio interval	Number of occurrences
1/2.99–1/2.50	1
1/2.49–1/2.00	6
1/1.99–1/1.50	21
1/1.49–1/1.00	52
1.00– 1.49	69
1.50– 1.99	35
2.00– 2.49	28
2.50– 2.99	18
3.00– 3.49	15
3.50– 3.99	3
4.00– 4.49	4
4.50– 4.99	3
5.00– 5.49	2
5.50– 5.99	2
Total	259

-metre echoes. This latter group (shown separately in Figure 2) includes only low alues of A_3 .

IV—DISCUSSION

(*i*) *Partial reflection from a large surface*

The partial reflection theory in its original form [8] assumes that the radiation s incident normally upon a large plane surface which forms the boundary between he ionized and non-ionized regions. The amplitude ratio of the reflected and inci- ent waves is a measure of the index of refraction and, hence, of the electron density ithin the ionized region. A plane surface would lead to the appearance of echoes nly at a single well-defined range and then only when the radar beam was incident ormally upon the surface. In fact, echoes are seen simultaneously at widely differ- ng ranges and bearings, so that the reflecting surface cannot be plane. An alterna- ive suggestion [3], which is more easily reconciled with the observational data, ssumes that the reflections occur at cylindrical surfaces. Since the plane case leads o a lower value of the electron density, it will be considered first.

The signal returned to the radar receiver from a perfectly reflecting plane surface ituated at a distance D from the radar station is the same as that which would be eceived by a similar receiver at a distance $2D$ from the transmitter. The appropri- te form of the transmission equation is [11]

$$A_0^2 P_r = P_t G^2 \left(\frac{3\lambda}{16\pi D}\right)^2 \quad \ldots\ldots\ldots\ldots\ldots\ldots\ldots\ldots\ldots\ldots (2)$$

here λ is the radio wavelength, G the aerial gain, P_t the transmitted power, A_0 ne numerical amplitude of the signal, and P_r the received power corresponding

to a signal amplitude of unity. For wavelengths considerably shorter than the critical wavelength, the amplitude reflection coefficient is given by [3,8]

$$\rho = \frac{Ne^2}{4\pi m f^2} \quad \ldots\ldots (3)$$

where N is the electron density (cm^{-3}), e and m are the electronic charge (esu) and mass (gm), and f the radiofrequency. Combining (2) and (3),

$$N = \frac{64\pi^2 m f^2 D A_0}{3e^2 G\lambda}\left(\frac{P_r}{P_t}\right)^{1/2} \quad \ldots\ldots (4)$$

The amplitude of the echo may be further modified by diffuseness in the boundary of the ionized region or by absorption. If the boundary is diffuse, the amplitude of the received signal is less than that predicted by (4). The precise form of the expression relating A (the measured amplitude of the echo) and A_0 is somewhat dependent upon the analytical expression which is chosen to represent the electron density gradient in the boundary. Herlofson has pointed out [8] that no great error is introduced by assuming

$$A = A_0 \exp\left(-\frac{4\pi^2 a^2}{\lambda^2}\right)$$

where a is the thickness of the boundary. Herlofson neglected the effect of absorption on the grounds that at the time of the observation made by Lovell, Clegg, and Ellyett [2] there was no evidence of general absorption below the 90-km level. In order to reconcile the theory with the present observations, it is necessary to include the effect of selective absorption. Provided the collision frequency of the electrons encountered by the radio waves is low compared with the wave frequency, the longer wavelength will suffer a greater attenuation. This dependence upon wavelength may be included in the expression for A in the following manner:

$$A = A_0 \exp\left(-\frac{4\pi^2 a^2}{\lambda^2} - \alpha\lambda^2\right) \quad \ldots\ldots (5)$$

where α is a constant of the wave path.

Taking $D = 750$ km (corresponding to the range of maximum occurrence of auroral echoes for the apparatus) and the other constants appropriate to the radar equipment, (4) reduces to

$$N = 3.7 \times 10^5 A_{03} = 7.1 \times 10^4 A_{05} \quad \ldots\ldots (6)$$

Hence

$$\frac{A_{05}}{A_{03}} = 5.2$$

The observed value of the amplitude ratio is

$$R = \frac{A_5}{A_3} = 5.2 \exp\left\{-4\pi^2 a^2\left(\frac{1}{\lambda_5^2} - \frac{1}{\lambda_3^2}\right) - \alpha(\lambda_5^2 - \lambda_3^2)\right\}$$

$$= 5.2 \exp\,(3.5a^2 - 20.5\alpha) \quad \ldots\ldots (7)$$

he total variation of R (Fig. 3) may be explained by suitable variations in the arameters a and α. The lowest possible value of electron density will result, if it is ssumed that $a = \alpha = 0$ when $R = 5.2$, which yields from (6)

$$N = 3.7 \times 10^5 A_3$$

or $R = 1/2$, the lowest value of N results when $a = 0$, $\alpha = 0.11$, and from (5) nd (6)

$$N = 1.8 \times 10^6 A_5 = 9.2 \times 10^5 A_3$$

he maximum values of the observed amplitudes for this value of R lead to

$$N \approx 8 \times 10^6$$

hese examples will serve to illustrate the application of the partial reflection heory to the dual frequency measurements. The electron density may be derived r any pair of the observations shown in Figure 2. The values arrived at in this anner are only valid if the thickness of the transition layer between free space nd the ionized region is small compared with the wavelength. It seems unlikely hat the boundary thickness of so large an ionized region should be less than, say, ne metre. Substituting this value for a in (7) and solving for α, we find from (5) nd (6), for $R = 5.2$,

$$N = 1.9 \times 10^8 A_3 = 3.7 \times 10^7 A_5$$

nd for $R = 1$,

$$N = 3.7 \times 10^8 A_3 = 3.7 \times 10^8 A_5$$

hese values are greater than the critical densities for reflection, namely,

$$N_{05} = 3.9 \times 10^7$$

nd

$$N_{03} = 1.4 \times 10^8$$

nd are inadmissible, since they imply the possible existence of a reflection coefficient greater than unity. The theory is only applicable when the reflection coefficient is much less than unity, and expressions (4) and (5) are only valid for $N \ll N_0$.

It was assumed in (4) that the reflecting surface was plane, although the assumption is not in accord with the characteristics of the echoes. This difficulty may be vercome by replacing the plane surface by a cylindrical one (as suggested by spinall and Hawkins [3]). Equation (4) should then be modified by the addition the factor

$$\left(\frac{b + D}{b}\right)^{1/2}$$

here b is the radius of the cylindrical surface. Aspinall and Hawkins suggested a dius of one kilometre, corresponding to the visual appearance of an auroral ray. or this value of b, equation (6) becomes

$$N = 10^7 A_{03} = 1.9 \times 10^6 A_{05}$$

and continuing the analysis, values of N greater than N_{05} are found even when the boundary layer is assumed to be infinitely thin.

There is further evidence that the assumption of a cylindrical surface is unjustified. The axis of the cylindrical surface should lie along the direction of the earth's magnetic field (as do the auroral rays). If the echoes arise by the process described above, the auroral ray must be perpendicular to the radar beam. This condition imposes a severe limitation upon the location of auroral displays from which echoes may be obtained. In particular, no echoes should be expected from auroral displays which occur to the south of the radar station. Since such echoes have been observed several times during the present investigation, it seems that the reflecting surfaces cannot be described simply as of cylindrical form.

It is evident that there are major difficulties involved in the application of the partial reflection theory to auroral radar echoes. Until these difficulties are resolved, the theory must be regarded as unsatisfactory.

(ii) Scattering from irregularities in an ionized region

The characteristics of the echoes suggest that the reflecting regions are confined to a relatively thin layer at a height of about 100 km above the earth's surface. The dimensions of a region giving rise to a single echo are apparently such that it subtends an angle, at the transmitter site, small compared with the angular dimensions of the radar beam. Moreover, the reflecting region characteristically extends over a range interval greater than that represented by the longer transmitter pulse (5.25 km). This is probably due to the finite width of the radar beam, since the apparent horizontal depth of a fully-developed auroral display is usually less than a kilometre.

The radar cross-section, S, corresponding to a given echo amplitude, A, may be found from the radar equation [11]

$$S = A^2 \frac{P_r}{P_t} \frac{4\pi}{G^2} \frac{D^4}{\lambda^2} \left(\frac{8\pi}{3}\right)^2 \qquad \text{.....(8)}$$

Taking $D = 750$ km as before,

$$\left.\begin{aligned} S_5 &= 3.8 \times 10^5 A_5^2 (\text{metre}^2) \\ S_3 &= 7.9 \times 10^5 A_3^2 (\text{metre}^2) \end{aligned}\right\} \qquad \text{.....(9)}$$

If the reflecting region is made up of a number of reflecting centres distributed in range, the maximum separation in range of two reflecting centres which may contribute simultaneously to an echo is just the range equivalent of the transmitter pulse width (duration). These range equivalents are 2.4 km for the 5-metre transmitter and 5.25 km for the 3-metre transmitter. For the purpose of comparing sensitivities, it is convenient to calculate radar cross-sections per kilometre range interval, namely,

$$\left.\begin{aligned} S_{05} &= 1.6 \times 10^5 A_5^2 (\text{metre}^2 \text{ per kilometre range}) \\ S_{03} &= 1.5 \times 10^5 A_3^2 \end{aligned}\right\} \qquad \text{.....(10)}$$

ence

$$R = \frac{A_5}{A_3} \approx \left(\frac{S_{05}}{S_{03}}\right)^{1/2} \quad \ldots\ldots\ldots\ldots\ldots\ldots\ldots\ldots (11)$$

According to Booker and Gordon [9], the back-scattering cross-section per unit olume of a region containing irregularities in the dielectric constant is

$$\sigma = \frac{\overline{\left(\frac{\Delta\epsilon}{\epsilon}\right)^2}\left(\frac{2\pi l}{\lambda}\right)^3}{\lambda\left[1 + \left(\frac{4\pi l}{\lambda}\right)^2\right]^2} \quad \ldots\ldots\ldots\ldots\ldots\ldots\ldots\ldots (12)$$

here σ is the scattered power per unit incident power density per unit volume nd per unit solid angle, l is the scale of fine structure, and $\overline{(\Delta\epsilon/\epsilon)^2}$ is the mean quared variation of the dielectric constant. If the metre is used as the dimension f length for σ, the relationship between S_0 and σ is given by

$$S_0 = (4\pi\sigma B)10^3 \quad \ldots\ldots\ldots\ldots\ldots\ldots\ldots\ldots (13)$$

here B is the area of the reflecting region when viewed in the direction of incidence f the radio waves, and the factor 4π is introduced because of a difference in defini- on between σ and the radar cross-section. Banerji has used the expression (12) to ıvestigate the sporadic E-layer [12].

The expression (12) may be modified for application to an ionized medium by ıbstituting the appropriate value of the dielectric constant [10]. This leads to

$$\sigma = \frac{\overline{\left(\frac{\Delta N}{N}\right)^2}\left(\frac{2\pi l}{\lambda_c}\right)^3}{\lambda_c\left[1 + \left(\frac{4\pi l}{\lambda}\right)^2\right]^2} \quad \ldots\ldots\ldots\ldots\ldots\ldots\ldots\ldots (14)$$

here N is the mean electron density and λ_c is the corresponding critical wavelength. t is assumed that the exploring wavelength is considerably shorter than λ_c , in ccordance with the initial assumption of electron densities less than the critical alue for reflection. The corresponding value of the amplitude ratio, R, is derived om equations (11), (13), and (14),

$$R = 1 + \left(\frac{4\pi l}{\lambda_3}\right)^2 \Big/ 1 + \left(\frac{4\pi l}{\lambda_5}\right)^2 \quad \ldots\ldots\ldots\ldots\ldots\ldots (15)$$

ccording to this theory, the minimum value of R is unity, which occurs when $\ll \lambda_3$, and the maximum value is 3.6 when $l \gg \lambda_5$. The inclusion of an absorption ·m would only tend to decrease the amplitude ratio. Since the higher measured alues of R (Fig. 3) represent a discrepancy between the observations and the ieory, the latter cannot be regarded as a satisfactory explanation of auroral reflec- ons.

(iii) Scattering from highly ionized regions

Two processes have been examined which seemed to offer some hope of recon- ling the existence of high frequency auroral reflections with relatively low electron

densities within the auroral structures. In the preceding paragraphs, the parameters a, α, and l were permitted to vary between certain limits. In fact, it is not likely that the variation assigned to each quantity could be justified physically. The behavior of R as indicated in Figure 3 seems to imply the operation of a threshold phenomenon similar to the reflection of radio waves from the ionosphere. Such a process was suggested in 1947 by Lovell, Clegg, and Ellyett [2], and later by Forsyth, Petrie, Vawter, and Currie as a result of single frequency observations [7]. The dual frequency observations permit a more critical examination of the suggestion.

For the purpose of this discussion, an auroral display may be thought of as a region consisting of a large number of clouds of ionization, each cloud resulting from the precipitation of a thin stream of charged particles (corresponding to the fine structure in visible aurora). The region of most intense ionization will coincide approximately with the region of greatest luminosity near the lower border. Although not essential to the theory, it may be assumed further that each cloud approximates a sphere of radius large compared with a wavelength, but much smaller than, say, one kilometre. The electron density within each cloud will fluctuate in response to variations in the density of the ionizing stream of particles. For radio waves of a particular frequency, f, a cloud will be nearly transparent when the electron density is appreciably below the critical value given by

$$N_0 = \frac{\pi m f^2}{e^2}$$

but the reflection coefficient will approach unity very rapidly as the electron density, N, approaches N_0.

The clouds may be classified into three groups according to their electron densities, as follows:

$$\text{Group I} \ldots\ldots N < N_{05}$$

$$\text{Group II} \ldots\ldots N_{05} < N < N_{03}$$

$$\text{Group III} \ldots\ldots N_{03} < N$$

where, as before,

$$N_{05} = 3.9 \times 10^7 \text{ cm}^{-3}$$

$$N_{03} = 1.4 \times 10^8 \text{ cm}^{-3}$$

There may be some variation in size of the clouds and, in general, a given cloud will not have the same apparent size for different wavelengths. Further, since the clouds are assumed to be nearly spherical in shape, the radar cross-section will approximate the physical cross-section. Accordingly, equation (10) gives a measure of the total cross-section (per kilometre of range) presented by the reflecting clouds in Groups II and III. From equation (11)

$$R = \left(\frac{\text{Total cross-section per unit range of clouds in Groups II and III}}{\text{Total cross-section per unit range of clouds in Group III}} \right)^{1/2}$$

the intensity of the ionizing process increases, the clouds will move from one oup to the next. The value of R will be great when many clouds are in Group II, t few in Group III, and will decrease to a limiting value of unity as the clouds ove from Group II to Group III. This simple picture explains adequately the servations, including the large number of echoes observed at 56 Mc/sec for which corresponding echoes were observed at 106 Mc/sec. The occurrences for which is less than unity may indicate the operation of selective absorption. The rapid vergence of the two histograms of Figure 3 for small values of R and the small mber of such occurrences support this view.

The appearance of auroral echoes at 56 Mc/sec is often preceded by a slight but stinct local increase of the apparent noise level. Since the increase appears within definite range interval, it must represent a reflected signal. The subsequent pearance of auroral echoes within the same range interval suggests that the signal returned from auroral ionization of low intensity. A similar effect at frequencies 46 and 72 Mc/sec, was observed by Lovell, Clegg, and Ellyett [2]. Their suggesn that these signals resulted from a scattering process seems valid. The amplitude too low to be measured accurately, but it is likely that the scattering process is at described by equation (14). If this is the case, the absence of a similar signal 106 Mc/sec indicates [according to equation (15)], that the scale of fine structure, is large compared with the wavelength. This is quite consistent with existing owledge of auroral phenomena and with the suggested size of the reflecting uds. As the intensity of the auroral display increases, the scattering process ould change over to the critical reflection process. The sudden increase in amplide associated with the appearance of typical auroral echoes is further evidence the threshold effect described above.

V—CONCLUSIONS

Of two suggested reflection processes involving low electron densities, one may erate during the early stages of an auroral display, but neither provides a satisctory explanation of radio echoes typically associated with visible aurora. On the her hand, these echoes are explained adequately by a simple theory which assumes e occurrence of electron densities as great as 10^8 per cubic centimeter within the roral structures. The principal objection to this result has been pointed out by ates, who suggests that so high an electron density would lead to a rate of emission light quanta greater than is observed [13]. It may be noted that according to the tical reflection theory, as presented above, the radio measurements lead only to cross-section for the ionic clouds having a given electron density. It is not possible determine the total volume occupied by the clouds without some information as the number of clouds which together contribute to the echo. In any case, the lume occupied by the clouds of highest electron density must be small compared th the total volume of the auroral display. The average electron density throughout the display is probably much less than 10^8 electrons per cubic centimeter. The dio observations also indicate that electron densities of this magnitude exist only short periods of time compared with the duration of the auroral display. Optical easurements provide a mean result, averaged with respect to both space and time.

Possibly the optical and radio measurements should be considered as complementary rather than conflicting types of evidence.

ACKNOWLEDGMENTS

Thanks are due Mr. F. E. Vawter and Mr. W. R. H. White, who assisted with the observations and measured some of the records. The auroral research program at the University of Saskatchewan is under the supervision of Dr. B. W. Currie to whom the author is indebted for many valuable discussions during the course of the work. The project is sponsored by the Defense Research Board of Canada. Dr. J. R. Wait, of the Radio Physics Laboratory, Defense Research Board, read an early draft of the paper and made several useful suggestions. The radar equipment was obtained by the Defense Research Board of Canada through the cooperation of the Geophysical Research Directorate, Air Force Cambridge Research Center, Cambridge, Massachusetts.

References

[1] L. Harang and W. Stoffregan, Nature, **142**, 832 (1938).
[2] A. C. B. Lovell, J. A. Clegg, and C. D. Ellyett, Nature, **160**, 372 (1947).
[3] A. Aspinall and G. S. Hawkins, J. Brit. Astr. Assoc., **60**, 130 (1950).
[4] R. K. Moore, J. Geophys. Res., **56**, 97 (1951).
[5] D. W. R. McKinley and P. M. Millman, reported at the Conference on Auroral Physics University of Western Ontario, London, Canada (July 1951).
[6] K. L. Bowles, reported in "A Review of V.H.F. Ionospheric Propagation," report of the Subcommittee on Ionospheric Propagation of the Wave Propagation Committee of the Institute of Radio Engineers (May 1952). [Edited by M. G. Morgan.]
[7] P. A. Forsyth, W. Petrie, F. Vawter, and B. W. Currie, Nature, **165**, 561 (1950).
[8] N. Herlofson, Nature, **160**, 867 (1947).
[9] H. G. Booker and W. E. Gordon, Proc. Inst. Radio Eng., **38**, 404 (1950).
[10] D. K. Bailey, R. Bateman, L. V. Berkner, H. G. Booker, G. F. Montgomery, E. M. Purcell, W. W. Salisbury, and J. B. Wiesner, Phys. Rev., **86**, 141 (1952).
[11] C. R. Burrows and S. S. Attwood, Radio wave propagation, New York, Academic Press Inc., p. 336 *et seq.* (1949).
[12] R. B. Banerji, Indian J. Phys., **25**, 359 (1951).
[13] D. R. Bates, Proc. R. Soc. (London), A, **196**, 217 (1949).

ON THE IONIZATION PRODUCED BY GAMMA RADIATION FROM THE GROUND AND FROM THE ATMOSPHERE

BY VICTOR F. HESS

Fordham University, New York, N. Y.

ABSTRACT

Two new methods for quick determination of the ionization produced by the gamma rays from the radioactive substances in the ground are discussed.

The first ("absorption method") utilizes partial screening of a portable ionization meter with a lead shield of one centimeter from the bottom and from the sides, and empirical determination of its absorbing power. This method was tried out in field experiments and its results agree very well with the results obtained with the conventional method (alternative measurements over soil and over water).

The second method ("well method") consists in placing a cylindrical ionization chamber inside an iron housing with a wall 10 cm thick, but open at the top and on the bottom. The chamber is used in two positions inside this "iron well" and from the difference of ionization observed at these two positions the total value of the terrestrial gamma radiation can be derived.

Both methods can also be used for determining the gamma radiation coming from the atmosphere ("air radiation"); however, the smallness of this effect makes it difficult to get reliable results. Discrepancies arising in this case are discussed.

§1. *Introduction*

The total ionization produced by hard gamma rays from the decay products of e uranium and thorium family and by potassium contained in rocks and soil terials (q_E) is usually determined by placing an ionization meter first over water d then over the ground. The difference of the ionization observed in both cases es the terrestrial gamma radiation ("earth radiation"). In field-work extending longer intervals of time, such determinations are not always reliable, because all leaks in the chamber in conjunction with barometric changes may produce an lux of atmospheric air containing measurable amounts of radon and thus falsify ults.

Recently, the author introduced an absorption method for the determination the ionization produced by gamma rays from the atmosphere [see 1 of "References" at end of paper], as well as for determining the one produced by gamma rays m the ground. In the latter case, a direct check of the reliability of the absorption thod is possible by comparing the results with the ones obtained with the conntional method mentioned above.

Experiments of this sort have been carried out and will be discussed below.

The use of the absorption method for measuring the "air radiation," first discussed in the paper of Hess and Vancour [1], leads to considerable difficulties on account of the smallness of the effect. W. F. Burns [2] carried out a long and careful series of observations in the summer of 1951 which were in substantial agreement with preliminary measurements of R. P. Vancour [1]. The results are, however, much higher than we can expect theoretically. Discussion of this discrepancy will be given later (see §5). At present, we will confine ourselves to the application of the absorption method for determinations of the earth radiation.

§2. *The principle of the absorption method*

The absorption coefficients of the hard gamma rays from RaC and ThC'' in lead are 0.531 and 0.472 cm^{-1}, respectively; the gamma rays from potassium have about the same penetrating power ($\mu = 0.516$ cm^{-1} in lead). Gamma rays from RaB are much softer and are almost completely absorbed in one centimeter of lead. Other hard gamma rays are emitted by UX_2, but their total intensity, compared with equilibrium amounts of the other members of the U-Ra series, is negligible [3].

If we call the ionization produced by the residual ionization from the walls of the ionization chamber q_0, from cosmic rays (soft plus hard components) q_c, from gamma rays from the ground q_E and from the atmosphere q_A, the total ionization observed in a chamber standing on the ground is

$$q_1 = q_0 + q_c + q_E + q_A \quad \ldots\ldots(1$$

If now the cylindrical chamber is surrounded with a lead screen of moderate thickness (D = about 1 cm) on the sides and below, but not on top, part of the terrestrial gamma rays is absorbed and we observe an ionization q_2:

$$q_2 = q_0 + q_c + q_E e^{-\mu \cdot D} + q_A \quad \ldots\ldots(2$$

The difference between the two observed values allows us to determine q_E if $\mu \cdot D$ is known:

$$q_1 - q_2 = q_E(1 - e^{-\mu \cdot D}) \quad \ldots\ldots(3$$

The effect of cosmic rays in both cases is the same, since the back scattering of cosmic rays from the one-centimeter lead screen into the chamber (wall-thickness 0.25 cm brass) is negligible.

The absorption coefficient μ in these equations corresponds to a composite value which can only be determined empirically, because in the first case when the brass chamber is used without lead screen the softer gamma rays from RaB can produce part of the ionization. Furthermore, some of the gamma rays from the ground penetrate the absorber in an oblique direction and, therefore, it would be inaccurate to insert for D simply the thickness of the lead screen.

§3. *Experimental procedure*

The ionization meter devised by O. H. Gish, K. L. Sherman, and V. F. Hess [4] was used for the experiments. The ionization chamber was filled with radon-free, aged air at atmospheric pressure. It was air-tight and of cylindrical shape (height =

times the radius); its volume was 13.17 litres (radius, 10.16 cm). The chamber as connected with a Lindemann electrometer which was used as a null instrument. or further details see [4] and [1].

Two semi-cylinders of lead and a bottom plate, all 0.98 cm thick, were used as bsorbers. The weight of the whole equipment was not excessive and could be asily handled by one person.

In a series of experiments in a subway tunnel and over water, the components , q_0 , and q_A were carefully determined. Thus, the earth radiation q_E was directly btained by subtracting $(q_0 + q_C + q_A)$ from the total ionization observed at the ifferent locations. This was done in each case (a) without and (b) with the one-entimeter lead screens around the cylinder. In this manner, the coefficient $e^{-\mu \cdot D}$ as evaluated experimentally. The average value of this exponential determined at ve different points in and around New York and near Poughkeepsie, N.Y., was

$$e^{-\mu \cdot D} = 0.382$$

his gives for $\mu \cdot D$ a value of 0.96. Inserting for $(1 - e^{-\mu \cdot D})$ the numerical value 618 in formula (3), I determined then q_E for five locations from the formula

$$q_E = \frac{q_1 - q_2}{(1 - e^{-\mu \cdot D})}$$

hese values are tabulated in Table 1, column 2, and then for comparison the values $_E$ for each point, obtained by the conventional method, are shown in column 3. he agreement is satisfactory. The absorption method will be valuable in cases here experiments are extended over long periods of time and where there is no me for checking the background of the chamber.

TABLE 1

Location	q_E (absorption method)	q_E (conventional method)
Seismic Station, Fordham University (garden)	3.06 I	3.02 I
Mt. St. Vincent College (over rock ledge)	4.23 I	4.30 I
Mt. St. Vincent College (over lawn)	3.36 I	3.39 I
Hillside Lake, N. Y. (near water's edge)	2.03 I	1.88 I
Hillside Lake, N. Y. (on lawn)	2.38 I	2.56 I

(The symbol "I" means ion pairs per cm^3 per sec in standard air.)

A more accurate procedure would be to use two concentric lead cylinders and two bottom lead plates, all one centimeter thick, and to compare the ionizations q_1 and q_2 with one and with two lead absorbers around the chamber. In this case, the experimental determination of $\mu \cdot D$ would be simplified and a mean absorption coefficient for the hard gamma rays from RaC, ThC'', and K (about 0.51 cm^{-1} in lead) could be used in formula (3). For field-work, the use of the double lead shields would be a disadvantage.

§4. *The well method*

This is a very simple and elegant method, which avoids the use of absorbing plates entirely and could be used, in principle, for the determination of earth radiation (q_E) and of air radiation (q_A) as well.

Suppose we place a Gish ionization chamber on the ground and build around it a wall of iron, 10 cm thick on all sides, except on the top and the bottom ("iron well"). The gamma rays from the ground can enter the chamber in a cone with a solid angle limited by the dimensions of the chamber.

If we raise the chamber from the ground to a position higher up in the iron well—for instance, by one-half of its total height (twice the radius) of the chamber—the solid angle through which gamma rays may enter from below is much reduced.

In both cases, only a fraction of the total gamma radiation from the ground is admitted, but these fractions are very different and they can be determined from the geometry of the arrangement.

For practical reasons, it will be better to use smaller ionization chambers for the "well method" in order to avoid excessive weight of the 10-cm iron screen.

If an ionization chamber is placed on the ground and its walls are thick enough to exclude beta rays, the gamma radiation entering it comes practically from the total half sphere (angle 2π steradians) below. If the chamber is placed in the iron well, only a fraction f can enter, which is

$$f = 1 - \cos \varphi$$

where φ is the mean semi-angle of the cone formed by all points along the vertical axis of the chamber connecting these points to the lower edge of the iron well.

If we choose two positions, one with the bottom of the chamber (radius r) directly on the ground (its center $2r$ above the ground) and the other one with the chamber raised to a point where the center of the chamber is at a distance $4r$ from the ground, we find by graphical integration the mean fraction of terrestrial gamma rays in the first case

$$f_1 = 1 - \cos \varphi_1 = 0.163$$

and in the second case

$$f_2 = 1 - \cos \varphi_2 = 0.033$$

Inserting these values in the equations for the total ionization observed in both cases, we have

$$q_1 = q_0 + q_C + q_A + q_E \cdot f_1 \qquad q_2 = q_0 + q_C + q_A + q_E \cdot f_2$$

ıd by subtraction

$$q_1 - q_2 = q_E(f_1 - f_2) = q_e(\cos\varphi_2 - \cos\varphi_1) \quad (4)$$

ɔm which q_E can be obtained directly.

For terrestrial radiation of about $3I$, this difference of the ionizations observed two positions would be

$$q_1 - q_2 = 3(0.163 - 0.033) = 0.39I$$

hich could be measured very easily.

Comparisons of the total ionization without the iron well and with the well and amber in the first position would not give an exact value for q_E, because the iron ell itself absorbs part of the cosmic radiation and of the air radiation.

§5. *Discussion of difficulties in determinations of the "air radiation"*

The "iron well method" could, in principle, be used also for the determination "air radiation," q_A. In this case, the chamber would have to be placed, first, with upper surface flush with the upper rim of the iron well (angle φ_1) and, then, sunk one-half of its height into the well (angle φ_2). The difference of the admitted actions of gamma rays from above would then be

$$0.163 - 0.033 = 0.13$$

ere, however, the total amount of air radiation to be expected is not much above $1I$, and 13 per cent of this would be very difficult to observe.

The same difficulty is in evidence if the absorption method is being used for the termination of the air radiation. W. F. Burns [2] carried out a great number of ch determinations on the grounds of the Seismological Station at Fordham and rived at value of $0.7I$ for the total air radiation (coming from the entire upper lf space). Thirteen per cent of this value could be detected if a sufficient number observations is made.

It should be pointed out, however, that from a theoretical standpoint it can rdly be understood that the ionization produced by the gamma radiation from e decay products of radium and thorium in the atmosphere could amount to $0.7I$. ıe radon content of the air around Fordham was determined by the author [5] 1943 and was found around 10^{-16} curie per cm^3. Its gamma ray effect, at ground el, would be

$$q = 2\pi K \int_0^\infty m e^{-\lambda\gamma}\, d\gamma$$

ere $m = 10^{-16}$ curie/cm^3. Inserting for K(Eve's constant) the value of $\times 10^9$ I per gram Ra and per cm^3 sec, and for the absorption coefficient of mma rays of RaC in air (λ) 4.6×10^{-5} cm^{-1}, we obtain for q the value

$$0.065I$$

is value may be doubled if we assume that the contribution of gamma rays from B + ThC in the atmosphere is equal to the one from the radon decay products.

So we would get for air radiation a value of $0.13I$, which is five times lower than the experimental value of W. F. Burns.

In order to clarify this discrepancy, further measurements, perhaps with the second method proposed above ("well method"), seem to be necessary.

The author wishes to thank Mr. E. Goodfried for permission to carry out measurements on his property at Hillside Lake, N.Y.

References

[1] V. F. Hess and R. P. Vancour, J. Atmos. Terr. Phys., London, **1**, 13-25 (1950).
[2] W. F. Burns, Thesis, Fordham University (1952).
[3] V. F. Hess, W. F. Burns, and W. D. Parkinson, Trans. Amer. Geophys. Union, **33**, 657-66 (1952).
[4] V. F. Hess, Trans. Amer. Geophys. Union, **27**, 670 (1946).
[5] V. F. Hess, Terr. Mag., **48**, 203 (1943).

THE DIURNAL VARIATION OF [OI] 5577 IN THE NIGHTGLOW: GEOGRAPHICAL STUDIES

BY F. E. ROACH, D. R. WILLIAMS, AND HELEN B. PETTIT

United States Naval Ordnance Test Station,
Pasadena and China Lake, California

(Received August 26, 1952)

ABSTRACT

In the region from north latitudes 36° to 44°, the nightglow radiation [OI] 5577 has been reported to undergo a diurnal change in intensity, resulting *on the average* in an intensity maximum approximately one hour after local midnight. The amplitude of the maximum is such that it is 1.3 times the mean intensity for the entire night. Marked departures from this average variation are noted on individual nights. Two simultaneous sets of observations at Cactus Peak in California and at the Haute Provence Observatory in France are studied in order to compare the diurnal variation at stations with a large difference of longitude. It is found that the variations have similar patterns in general, but with significant differences in detail. On two occasions, approximate triangulations on emission maxima yield a height of 180 km. Attention is called to a similarity between the diurnal variation of the nightglow 5577 at low latitudes and of the polar aurora at high latitudes.

I—INTRODUCTION

In a series of papers from this Laboratory, the diurnal variation of the forbidden ygen radiation 5577 ($^1S_0 - {}^1D_2$) as observed in the nightglow at Cactus Peak, alifornia, has been discussed [see 1, 2, and 3 of "References" at end of paper]. articular emphasis has been placed on an attempt to interpret the observations t only in terms of the local intensity of radiation over Cactus Peak, but also of at over other parts of the earth within a small circle centered at Cactus Peak and cluded within the hemisphere of the sky visible at any instant. Such an approach s indicated the desirability of simultaneous observations at several stations in der to test the conclusions drawn from single-station data.

One possibility is to locate stations so that they can observe the same part of e upper atmosphere simultaneously. This procedure is feasible, especially in the uthwestern part of the United States, where good observing conditions exist over wide area. We have made some preliminary attempts in this direction by placing iotometers at White Mountain and Cactus Peak, separated by 165 km, in a rection 11° west of north (White Mountain from Cactus Peak); and at Palomar ountain and Cactus Peak, separated by 317 km, in a direction 16° west of north actus from Palomar). The data are under analysis, and at this point it might

simply be mentioned that the base-line in both cases was too short to yield precis conclusions with the instruments then at our disposal. In future attempts of thi sort, we would recommend that stations be separated by 700 to 1,000 km.

Another procedure is to separate the stations by a large fraction of the earth' circumference in *longitude*, so that, although simultaneous observations of the same part of the upper atmosphere are not possible, it is feasible to compare the diurna variations at each station with respect to *local* time. The present paper is concerned with such a study. During a period of a little over one year, there were in operation at Cactus Peak and at the Haute Provence Observatory in France similar photometers for the observation of 5577. The two stations are separated in longitude by $08^h\ 14^m$. Thus, at the start of observations in the evening at Cactus Peak, the dawn is approaching at Haute Provence. Only on long winter nights can the two observations be simultaneous in time, and even then entirely different portions of the upper atmosphere are under surveillance.

Such a combination of stations is, however, very useful in examining the suggestion of Roach and Pettit [2] that there may be a "semi-fixed" pattern of excitation on the night side of the earth under which an observer seems to rotate with the earth. According to this picture, the observer at Haute Provence should "see" the same pattern eight hours earlier by Greenwich time than the Cactus Peak observer but at the same local apparent solar time. The difference of latitude of the two stations introduces a complication, but, if the height to the emitting layer is of the order of 200 km as our observations indicate, there should be a substantial overlap in the north-south direction. As a matter of fact, we shall discuss later the possibility of triangulating on an emission patch which appears in different orientations at the two stations as a consequence of the difference of latitude.

During the period of the concurrent program, there were two occasions in 195 when the weather was propitious at both stations so that it was possible to get a satisfactory series of observations. These will be discussed in detail in Section III after a general survey of the literature on the subject of the diurnal variation o 5577 in the nightglow in Section II.

II—LITERATURE SURVEY

In our recent work with recording photoelectric photometers, it has been possible to survey the *entire* sky systematically and repeatedly throughout the night. However, this has not been possible for observers using visual photometers o spectrographs who, in general, have observed one part of the sky, such as the zenith, or the pole or in some cases two parts of the sky 90° apart. It has been our experience that, except for the kind of detail available from precision recording photometers, the entire sky may be considered to go through similar variations with time, so that the time variation of *any* part of the sky is fairly representative. With this in mind, we have examined all the references known to us in which the nightglow radiation 5577 has been isolated for study, either by filters or by a spectrograph, and systematically followed throughout the night. From the data or plots in the original papers, we have estimated the mean time of maximum shown in column 4 of Table 1 and the ratio of the intensity at maximum to the mean for the entire night in column 5. It is rather striking that in the zone from north latitude

° to north latitude 44° and over a change of longitude of 10^h 40^m the time of
ıximum occurs approximately one hour after local midnight. Equally impressive
the agreement of the several observers with respect to the mean amplitude of the
riation. These observations include data collected from 1928 to the present time
d strongly support the thesis that the usual pattern of variation in the indicated
ographical zone is a steady increase of intensity during the night until one hour
ter local midnight to approximately double the initial value, followed by a fairly
mmetrical decline toward dawn.*

TABLE 1—*Diurnal maxima of 5577*

Location	Latitude	Longitude	Local time of maximum	Ratio maximum/mean	Reference
	° ′	° ′	*h*		
ount Elbrus (Russia)	N 43 17	E 42 18	1.6	1.3	6,7,8,9
ute Provence (France)	N 43 56	E 5 45	1.5	1.2	10
ute Provence (France)	N 43 56	E 5 45	23.7	1.3	4
agstaff, Arizona	N 35 13	W 111 40	1.5	1.3	11
ctus Peak, California	N 36 05	W 117 49	0.2	1.3	12
ean	.....	.....	1.0	1.3	..
ona (India)	N 18°	E 74°	Minimum at about 01^h	....	13

Although the general description given in the preceding paragraph is true *on e average* and probably represents the over-all diurnal variation to be expected, ide departures from this "normal behavior" have been noted. At Cactus Peak, r example, we have found maxima as early as 09^h 30^m in the evening and as late 03^h in the morning. Out of the 49 nights included in the Cactus Peak entry of able 1, three showed no maximum at all. Barbier, Dufay, and Williams [4] have iso recorded occasional nights of low intensity at Haute Provence in which the iurnal variation was almost negligible. Frequently we have observed more than ne maximum during a night and on one occasion we observed a *minimum* near

*It is important to note here that the diurnal variation of intensity is not the same for all ightglow radiations. Our studies of [OI] 6300 and of NaI 5893 show that they have no obvious lationship to [OI] 5577 and therefore the deductions of this paper should not be extrapolated to *ny* emission other than 5577. Also, attention is directed to the fact that the observations of arandikar [13] made at Poona, India, at a latitude of 18° north showed a *minimum* near mid-ight. It is suggested by the present data that the midnight maximum of 5577 may not be uni-ersally observed over the entire earth's surface. The studies of Lord Rayleigh [5] on the diurnal ariation of the nightglow have not been included in Table 1, since he used a rubidium photo-lectric cell insensitive to radiation in the green.

TABLE 2—*Comparative data on the absolute intensity of 5577*

Author	Intensity	Reference
	(*quanta*/$cm^2 \cdot sec$)	
Lord Rayleigh (England)	1.8×10^8	17
Cerniajev, Khvostikov, Panschin (Russia)	2.0×10^8	18
Rodionov, Pavlova, Rdultovskaya (Russia)	2.8×10^8	9
Roach and Pettit (Cactus Peak)	1.5 to 4.4×10^8	2
Barbier, Dufay, Williams (Haute Provence)	1.5×10^8	4
Barbier and Pettit (Alaska, no aurora)	3.0×10^8	19
Chiplonkar and Ranade (India)	1.8 to 6.9×10^8	20
Mean	2.6×10^8	..

local midnight. In one case, the sequence could be followed from the eastern to the western part of the sky, in the sense that the intensity began to increase in the east before it did in the west, consistent with the idea that the excitation pattern was following the same local-time sequence over a considerable range of longitude [3]. On the other hand, the regular diurnal variation usually has irregularities superimposed on it that make such a quantitative test difficult. In the light of the evidence

TABLE 3—*Nights selected for comparative study*

Location	Date 1950	Local time of maximum	Relative intensity at maximum
Cactus Peak	15 February	1.3	1.46
Haute Provence	17 February	1.8	1.15
Cactus Peak	17 February	3.4	1.24
Haute Provence	18 February	0.2	1.36
Mean	February	1.7	1.30
Haute Provence	10 July	0.7	1.18
Haute Provence	11 July	(2)	(1.3)
Cactus Peak	11 July	1.40	1.22
Haute Provence	12 July	1.10	1.16
Cactus Peak	12 July	2.40	1.26
Cactus Peak	13 July	1.40	1.05
Mean	July	1.50	1.20

ted in this paragraph, it is possible to make a second generalization, namely, that ne departures from the average diurnal variation are a first-order effect and must e considered to be an important part of the over-all picture.

Some comparative data on the absolute intensity of 5577 are collected in able 2. All investigators are in agreement that the intensity in the zenith corre-ponds to 2×10^8 to 5×10^8 quanta/cm^2 column·second. We are now able to etermine this quantity with precision, but even the classical determination made y Lord Rayleigh [17] under difficult conditions is very close to the one currently ccepted.

III—A COMPARATIVE STUDY OF OBSERVATIONS AT HAUTE PROVENCE AND CACTUS PEAK

In Table 3 we show the data regarding the nights chosen for a comparative tudy. The variation of the zenith intensity with local time is shown in the left

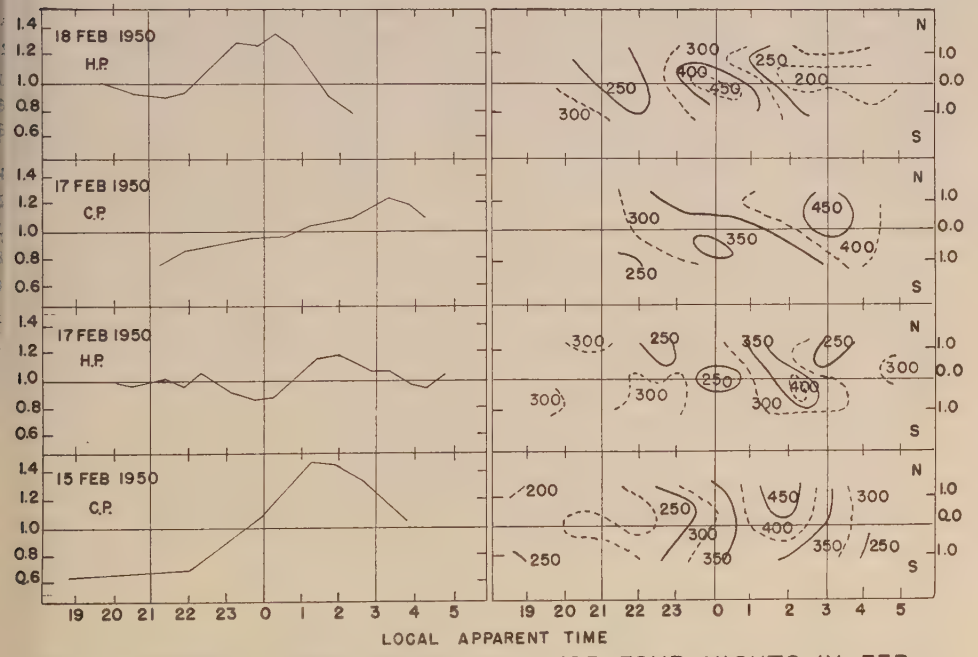

FIG. 1—DIURNAL VARIATION OF 5577 FOR FOUR NIGHTS IN FEBRUARY 1950 AT CACTUS PEAK (C.P.) AND HAUTE PROVENCE (H.P.); THE LEFT-HAND PLOTS GIVE THE MEAN INTENSITY VERSUS TIME, WHILE THE RIGHT-HAND PLOTS GIVE THE TIME VARIATION OF THE NORTH-SOUTH SWEEPS

portion of Figures 1 and 2. For both the February and July sequences we note that he comments made in Section II are illustrated. The *mean* values of the local time of maximum and of its amplitude are in essential agreement with the means of all he data in the literature shown in Table 1. But on examining the plots in detail, one is struck as much by the differences among the nights as by the similarities.

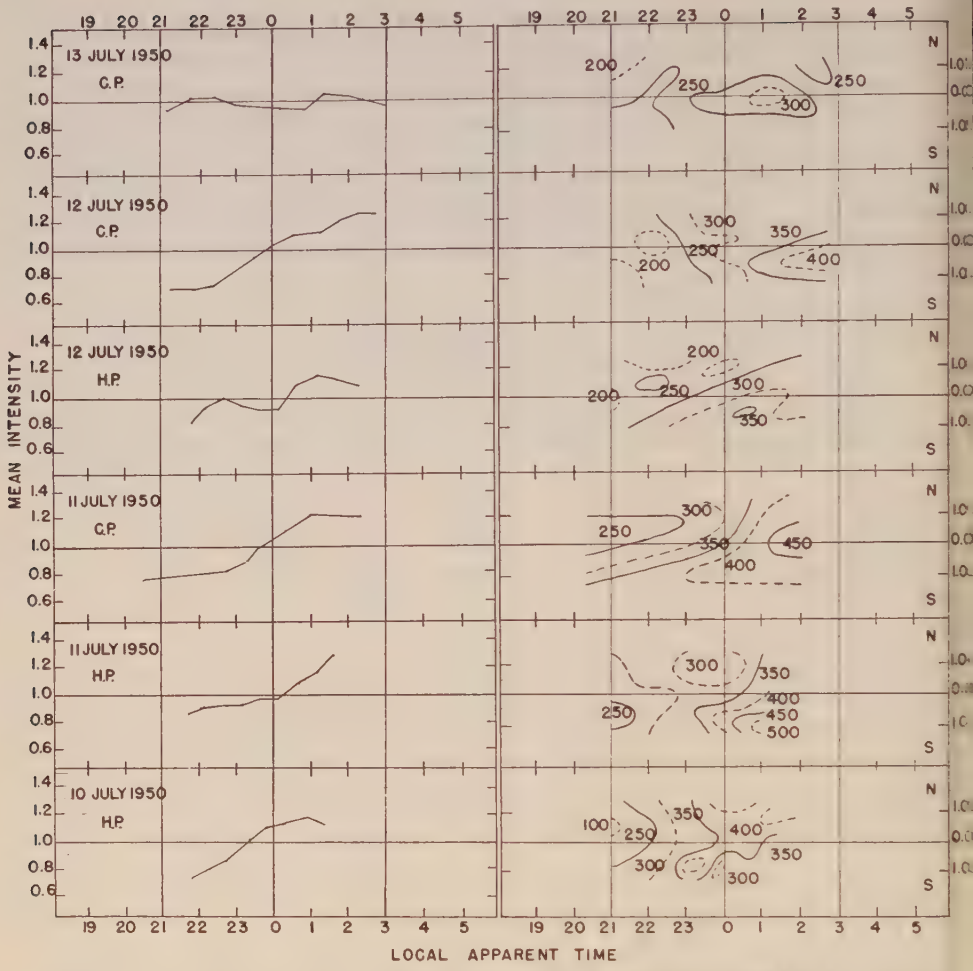

FIG. 2—DIURNAL VARIATION OF 5577 FOR SIX NIGHTS IN JULY 1950; THE METHOD OF PLOTTING IS THE SAME AS FOR FIGURE 1

Even the sets of observations made on the same night at the two stations on 17 February and 11 July are similar only in a general way.

The conclusion is thus forced upon us that the sequence of nights under study tells a double story: a broad diurnal variation in agreement with the general average, together with marked deviations localized in time and place which almost obscure the general effect.

We now consider another way of showing empirically the diurnal variation of intensity. The first sweep of each complete sky survey is in the observer's prime meridian; that is, the photometer goes from the north horizon through the zenith to the south horizon.* This first sweep "looks at" successive portions of the earth's upper atmosphere, first at some distance to the north (the exact distance measured

*Subsequently, seven other sweeps at other azimuths cover the entire sky. See reference [2] for a detailed description of the observing pattern.

ong the earth's surface depends on the height to the emitting layer), then the rtion of the atmosphere directly over the observer as the photometer records the nith intensity, and finally regions to the south. The interesting fact is that, for is one sweep, all the portions of the atmospheric emitting layer under successive rveillance *are at the same local apparent time*. Thus, the observations may be insidered homogeneous, time-wise. In previous discussions [2,3], it has been shown ow the actual intensities at large zenith distances (slant intensities) can be pproximately reduced to the intensity that would be seen by an observer directly nder the emitting portion of the upper atmosphere (local zenith intensities). This accomplished by dividing the observed slant intensity, I_z , by the mean ratio for e entire night (all sweeps) of I_z/I_O . The resulting local zenith intensities in the rth-south sweep thus represent intensities as they would appear to an observer oving at approximately the same local time from several hundred kilometers rth to a similar distance south with his photometer always pointed at his zenith. the successive intensities of the north-south sweeps are plotted against time roughout the night, the diurnal variation of 5577 over a wide belt of latitude is own. In Figures 1 and 2 (the right-hand portions), we show such plots represent-g the nights under study, the unit being 10^6 quanta/cm^2 column·second. Maxima ow show up as *regions* having extension in both space (ordinate) and time (ab-issa). An alternative way of visualizing the maps is to imagine them as excitation atterns on the night side of the earth under which the observer seems to move as e earth rotates, in which case the excitation configurations are thought of as pure ace patterns, the time being introduced incidentally by the earth's rotation.

Figures 1 and 2 again bring out the dual character of the diurnal variation—all aps show a well-defined maximum but have significant differences in detail. One teresting feature of the February sequence is that on both the Cactus maps the nter of the maximum is definitely to the north, whereas in the Haute Provence aps it is to the south on 17 February and overhead on 18 February. This empirical ct is consistent with the hypothesis of a pattern fixed in latitude for which a region maximum intensity could appear in opposite directions as seen from the two ations (see Fig. 3). On 11 July, maxima are noted overhead at Cactus and well to e south at Haute Provence. From this point of view, we have examined the posi-on of the maximum on the maps closest together in time, for both February and ly, between which there elapsed only the eight hours due to the difference of ngitude of the two stations. On 17 February the zenith distance of the center of e maximum is estimated to be 70° south for Haute Provence and 70° north for actus Peak. A "triangulation" as in Figure 3 then places the position of the aximum on 17 February at north latitude 40° and at a height of 180 km. A similar mparison of the maps at the two stations for 11 July indicates that a maximum the early morning hours occurs overhead at Cactus Peak and 82° to the south at aute Provence, again leading to a height of emission of 180 km. This value of the eight of emission is in substantial agreement with all the determinations at this aboratory by the Van Rhijn method.* Because of the possible change of position the maximum with time, we do not wish to stress this independent determination

*From an unpublished study of all our records for the calendar year 1951, we find an average an Rhijn height of 200 km for the layer emitting 5577. Also cf. references [2,3].

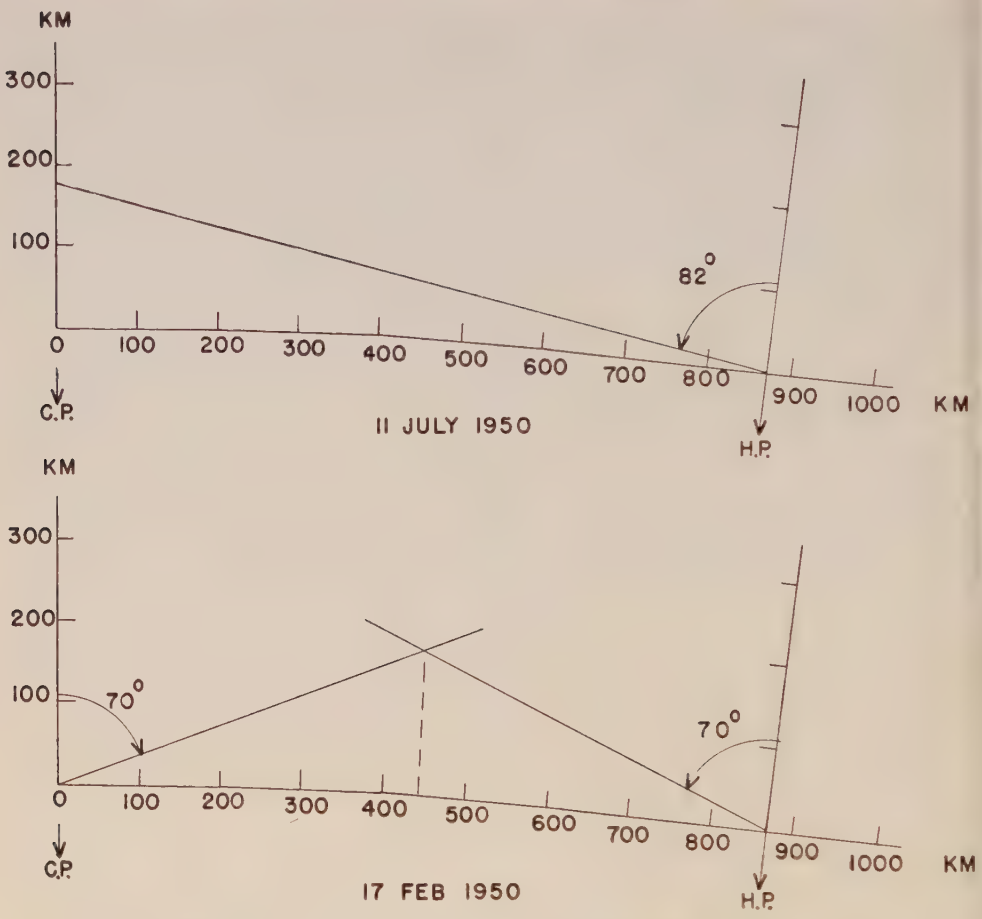

FIG. 3—HEIGHT TO REGIONS OF MAXIMUM INTENSITY OF 5577 ON 17 FEBRUARY 1950 (SEE FIG. 1) AND ON 11 JULY 1950 (SEE FIG. 2) BY TRIANGULATION IN THE NORTH-SOUTH SENSE BETWEEN CACTUS PEAK AND HAUTE PROVENCE

of the height of the emitting layer, but believe it is of interest in illustrating a useful technique that might be employed by two stations at the same longitude and separated in latitude by 8° to 10°, in which case the local time would be the same for both.

It is of interest to note the tendency during both the February and July sequences of observations for the maximum of intensity to be to the south of Haute Provence. In their systematic study of 5577 at Haute Provence, Barbier, Dufay, and Williams [4] have shown (cf. their Fig. 12) that in a large fraction of the nights this southward maximum exists. The large quantity of data which has been accumulated at Cactus Peak is now under analysis and the details will be reported later, but it is apparent that with respect to Cactus Peak there is an approximately equal distribution of maxima to the north and south. The suggestion inherent in these

facts is that there may be a geographical zone of nightglow maximum in the general vicinity of 36° north latitude, somewhat analogous to the zone of maximum polar aurora activity farther north.

IV—THE DIURNAL CHANGE OF 5577 IN THE POLAR AURORA

It is customary to make a sharp distinction between the polar aurora and the nightglow, even though the term "permanent aurora" which many of the early writers used for what is now called the nightglow or night airglow implied that the difference was one of intensity and not of kind. The current thinking which separates the two phenomena into distinct categories is based in large part on the great differences in the nature of their spectra. Although the forbidden oxygen lines 5577 and 6300, 6363 are common to both, there are so many other spectral differences that it is obvious that the nature of the excitation process cannot be identical [14].

One is impressed, however, by the empirical fact that the polar aurora undergoes a diurnal change similar to that which has been so widely observed for 5577 in the nightglow. Various indices of auroral activity appear in the literature, but a direct measurement of 5577 in the polar aurora is reported by Currie and Edwards [15], based on observations made at Chesterfield, Canada (63° 20′ north, 90° 42′ west). They found a definite maximum of intensity near local midnight, with an amplitude having the same order of magnitude as the value reported by us in this paper for nightglow 5577. According to Vegard [16], who made a statistical study of the auroral diurnal variation (based on the number of visible aurorae, not on 5577 intensities), the maximum occurs about one hour before *magnetic* midnight and hence at a spread of local times for observers at various locations. In a similar study, Currie and Jones [21] find a diurnal variation of the polar aurora in which the maximum seems to be more closely associated with local midnight than with magnetic midnight. Dauvillier [17], in a study of Scoresby Sound auroral data during the 1932-33 polar year, reports an evening maximum at $21^h\ 00^m$ local time and a somewhat smaller amplitude morning maximum at $04^h\ 30^m$.

The similarity of the general time variation for 5577 in both the nightglow at low latitudes and the polar aurora at high latitudes may be simply a coincidence, but it does raise the question of whether the nightglow may be a "permanent aurora" of low intensity and excitation. Or to reverse the question: Is the polar aurora a high-intensity, high-excitation form of the nightglow with each having a similar but not identical basic mechanism of excitation?

V—CONCLUDING REMARKS

In this report we have discussed the general tendency for the 5577 nightglow radiation to undergo an intensity maximum shortly after local midnight. We have further emphasized that the departures from the average diurnal variation are large. Both of these features, regularity in a general diurnal pattern and irregularity in the detailed pattern, are characteristic of tropospheric phenomena known generically as "weather." In this regard, we may consider our excitation pattern maps as analogous to upper atmosphere weather maps. Whether this is merely an analogy or has some deeper physical significance is an interesting conjecture.

ACKNOWLEDGMENTS

It is a pleasure to record our thanks to Drs. D. Barbier and J. Dufay for their help in obtaining the observations at the Haute Provence Observatory. One of us (F.E.R.) was privileged to carry out part of the analysis of the data at the Institut d'Astrophysique, in Paris, as a Fulbright Research Scholar during 1951-52.

References

[1] D. G. Marlow and J. C. Pemberton, An automatic scanning and recording photometer for night sky studies, Rev. Sci. Instr., **20**, 724 (1949).
[2] F. E. Roach and H. B. Pettit, On diurnal variation of [OI] 5577 in the nightglow, J. Geophys. Res., **56**, 325 (1951); and Excitation patterns in the nightglow, L'étude Optique de l'atmosphere terrestre, Mém. Soc. roy. sci. Liége, **12**, 13-42 (1952).
[3] D. N. Davis, J. Geophys. Res., **56**, 567 (1951).
[4] D. Barbier, J. Dufay, and D. R. Williams, Ann. Astrophys., **14**, 399 (1951).
[5] Lord Rayleigh, Proc. R. Soc., A, **124**, 345 (1929).
[6] N. Dobrotin, I. Frank, and P. Cerenkov, Doklady Akad. Nauk USSR, **1**, 114 (1935).
[7] I. A. Khvostikov and A. Lebedev, Doklady Akad. Nauk USSR, **1**, 118 (1935).
[8] N. Wassmuth, V. Werzner, S. Tibilov, and S. Freivert, Doklady Akad. Nauk USSR, **19**, 405 (1938).
[9] S. F. Rodionov, E. N. Pavlova, and E. V. Rdultovskaya, Doklady Akad. Nauk USSR, **66**, 55 (1949).
[10] J. Dufay and Tcheng Mao-Lin, Ann. Géophys., **2**, 189 (1946).
[11] J. C. McLennan, J. H. McLeod, and H. J. C. Ireton, Trans. R. Soc. Can., **22**, 397 (1928).
[12] Based on an, as yet, unpublished summary of a study of 5577 from 1948 to 1952.
[13] J. V. Karandikar, Indian J. Phys., **8**, 547 (1934).
[14] Many recent authors have suggested, however, that the nightglow and polar aurora are related. See, for example, A. Dauvillier, Rev. Gén. Électricité, **31**, 303, 433, and 437 (1932); C. T. Elvey, Rev. Mod. Phys., **14**, 140 (1942); D. R. Bates, Mon. Not. R. Astr. Soc., **106**, 509 (1946); Observatory, **67**, 46 (1947); F. Hoyle, Report to the Meeting of the Gassiot Committee (1947); L. Biermann and P. ten Bruggencate, Veröff. Sternwarte, Göttingen, No. 83 (1947).
[15] B. W. Currie and H. W. Edwards, Terr. Mag., **41**, 265 (1936).
[16] L. Vegard, Phil. Mag., **23**, 211 (1923).
[17] Lord Rayleigh, Proc. R. Soc., A, **129**, 458 (1930).
[18] V. I. Cerniajev, I. A. Khvostikov, and K. B. Panschin, J. Phys. Radium, **7**, 7, 149 (1936).
[19] D. Barbier and H. B. Pettit, Ann. Géophys., **8**, 232-247 (1952).
[20] M. W. Chiplonkar and J. D. Ranade, J. Univ. Bombay, **14**, pt. 3, 14 (1945); Proc. Indian Acad. Sci., A, **18**, 121 (1943); Bull. Astron. Inst. Czechosl., **2**, 79 (1950).
[21] B. W. Currie and C. K. Jones, Terr. Mag., **46**, 269 (1941).

EXTENDED-RANGE RADIO TRANSMISSION BY OBLIQUE REFLECTION FROM METEORIC IONIZATION*

BY O. G. VILLARD, JR., A. M. PETERSON, L. A. MANNING, AND VON R. ESHLEMAN

Radio Propagation Laboratory, Stanford University, Stanford, California

(Received September 18, 1952)

ABSTRACT

It has been found that radio communication between relatively low-power stations operating at 14 Mc and separated by distances of roughly 1,200 km may be maintained at times when no layer transmission to any point on the earth's surface can be demonstrated to be present. The signal obtained is subject to considerable fading, but some signal is nearly always detectable. The contribution of overlapping oblique-incidence meteor reflections to the observed signal is considered in the light of some preliminary theoretical and experimental findings. It is clearly important to assess the meteoric contribution with care, since the possibility that meteoric reflections alone could account for the signal does not seem unreasonable. Suggestions for further investigation are given.

During tests of a technique for determining those areas on the earth's surface to which strong radio transmission is possible at any given time and frequency [see 1 and 2 of "References" at end of paper], it was found that radio communication with a station 1,200 km away was still possible at a time when no sizable reflecting region—such as the *F*, *E*, or sporadic-*E* layer—could be shown to be present. The frequency employed was 14.3 Mc. Both stations had power outputs of the order of 100 watts, and were located at sites free of obstructions to low vertical-angle radiation. Rotatable beam antennas, mounted at heights of roughly 40 feet and having gains of 6 to 8 db, were used. The receivers were of the standard communications type, having fair sensitivity and half-power band-widths of the order of 4 kc.

Characteristics of the signal obtained under these conditions may be summarized as follows. The strength varied over wide limits, dipping occasionally into the noise level, but frequently rising as much as 20 or 30 db above. The five-minute average value is perhaps 10 db above the noise. The most significant feature of this signal is the fact that it is always present, except for the fades. It has been observed on a large-enough number of occasions to rule out the possibility that it might be a transient or sporadic effect. With suitable limiting, the signal is entirely satisfactory for hand-keyed c.w. transmission.

The sudden, strong increases in signal strength are clearly caused by reflections

*Prepared under Contract N6onr-251 Consolidated Task No. 7 (NR-078-360) for Office of Naval Research, the Signal Corps, and the U. S. Air Force.

from individual meteor ionization trails. The relatively continuous background, however, requires further explanation. It is the purpose of this paper to investigate the contribution to this signal provided by overlapping reflections from the relatively large number of meteor trails present at any given time.

Absence of layer reflections

In order to establish that no layer-type transmission was contributing to the measured field strength, the scatter-sounding apparatus described in reference [1] was used. This consisted of a 1-kw 14-Mc transmitter connected to a rotatable directional antenna and adapted so as to excite and display back-scatter echoes from the ground. These echoes appear in detectable strength only when a radio-reflecting region of reasonable size (of the order of several hundred square kilometers or larger) is present. Tests have shown the indication to be quite sensitive; as soon as one-way layer-propagated signals of medium strength are heard, back-scattered echoes appear on the indicator.

Scatter-soundings and transmission tests were performed at Stanford University, California, between the hours of 11 p.m. and 4 a.m., Pacific Standard Time, during the months of December, 1951, and January, 1952. The remote station providing the opposite terminus of the transmission path was located at Spokane, Washington, at a bearing of 16° true from Stanford, California.

At those hours and at that time of year, *F*-layer transmission is almost invariably absent. Sporadic-*E* transmission, however, is always a possibility. Although the presence of a sporadic-*E* cloud of the usual type along the transmission path would manifest itself as a tremendous increase in signal strength over that being considered here, together with a large reduction in the average fading period, the possibility always exists that such a cloud might form to one side of the path and contribute to the total observed signal at each terminus by oblique back-scattering from the ground. The strength and fading characteristics of signals propagated by such oblique back-scattering make them very difficult to distinguish from signals propagated by the type of transmission being considered herewith. Hence it is essential in tests of this sort to rule out the possibility of a back-scattered contribution to the total signal.

To demonstrate the absence of a back-scattered component, repeated scatter-soundings were made during the course of the transmission tests. On about half the nights during the period under discussion, sporadic-*E* patches of varying intensity and in varying locations, were found with the aid of the scatter-sounder. (A vertical-incidence model C-3 ionosphere recorder, operated at Stanford University, showed far less sporadic-*E* activity, as would be expected in view of its limited area of surveillance.) Since tests on these occasions showed clearly that a suitably-located off-path sporadic-*E* patch did contribute to the total signal, forward-transmission test results were considered reliable only when all detectable sporadic-*E* was absent.

Use of rotatable unidirectional antennas at both ends of the forward-transmission circuit provided another means for assessing the contribution of off-path scatter to the total signal. In the absence of sporadic-*E*, it is found that if either antenna is directed away from the other station, the steady background component of the signal fades down and is soon lost. In fact, the signal is readily detectable at

e aforementioned power levels only when the extra gain provided by the beam ntennas is present. When an off-path sporadic-*E* patch is present, a relatively rong signal can usually be obtained when each antenna is pointed, not at the pposite station, but rather in the general direction of the scatter patch and the ound-scattering area which lies beyond it.

Further transmission characteristics

To demonstrate that the same type of background signal is observable over a milar path in a different direction, tests were made with a station in Tucson, rizona, about 1,175 km distant and at a bearing of 115° true from Stanford, alifornia. The Arizona station had equipment substantially equivalent to that at pokane in respect to power, antenna arrangements, and site. The transmission naracteristics of the Tucson path proved to be indistinguishable from those of the rcuit to Spokane.

It was found that an increase in transmission frequency caused the background gnal to decrease very rapidly. Tests with Spokane, using moderately high-power ulsed transmissions at 23 Mc, showed that the steady background had disappeared; signal was received only during the strongest meteor bursts. The same was true or continuous-wave signals over the Tucson path when operating frequency was ncreased from 14.2 to 28.6 Mc, with all other circumstances of the test essentially quivalent.

In an effort to determine the maximum range at which this type of transmission ould be maintained, a 14.2-Mc continuous-wave test was made between Stanford, alifornia, and a station in Aberdeen, South Dakota, which is some 2,280 km dis- ant. This range is close to the maximum for one-hop transmission via *E*-region eflection. Once again, the antenna arrangements, power, and site characteristics t both ends of the circuit were substantially equivalent. It was found that signals rom the opposite station could be received only at relatively infrequent intervals y reflection from individual meteor columns. There was no trace of a steady ackground.

Effect observable on short-wave broadcast transmissions

Further study of the type of transmission which is the subject of this discussion vas conducted with the aid of signals from a 50-kw short-wave broadcasting station ocated at Delano, California, approximately 315 km southeast from Stanford. During the early spring of 1952, this station transmitted during the evening hours imultaneously on 15.31 and 17.77 Mc, employing beam antennas so directed that tanford University lay within their half-power horizontal beam-width. On many venings, *F*-layer transmission from this station to any point on the earth's surface ailed well before sign-off time. In the absence of sporadic-*E* reflection, background ransmission of the type previously described could clearly be heard on both requencies.

The 17-Mc signal was observed on an instantaneous direction-finder originally esigned for meteor azimuth determination [3]. Just before failure of *F*-layer trans- nission, the signal from Delano was relatively strong, with an azimuth toward the outhwest. Since this is the direction in which the *F*-layer-propagated scatter-echoes

are last seen on the scatter-sounder as F-layer transmission fails at night, it is clear that F-layer back-scatter was the predominant mode of transmission from Delano at that hour. After disappearance of all F-layer transmission, and hence F-layer back-scatter, the bearing of the now appreciably weaker Delano signal shifted to the southeast; that is, to the approximate bearing to the station.

Individual meteor bursts would cause this signal to fade up momentarily to very high levels. When this occurred, the bearing to the meteor burst could be obtained with good accuracy. The meteor reflections were found to be coming from all directions about the receiving point. The vertical angle of fire of the Delano beam is so low that the maximum of the main lobe intersects the 100-km region of the ionosphere some 200 km beyond Stanford toward the northwest. The presence of minor lobes in the beam pattern assures reasonably uniform illumination of the ionosphere above Stanford.

When the large identifiable meteor reflections faded down, and only the background signal was visible, the indicated bearing would again return approximately to the southeast. A continual small shift of this bearing about the mean value was observed, in a manner which suggested that no single, fixed point of reflection was responsible for the entire signal.

Comparison of forward and back-reflection recordings

Field-strength recordings of the 1,200-km 14-Mc transmissions were made with the aid of a direct-inking magnetic "pen-motor" recorder, capable of a response up to 100 cps. These records were found to have a great many features in common with recordings previously made with the same equipment at Stanford University for the purpose of meteor ionization studies [3,4]. Continuous-wave signals at approximately the same power levels and operating frequencies had been used for the meteor investigations, which had been concerned with backward reflection from ionization trails at perpendicular incidence.

The most striking difference between the backward and oblique recordings is the presence in the latter of a steady background component. In both cases, individual meteor reflections can be clearly discerned in so far as their time of beginning is concerned. Although the duration of each echo is well defined at perpendicular incidence, since the individual echoes are well separated along the trace, at oblique incidence this duration cannot readily be determined. It is clear that the individual echoes have, on the average, considerably increased durations, although the exact time of ending of each one tends to be obscured, since it fades into and merges with the continuously-fluctuating background.

The question at once arises, can the background signal itself be accounted for as a consequence of the overlapping of many individual meteor echoes? Clearly, if overlapping occurs on a consistent-enough basis, a mechanism is at hand whereby continuous transmission could be supported. In partial answer to this question, it is first necessary to consider the expected increase in echo duration when reflection from a meteor column occurs at oblique rather than perpendicular incidence.

Theoretical considerations

At the present time, it is not possible to predict accurately the nature and

haracteristics of the radio echo which will be produced by a given meteoric particle. he chief difficulty is lack of direct knowledge of the physical processes involved in ormation of the ion column, and consequent uncertainty as to the size and distribution of the ionic disturbance whose reflecting powers are to be predicted. Moreover, elatively little is known about the number, size, and velocity distributions of the cho-producing particles themselves. On the basis of experience, however, a model lectron column has been postulated [5], the radio echo characteristics of which ould agree fairly closely with those of the majority of meteor echoes observed in ractice. Calculation of the reflected field strength for this model column is straightorward and involves summing the contributions of each electron considered as an ndependent scattering source under the influence of the incident electromagnetic ield.

Using generally-accepted recombination and diffusion coefficients for the "*E*" egion of the ionosphere, in which the majority of ion columns occur, it may be hown that if the number of electrons per meter of trail length is less than 10^{14}, and he initial radius of the column is of the order of a molecular mean free path (a easonable assumption), there is virtually no loss of electrons by recombination. Back-reflection meteor studies made at Stanford University [5] at a frequency of 3 Mc have indicated that the majority of meteor trails—that is, those whose haracteristics are best matched by the model—have a line density of less than 10^{14} lectrons per meter. On the basis of this and other evidence, recombination is not elieved to be an important factor in meteor ionization.

The model column, accordingly, has an initial size as given above, and expands utward in accordance with the classical diffusion equation as applied to cylindrical eometry. Solution of this equation leads to a Gaussian distribution of electron lensity as a function of radius measured from the axis of the column. Although it is ighly probable that actual meteor trails have a more complicated distribution of onization than this, the Gaussian distribution represents a useful working model.

Accepting these premises, we have a column at first small compared with a wavelength. When a radio wave strikes this column perpendicularly, the contributions of each individual electron to the back-scattered energy in the vicinity of the perpendicular reflection point add up substantially in phase, and a strong backreflected or back-scattered signal results. Then, as the column expands and its size becomes comparable to a wavelength, the contribution from the outermost edge begins to cancel that from the inner edge, owing to the path-length difference. For a given rate of diffusion, this will happen relatively quickly during the life of a backscattering ionization column. However when the reflection or scattering is oblique, a longer time must elapse before the meteor trail can expand to the point where an equivalent path-length difference exists.

For both forward and back scattering, the amplitude of the radio signal propagated via the column will decay with time in an exponential manner. An example of an echo showing this behavior will be found in Figure 1 of reference [3].

Echo duration and amplitude

Evaluation of the ratio of the time of echo duration for forward scattering τ_F, o the time of echo duration for back scattering τ_B, may proceed with the aid of the

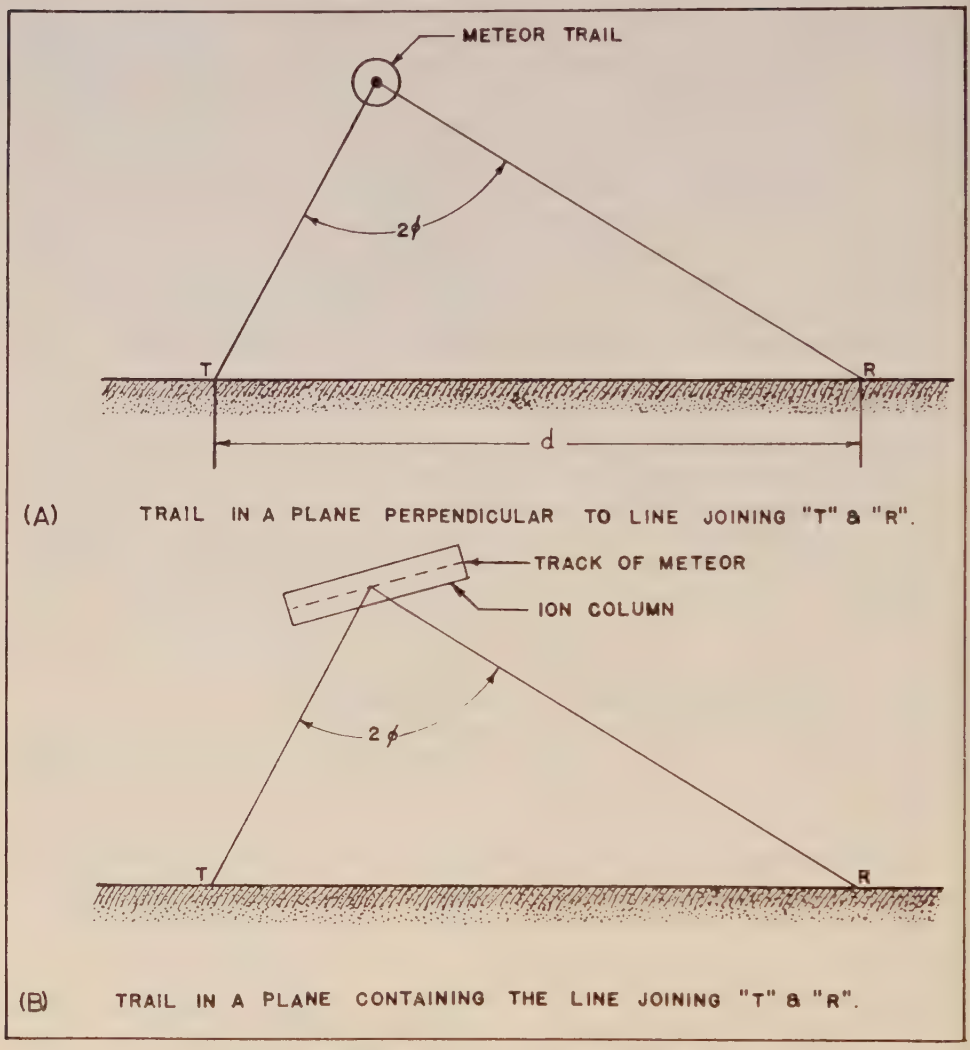

FIG. 1—REFLECTION GEOMETRY

geometry illustrated in Figure 1. Both of these times are defined as the time interval between initial and 37 per cent amplitude. Let 2ϕ be the forward-scattering angle.

For the geometry of either (*A*) or (*B*) of Figure 1, it may be shown on the basis of the preceding assumptions that the echo duration to 37 per cent of the initial amplitude τ_F is given by

$$\tau_F = \frac{\sec^2 \phi}{4k^2 D} \text{ seconds} \quad \ldots\ldots\ldots\ldots\ldots\ldots\ldots\ldots\ldots\ldots (1)$$

where $k = 2\pi\ \lambda$ and D = the diffusion coefficient, approximately 3 meters^2, sec in the *E*-region.

From equation (1), the ratio of durations for the forward- and back-scattering cases is

$$\frac{\tau_F}{\tau_B} = \sec^2 \phi \quad \ldots\ldots\ldots\ldots\ldots\ldots\ldots\ldots\ldots\ldots (2)$$

In assessing the average duration increase produced by this effect for a particular forward-scattering path, account must be taken of the location of the individual meteors with respect to the end-points, since this will sharply effect the value of ϕ

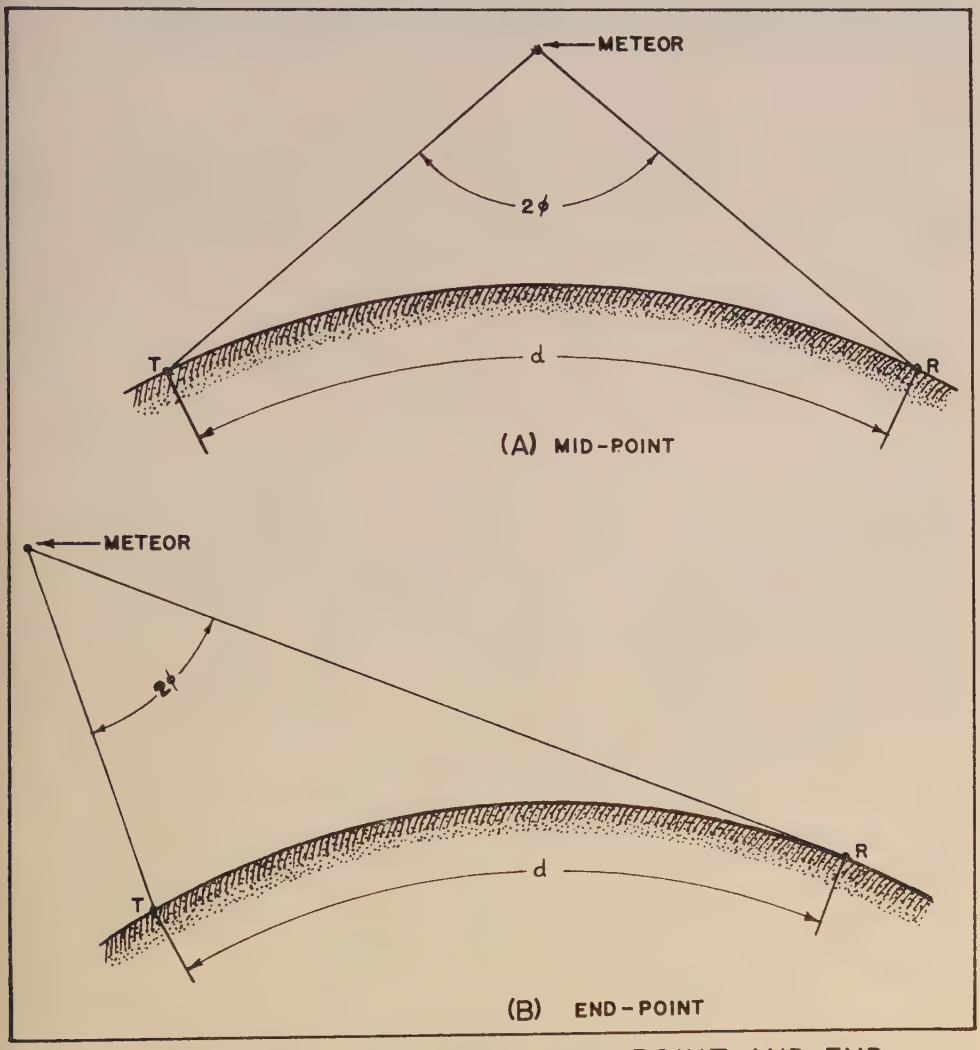

FIG. 2—DIFFERENCE BETWEEN MID-POINT AND END-POINT GEOMETRY

and thus the echo duration. The situation is illustrated in Figure 2 (*A*) and (*B*).

From the standpoint of the amplitude of the reflected signal, on the other hand, the geometry of Figure 1 (*B*) proves to be the more favorable, owing to the way in which the Fresnel zone contributions add up in comparison with part (*A*) of the

Figure. Whereas in (*A*) the forward-scattered signal will have the same strength as a back-reflected signal traveling over a path of equivalent length, in (*B*) the amplitude of the forward-scattered signal exceeds that of an equivalent back-scattered signal by the factor sec ϕ.

A further factor affecting reflected-signal amplitude can be understood by reference to Figure 2. As the separation distance d increases, reflections of the sort shown in part (*B*) become weaker owing to the very low angle of take-off or arrival required for signals at one end of the circuit. Antenna systems in practice rapidly lose sensitivity at very low angles.

Experiment involving three paths of differing lengths

In an effort to obtain at least a qualitative experimental verification of these considerations, a test was undertaken whereby a simultaneous recording was made at Stanford of three 14-Mc signals on closely adjacent frequencies, one originating from a location 15 km away, another 475 km away, and the third 1,175 km away. All three stations had powers of the order of 500 watts. The closest-in station employed a quarter-wave dipole antenna, one quarter-wave above ground, but both the more distant ones had Yagi beams giving 6 to 8 db gain, and located about 40 feet above ground. Absence of layer transmission of any sort was verified by scatter-sounding. Ground-wave transmission from the nearest station was suppressed by suitable choice of location and antenna orientation.

An effort was made to determine the total duration of the discernible meteor echoes for each of the three paths by examination of the records. The *total* duration of a given meteor was selected as a criterion, because the non-linearity and limited dynamic range of the recorder made it impractical to determine the time interval between a given value and 37 per cent of that value. Total duration can be determined with accuracy only for the shortest path, where the individual echoes are well separated. It could only be estimated for the longer paths because of the difficulty of distinguishing the time of cessation of a given echo in the presence of the continuously-fluctuating background.

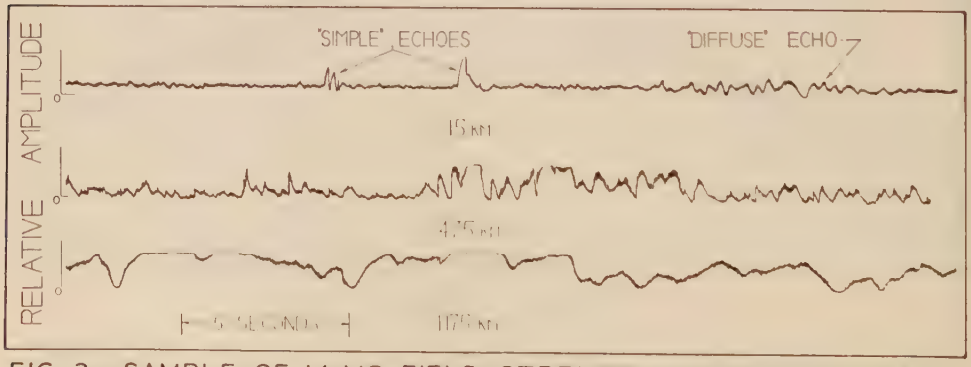

FIG. 3—SAMPLE OF 14-MC FIELD-STRENGTH RECORDINGS MADE SIMULTANEOUSLY OVER PATHS OF DIFFERING LENGTH, AT A TIME WHEN NO LAYER-TYPE REFLECTION TO ANY POINT ON THE EARTH'S SURFACE COULD BE SHOWN TO BE PRESENT

Figure 3 shows a sample of the records obtained. The "diffuse" echo shown on the 15-km recording is believed on the basis of considerable experience to be a non-perpendicular reflection from a meteor column grown so large (or so distorted by winds) as to have become amorphous. These echoes are relatively rare compared with the "simple" type echoes, the behavior of which is well predicted by the assumed model.

At a frequency of 14.2 Mc, and assuming a diffusion coefficient of 3 meters^2/second, the calculated forward-scattering times to 37 per cent amplitude, τ_F, and the ratios of τ_F to τ_B for the two oblique paths, are summarized in the following Table:

TABLE 1

For reflection at mid-point (Fig. 2A)			For reflection over one station (Fig. 2B)		
τ_F		τ_F/τ_B	τ_F		τ_F/τ_B
Path	Time		Path	Time	
km	*sec*		*km*	*sec*	
475	6.2	6.7	475	1.5	1.6
1,175	21.4	23.1	1,175	1.6	1.7

Data were taken for the three paths simultaneously for a total time of roughly three hours. The rate of detection of meteor reflections, distinguishable as such, was 2.7 per minute for the 15-km path, 3.2 per minute for the 475-km path, and 1.0 per minute for the 1,175-km path. The lower rate for the longer path is unquestionably due to the great difficulty of distinguishing individual echoes in the fluctuating background.

For those meteor reflections which could be distinguished as such, it was found that the average duration for the 475-km path was 3.1 times as great as that for the local path. The average duration for the 1,175-km path was 4.5 times as great as for the local path.

An attempt was made to add up the total time during which *distinguishable* meteor echoes were present on the three records. Such echoes were present for 7.5 per cent of the time over the local path; 27 per cent of the time over the 475-km path, and 12 per cent of the time for the 1,175-km path. The last figure is again indicative of the difficulty of distinguishing individual echoes in the fluctuating background.

Conclusion

These experimental results, rough as they are, are interpreted as providing qualitative support for the theory. It is evident that durations are considerably increased over the oblique path, as predicted. If echoes are present for 7 per cent of the time at vertical incidence, and if a duration increase of up to 23 times for favorably-situated columns is to be expected over the oblique path, it seems clear that the contribution of overlapping meteor echoes to the total forward-scattered

signal must be assessed with care, since the possibility that these echoes themselves may account for the total observed signal is not unreasonable.

No attempt is made at this point to offer a final explanation for the signal actually observed over the 1,200-km oblique path. It should be kept in mind that the scatter-sounding apparatus could only demonstrate the absence of strong layer transmission. Very weak and patchy sporadic-E ionization along the path between the stations could conceivably account for the observed signal, and might not be detectable on the back-scatter equipment.

Although observations similar in many details have been made at the higher frequencies [6], it is not yet demonstrated that the same explanation would be applicable to the two cases.

Need for further investigation

Prediction of the total field strength over an oblique path due to meteoric scattering involves a number of considerations. First, the proportion of meteors following a path which satisfies the geometrical requirements for transmission of a signal must be evaluated. It is known that the radiants of sporadic meteors are not distributed entirely at random, and that the actual distribution may change from hour to hour. Further, the number of ion columns formed nearly horizontally to the earth will be small because the meteoric particle forming such a column must have survived a relatively long passage through the ionosphere. Yet nearly horizontal columns are required to produce a reflection near the mid-point of a long path.

Those meteors producing signal transmission will contribute a component whose duration is determined by the forward-scattering angle 2ϕ, and whose amplitude will be influenced by the trail orientation (whether parallel or perpendicular to a line joining the two stations). Finally, for given transmitting and receiving parameters, the per cent time that the overlapping contributions will exceed the limit of detectability must be determined.

The present uncertainties in such a calculation may be listed as follows:

(1) The per cent of all meteors producing more than 10^{14} electrons per meter of path, and hence giving rise to echoes more complicated than the simple exponential ones considered above, should be established and their effect on the calculation determined. Some excellent examples of these echoes have been shown by McKinley [7]. There may be seasonal variations in this percentage, perhaps connected with the faster annual meteor showers.

(2) It is desirable to know the number of detectable meteor echoes with greater accuracy, and particularly the variation of this number with time of day and season of the year. It is likely that the number detected will depend on frequency, being sharply reduced for radio frequencies above 30 or 40 Mc.

(3) The radiant distribution of sporadic meteors should be studied. The favored directions known to exist early and late in the day should be verified and included in more complete calculations.

It is felt that these uncertainties can be reduced by a suitable experimental program to the point where the calculations would yield an answer meriting considerable confidence.

Acknowledgment

The authors wish to express their thanks to Messrs. Rodney O. Beaudette, Ben C. Fidler, Cameron G. Pierce, and Alvin C. Haugen for their assistance in the tests involving Spokane (Washington), Tucson (Arizona), Pasadena (California), and Aberdeen (South Dakota), respectively.

References

[1] O. G. Villard, Jr., and A. M. Peterson, Instantaneous prediction of radio transmission paths, QST, **36**, 11-20 (1952).

[2] O. G. Villard, Jr., A. M. Peterson, and L. A. Manning, A method for studying sporadic-*E* clouds at a distance, Proc. Inst. Radio Eng., **40**, 992-994 (1952).

[3] L. A. Manning, O. G. Villard, Jr., and A. M. Peterson, Radio Doppler investigation of meteoric heights and velocities, J. Appl. Phys., **20**, 475-479 (1949).

[4] L. A. Manning, O. G. Villard, Jr., and A. M. Peterson, Meteoric echo study of upper atmosphere winds, Proc. Inst. Radio Eng., **38**, 877-883 (1950).

[5] Von R. Eshleman, The mechanism of radio reflections from meteoric ionization, Tech. Rep. No. 49, Electronics Research Laboratories, Stanford University (July 15, 1952).

[6] D. K. Bailey, *et al.*, A new kind of radio propagation at very high frequencies observable over long distances, Phys. Rev., **86**, 141-145 (1952).

[7] D. W. R. McKinley and P. M. Millman, A phenomenological theory of radar echoes from meteors, Proc. Inst. Radio Eng., **37**, 364-375 (1949).

HIGHER-ORDER APPROXIMATIONS IN IONOSPHERIC WAVE PROPAGATION

BY C. O. HINES

Fitzwilliam House, Cambridge, England

(Received October 3, 1952)

ABSTRACT

Because of non-linearities in the basic equations governing ionospheric wave propagation, the usual (perturbation) treatment involving a single frequency of oscillation does not provide a complete solution. The difficulty has been treated in the literature by the introduction of harmonics but, because of a misinterpretation of the mathematical symbolism, the results are not immediately applicable to the physical problem for which they were intended. A corresponding treatment, physically more appropriate, is undertaken here. Certain results of the earlier inquiry—in particular, those concerning resonance—are regained at some levels of approximation, but the general validity of the approach is found to be doubtful.

1. *Introduction*

Three non-linearities occur in the equations governing the ionosphere, even in a non-relativistic mean-value theory of homogeneous plane-wave propagation: (*A*) the macroscopic electronic current involves the product of mean particle density N with mean particle velocity $\mathbf{U}$, and both these generally vary in space and time. (*B*) The acceleration to be used is $d\mathbf{U}/dt = \partial\mathbf{U}/\partial t + (\mathbf{U}\cdot\nabla)\mathbf{U}$. (*C*) The force acting on the charge depends on $\mathbf{U} \times \mathbf{H}$, where $\mathbf{H}$, the macroscopic magnetic field, is also varying. Further, a second-order effect of the "Lorentz polarisation" type could conceivably exist, and would introduce yet another non-linearity; this possibility will be disregarded here, however.

The attendant difficulties can be removed from elementary theory by a perturbation treatment, in which the variations from static conditions are assumed small and their products negligible. However, it is of some interest to discover the results of a more complete analysis which takes full account of the non-linear terms and of their effects. To this end, J. Feinstein* undertook a treatment in which the variables had the form

$$f = \sum_{n=0}^{\infty} \{f_n \exp i\psi_n\} \quad \ldots\ldots\ldots\ldots\ldots\ldots\ldots\ldots (1)$$

where

$$\psi_n = n(\omega t - S_n x - q_n y) \quad \ldots\ldots\ldots\ldots\ldots\ldots\ldots\ldots (2)$$

*J. Feinstein, J. Geophys. Res., 55, 161-170 (1950).

[Cf. his equations (8) *et seq.*, rather than his (6), in which the left-hand parenthetical signs appear to be misplaced.] On inserting these into the basic equations, product terms in $\exp i(\psi_r + \psi_s)$ occurred and were combined with linear terms in $\exp i\psi_{r+s}$ to produce new equations: each of the original relations gave rise to an infinite number of new ones determined by the various orders of the exponentials. The amplitude coefficients of the variables could then be determined for each harmonic in turn, after beginning with constant ($n = 0$) terms and the fundamental mode ($n = 1$).

In the simple case arising when $\mathbf{U}_0 = 0$—to which we shall confine our attention in the present paper—the characteristic Appleton-Hartree equations for the fundamental mode appeared, indicating that it was unaffected by the higher-order modes. The development was carried to the second order only, but some general results found there are common to all higher orders: the values of the S_n's and q_n's are independent of n—all modes are propagated with the same phase velocity (complex, in general)—and the higher-order amplitudes appear in forced-oscillation equations, the forcing terms being dependent only on lower modes. Resonance could occur for any mode which had a characteristic refractive index equal to that of the fundamental, and hence strong ordinary-extraordinary coupling could exist at multiple frequencies.

Although mathematically correct, these results are not directly applicable to the physical problem, since, in physics, the observables must be real; complex solutions are of use in treating linear equations only because their real (and imaginary) parts are themselves solutions, but this is not the case with non-linear equations. It was thought desirable, then, to undertake a similar treatment, assuming real solutions from the start, and so determine what alterations might be in order. The new development is given, in outline only, in the following sections.

2. *Solutions for real phase angles*

We shall begin with the propagation of homogeneous plane waves through a homogeneous non-absorbing medium, with a real above-critical frequency of the fundamental mode. The phase angles ψ_n are then real and, by a reorientation of axes, may be written as

$$\psi_n = n(\omega t - qz) = \psi_n^* \qquad (3)$$

In this, we anticipate one of the conditions of validity by introducing a single q rather than a sequence of q_n's; the asterisk is used to denote a complex conjugate.

The variables are assumed to have the real form

$$f = \frac{1}{2}\sum_{n=0}^{\infty}\{f_n \exp i\psi_n + f_n^* \exp - i\psi_n\} \qquad (4)$$

and, in this form, may be introduced into the basic equations governing ionospheric propagation. The product terms which then occur are of two types—those found in $N\mathbf{U}$ and $\mathbf{U} \times \mathbf{H}$, with the general form

$$\left.\begin{aligned} 4AB = \sum_{n=1}^{\infty}\left\{\left(\sum_{r=0}^{n} A_r B_{n-r} + \sum_{r=0}^{\infty} A_r^* B_{n+r} + \sum_{r=n}^{\infty} A_r B_{r-n}^*\right)\exp i\psi_n\right\} \\ + \sum_{n=1}^{\infty}\{(\cdots)^* \exp - i\psi_n\} + A_0 B_0 + A_0^* B_0^* + \sum_{n=0}^{\infty}\{A_n^* B_n + A_n B_n^*\} \end{aligned}\right\} \qquad (5)$$

and those resulting from the components of $(\mathbf{U}\cdot\nabla)\mathbf{U}$, having the form

$$\left.\begin{aligned} 4A\partial B/\partial z = &-iq\sum_{n=1}^{\infty}\left\{\left[\sum_{r=0}^{n}(n-r)A_rB_{n-r}+\sum_{r=0}^{\infty}(n+r)A_r^*B_{n+r}\right.\right.\\ &\left.\left.-\sum_{r=n}^{\infty}(r-n)A_rB_{r-n}^*\right]\exp i\psi_n\right\}\\ &+iq\sum_{n=1}^{\infty}\{[\cdots]^*\exp -i\psi_n\}-iq\sum_{n=1}^{\infty}\{nA_n^*B_n-nA_nB_n^*\}\end{aligned}\right\}\quad\ldots.(6)$$

In addition to the sum-frequency products which entered Feinstein's work, we here find difference-frequency terms, resulting from the use of real solutions. (Cf. explicit products of sines and cosines.) These difference-frequency effects—mentioned physically by Feinstein, but absent from his mathematics—produce a complete alteration in the further development of the method. We obtain an infinite set of new relations as before, by separating out the various exponentials in turn, but this set can no longer be solved step by step from the lowest orders upwards. Instead, the interaction of high harmonics to produce lower ones results in a complete intertangling of amplitude coefficients of all orders, and prevents their sequential determination; the whole infinite quadratic set must be solved simultaneously.

In practice, of course, we can only attempt some approximation method, for the problem would otherwise be beyond solution. The most appropriate method which occurred to the author was the following: Consider an n^{th}-order amplitude coefficient as being a small quantity of order n, and disregard all small terms of some order $m+1$ and higher, as an m^{th}-order approximation. If this is done, then the set becomes finite (since all equations resulting from above-m^{th}-order modes may be ignored) and each equation contains only a finite number of terms (since difference terms resulting from the interaction of r and s modes can be neglected if $r+s>m$); a solution can then be determined with a finite amount of labour. This procedure is suggested by the more usual perturbation method and by the fact that, in Feinstein's development, successive amplitude coefficients were found to decrease in magnitude by ratios of the order particle-speed/phase-speed.

This approach works well in the first approximation ($m=1$), which yields the perturbation formulae and the standard Appleton-Hartree relations for ionospheric propagation. In the second order ($m=2$), Feinstein's results are regained: the Appleton-Hartree formulae still govern the fundamental mode, and resonance can occur in the second. [The driving force must, however, be altered to take account of the $(\mathbf{U}_1\cdot\nabla)\mathbf{U}_1$ term which was omitted from his equation (5*b*).] The zero-order (constant) values must undergo a slight change from those normally contemplated, however, due to second-order interactions; for example, the terms $N_1^*\mathbf{U}_1+N_1\mathbf{U}_1^*$ lead to a constant electronic current which must be balanced by a compensating current of positive charge or by relaxing the $\mathbf{U}_0=0$ condition.

In the third-order approximation ($m=3$), new difficulties arise. The first and second modes then interact to produce a first-mode term of a magnitude which is no longer to be neglected. The relations which previously yielded the fundamental dispersion equation as a condition for solution become, by this interaction, quad-

ratic in the amplitude coefficients, and they can only be solved in conjunction with similar relations resulting from the second mode—those that previously gave a forced oscillation and a possible resonance. The amplitude coefficients of the first two modes and the phase speed are, then, mutually dependent; no self-contained dispersion equation, governing the wave motion, can be obtained. The third mode is, however, in forced oscillation, and can exhibit resonance under suitable circumstances.

A similar situation obtains in all higher orders of approximation; in the m^{th}, it is found that the m^{th} mode is driven by the lower ones, does not affect them, and can become resonant, while the amplitude coefficients of the lower modes are completely intertangled, together with ω and q, in a set of quadratic equations.

From the form of the exact equations, it would appear that the difficulties encountered here are inherent in the form of solution assumed, and not simply in a poor (and possibly illegitimate) approximation procedure. Whether or not this is so, we shall now discover that the whole approach can have little general validity, for absorption inevitably occurs, and then the method appears to break down completely.

3. *Solutions for complex phase angles*

Consider a wave, traversing an absorbing medium (or at a frequency below the critical), for which the phase angles are

$$\psi_n = n(\omega t - q_R z - i q_I z) \quad \ldots\ldots\ldots\ldots\ldots\ldots\ldots\ldots (7)$$

with ω, q_R , and q_I real and independent of n, and $q_I \neq 0$. Solutions of the form

$$f = (1/2) \sum_{n=0}^{\infty} \{f_n \exp i\psi_n + f_n^* \exp - i\psi_n^*\} \quad \ldots\ldots\ldots\ldots (8)$$

may be assumed, and may be inserted into the basic ionospheric equations.

We now proceed as before, deriving an infinity of sets of equations by separating out those terms which, for each n in turn, contain the common factor $\exp in(\omega t - q_R z)$—a factor which may subsequently be cancelled out. The die-away factor $\exp nq_I z$, which results from linear and sum-frequency terms, could likewise be cancelled in Feinstein's development, leaving quadratic relations between the constant amplitude coefficients as before. But such a procedure is now impossible, for the difference-frequency terms contain die-away factors of the form $\exp (2r \pm n)q_I z$, with r ranging over an infinite set of integers. This situation demands a further subdivision: each equation yields a new infinite set, determined by extracting each type of die-away in turn. As a result, a two-fold infinity of conditions is imposed on the one-fold infinity of amplitude coefficients, and an incompatibility results unless the latter vanish, leaving a useless solution.

The situation is somewhat relieved by assuming

$$\psi_n = n(\omega t - q_R z) - i q_I z \quad \ldots\ldots\ldots\ldots\ldots\ldots\ldots\ldots (9)$$

with ω, q_R , and q_I again real and independent of n. This leads to terms of only two types—containing $\exp q_I z$ (from linear terms) or $\exp 2q_I z$ (from products)—in each equation. This is the best we can do, but it still produces twice too many conditions, and we are again reduced to vanishing variations. It would therefore appear that the present approach to the problem of nonlinearities cannot generally be applied.

AN IONOSPHERE RECORDER FOR LOW FREQUENCIES

By J. C. Blair, J. N. Brown, and J. M. Watts

Central Radio Propagation Laboratory, National Bureau of Standards, Washington 25, D. C.

(Received October 10, 1952)

ABSTRACT

Application to the low frequency case of techniques heretofore used in high frequency ionosphere recorders is described. The beat frequency method of generating wide frequency sweeps is used, covering frequencies from 50 kc to 1,000 kc in a short time without band switching. Advantage is gained by the use of transformers containing ferromagnetic cores in the wide-band transmitter amplifiers, but the antenna system, for practical reasons, is very inefficient. Sample records are shown.

The development of equipment for investigating ionosphere characteristics at low frequencies is a logical addition to the radio propagation research program of the National Bureau of Standards. Since the early days of radio, the communications industry has been expanding into the high frequencies, so that interest in the low frequencies lagged. Recently, however, attention has been drawn to frequencies below 1 Mc, not only by the need for more communications channels, but also by the possibility of greater reliability at very low frequencies, and by the proposals of new kinds of radio navigation and location systems using both pulse and phase measuring schemes at low frequencies.

Regular sweep-frequency measurements of ionosphere virtual heights have been made at the National Bureau of Standards since 1933. However, with the exception of recordings made with apparatus now obsolete, all the available records are of frequencies above 1 Mc. The high frequency equipment now used by the National Bureau of Standards nominally includes frequencies from 1 to 25 Mc [see 1 of "References" at end of paper].

The work on low frequencies was started in 1949. By early 1950, a pulse transmitter was completed which was operated on a fixed frequency basis. That transmitter was of the master oscillator-power amplifier type, using four type 527 tubes in the output stage. It was capable of delivering pulses of over one megawatt power with a duration of about 100 microseconds. As soon as it was available, a series of experiments were performed, at first on an exploratory basis. Vertical-incidence reflections were obtained at 37 kc, which is believed to be the lowest frequency at which such an experiment has been successful. Other frequencies tried were 50 kc, 100 kc, and 160 kc. However, the results of these experiments were not of sufficient value to describe the relation between apparent reflection height and frequency, which is one of the important parameters used in ionospheric analysis.

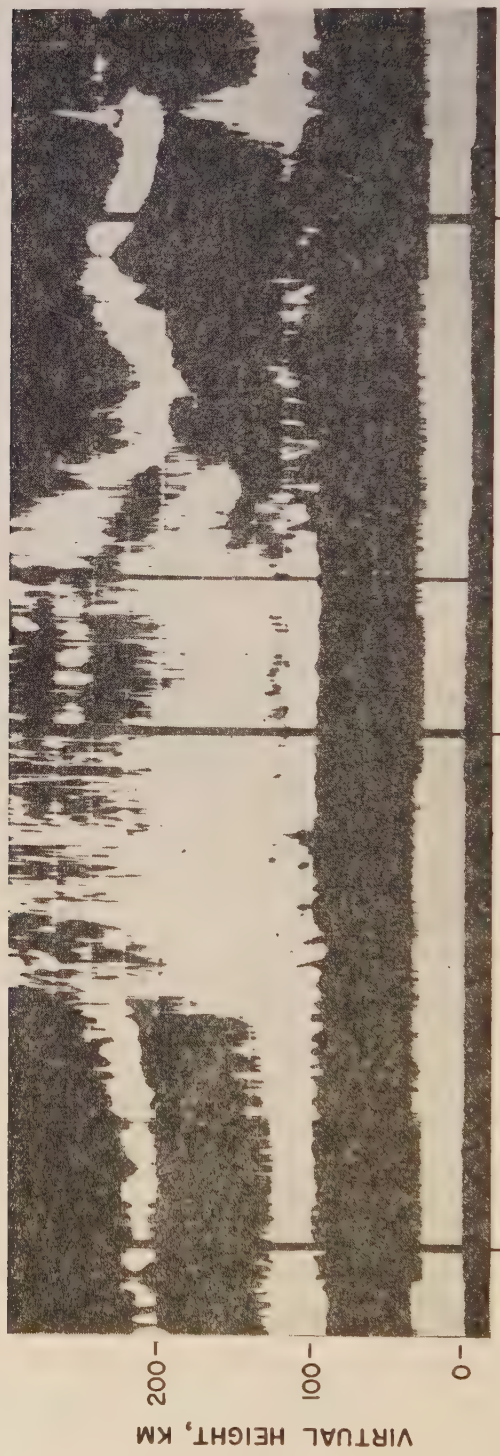

FIG. 1—VARIATION OF REFLECTION HEIGHT WITH TIME AT 160 KC

Figure 1 shows an example of the variation of reflection height with time at 160 kc. The complicated structure exhibited at times on this type of recording seemed to have a dependence upon the degree of geomagnetic activity [2], time of day, and frequency. Records made at 100 kc and below were, in general, less complicated than those made at 160 kc. However, the variation from day to day was so large, and the characteristics at times were so complicated, that single frequency data demonstrated primarily the great desirability of performing the more elaborate sweep-frequency type of exploration.

Design and assembly of a sweep-frequency apparatus were begun in late 1950.

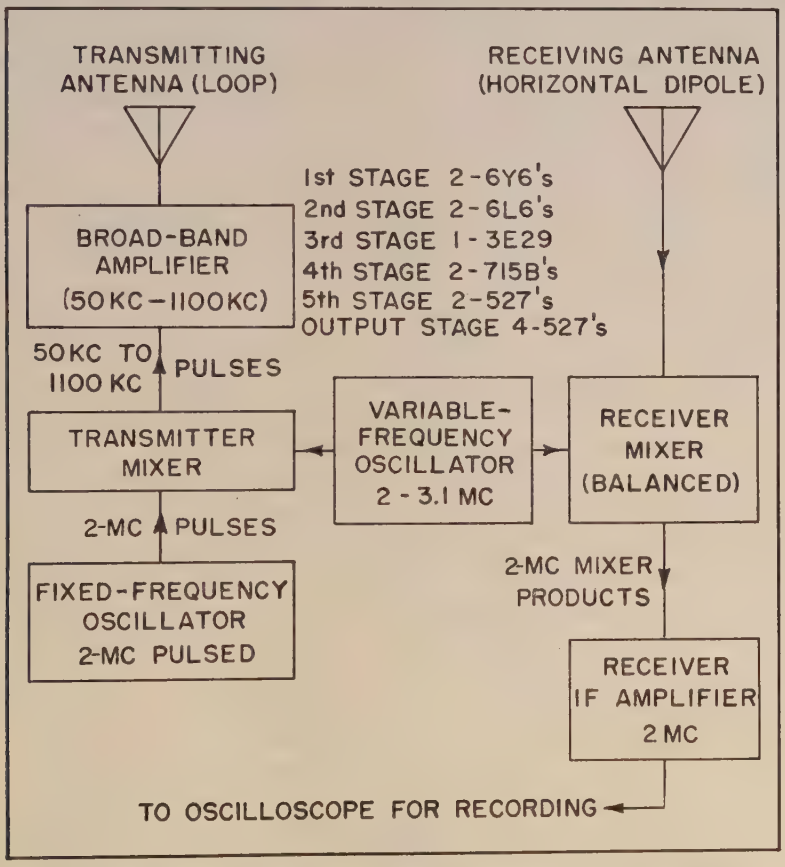

FIG. 2—ELEMENTARY BLOCK DIAGRAM OF SWEEP-FREQUENCY TRANSMITTER AND RECEIVER

A description of the system, which was put into operation in December, 1951, follows.

The principles first used by T. R. Gilliland in 1924 [3] and by P. G. Sulzer [4] for high frequency ionosphere recorders were adopted, since the advantages of mechanical simplicity and low cost were not to be ignored. The transmitter consists of a series of wide-band amplifiers fed by the output of a mixer. The mixer produces the beat frequency between two oscillators, one a continuous-wave oscillator vari-

able in frequency from 2 Mc to 3.1 Mc, the other a pulsed oscillator at a fixed frequency of 2 Mc. A block diagram of the transmitter and receiver arrangement is shown in Figure 2. As in Sulzer's equipment, the variable-frequency oscillator is used as the converting oscillator in the receiver mixer, so that reflected pulses are automatically converted to 2 Mc, which is the i.f. frequency of the receiver. There is a slight detuning during a sweep because of the elapsed time during the pulse travel to the ionosphere and back, but for the sweep speeds and band width used this is negligible.

In some ways, the design of the low frequency equipment was less difficult than the design of the high frequency equipment. The band width is only about 1 Mc compared to 25 Mc. Also, the low frequencies permit the use of ferromagnetic cores in all transmitter stages. Therefore, push-pull operation with appreciable inductive coupling between the plate circuits is possible, which allows the high power stages to operate Class B with reasonably good waveform. Several sizes of thinly laminated, grain oriented, steel cores were available, as well as small standard size ferrite cores which were originally designed for use in television deflection circuits. Successful transformers could be made from all of these, but there are indications that ferrite cores are more efficient. Of particular interest is the output transformer of the last stage. The only core immediately available which was large enough for the power level delivered by the push-pull parallel 527 tubes was a Type C hypersil core composed of 0.005-inch strip. The core losses are so high that enough heat is generated to destroy the polyethelene insulation of the winding if prolonged operation is attempted. Procurement of a ferrite core large enough for this power level should increase the output power by a considerable amount.

Adjustment was made for flatness of over-all transmitter response with a dummy load of 500 ohms connected. Since there are six stages, identical frequency response characteristics in each stage would produce an over-all response of greatly exaggerated unevenness. For this reason, each stage was adjusted separately while

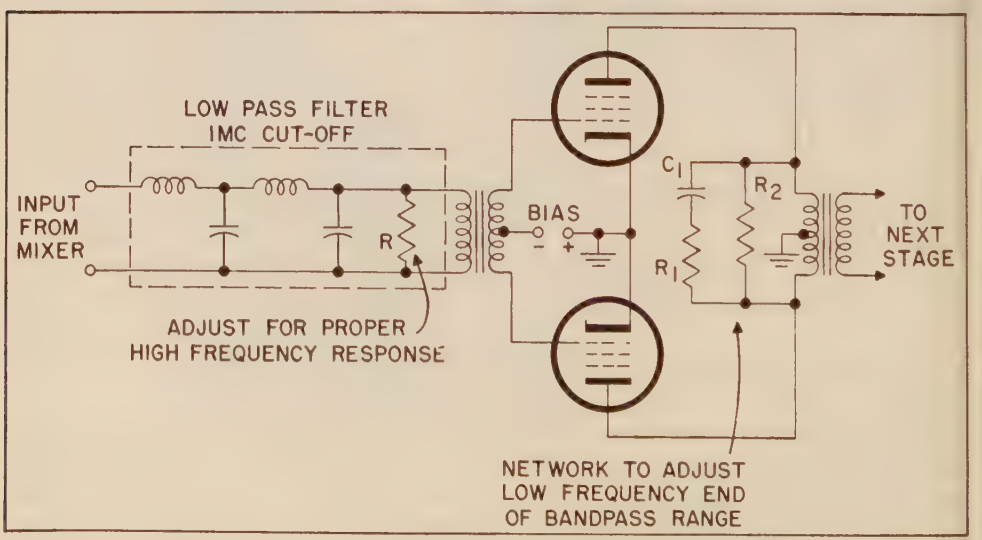

FIG. 3—EXAMPLE OF EQUALIZING USED IN TRANSMITTER

observing the over-all response at the driver stage output. Figure 3 shows the broad-band amplifier succeeding the transmitter mixer stage. It is compensated in two ways, as follows:

(1) The resistance, R, terminating the low pass filter is adjusted to mismatch the filter, thus causing a peak in the filter output at the cut-off frequency (1 Mc). The size of the peak is adjusted by varying R. By this means alone, the high frequency power output of the driver stage is made slightly greater than in the mid-frequency range.

(2) The plate circuit of Figure 3 contains C_1 , a capacitor large enough to tune out the open circuit inductance of the transformer at approximately 50 kc. R_1 is inserted to reduce the resonant circuit Q to approximately 2, and R_2 provides a small amount of loss at all frequencies to improve the waveform delivered by the beam power tubes.

Similar equalization in other stages is satisfactory for producing a response which is almost perfectly flat from 50 kc to 1 Mc, measured at the grids of the final amplifier. The power delivered by the final amplifier into a 500-ohm resistive load is shown as a function of frequency in Figure 4.

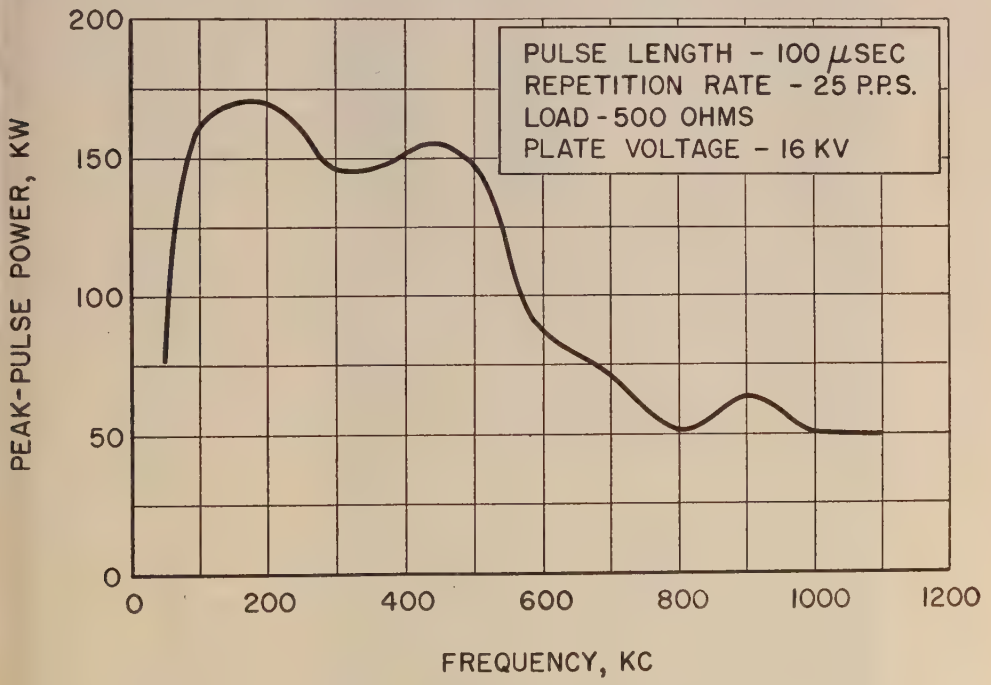

FIG. 4—POWER OUTPUT OF TRANSMITTER INTO DUMMY LOAD

A single antenna which would perform efficiently through the entire frequency sweep is not practical. The dimensions of such a system would be of the order of a half wavelength at the lowest frequency (9,830 feet at 50 kc), and the broad-band wave antennas such as rhombics, V-type, and deltas are out of the question, since the desired direction of transmission is vertical. Older types of high frequency

FIG. 5—SAMPLE NIGHT RECORD MADE BY SWEEP-FREQUENCY RECORDER, MARCH 28, 1952, AT 0015

ionospheric recorders used a series of horizontal dipoles, each broad-banded by using a cage-type construction which made the effective diameter large. Several of these of different lengths and heights were switched in sequence throughout the frequency sweep to produce a relatively constant radiated power. This system would probable be feasible for low frequency work, but it still is expensive in land and materials compared to the single loop antenna which is used. This loop is suspended between two vertical supports, and is approximately 350 feet long and 150 feet high. An idea of the efficiency of this antenna is given by the calculated radiation resistance in free space, which is approximately 13 milliohms for the one-turn loop at 100 kc. Measurement of peak-pulse antenna current at this frequency indicates that the radiated power is probably in the order of 5 watts. In spite of this, reflections are frequently recorded at 100 kc during the night hours.

Since the antenna efficiency decreases with frequency, it is fortunate that ionospheric absorption also decreases with frequency at low frequencies (below about 1.2 Mc). However, they obey completely different laws since, as the frequency is lowered, the antenna radiation resistance decreases much faster than does ionospheric absorption.

The record of apparent reflection height *versus* frequency is made in the conventional way by intensity modulation of an oscilloscope beam to which a line deflection type of time base is applied. The line thus produced is photographed by a camera, the film of which moves in synchronism with the frequency-change motor of the transmitter and in a direction of travel perpendicular to the time base line. Figure 5 is an example of one such record made at night. A considerable advantage is derived from the ability of the film to integrate, since the time base sweeps overlap. This has the effect of discriminating against random interference, such as modulated signals, static, etc., yet retaining the desired pulse signals which are correlated with the start of the time base. The fact that low frequency transmitting stations almost always use vertically polarized antennas has been utilized in the receiving antenna design. This antenna is a low, horizontal dipole which is very effective for reception of downcoming signals, but which has low sensitivity to the nearly vertically-polarized interfering signals. Despite these advantages, the effective sensitivity of the receiver is lowered greatly at some frequencies due to the presence of interfering stations. One interfering signal, which comes from a radio range transmitter only three miles distant, effectively blocks the receiver in spite of the antenna orientation and the use of a special shielded input transformer. The records of Figures 5 and 6 show no ionospheric reflections near 232 kc because of this station. The standard broadcast band, beginning at 550 kc, causes some interference, but not as much as had been anticipated. The part of the records below 100 kc is blank because the receiver i.f. amplifier is partly blocked by the strong signal from the variable-frequency oscillator, which is not completely balanced out in the receiver mixer. Pips from a 7,500-cps oscillator form the horizontal markers, which represent 20-km intervals in apparent height. The direct pulse from the transmitter forms the uneven trace at the bottom. Frequency marks at 100-kc intervals, plus one mark at 50 kc, show as vertical lines. These are produced by a cam-operated microswitch at the frequency change mechanism.

Interpretation of the actual records is beyond the scope of this article, but a

FIG. 6—SAMPLE DAY RECORD MADE BY SWEEP-FREQUENCY RECORDER, MARCH 27, 1952, AT 1606

comparison of Figure 5, which is a typical night-time record, with Figure 6, a daytime example, indicates the usual type of diurnal variation. Traces labelled "*A*" in both records are from the ionospheric *E* region. The extraordinary component of the *F* layer, "*B*", and the ordinary component, "*C*", appear only at night. Occasionally, at night, there appears between the *E*- and *F*-layer traces another trace or group of traces which seems to be very similar to what have been called *E*2-layer traces when observed on the conventional daytime high frequency ionosphere records; the night-time characteristics of this are still to be determined.

References

[1] J. M. Carroll, Automatic ionosphere recorder, Electronics, **25**, 128-131 (1952).
[2] J. M. Watts and J. N. Brown, Effects of ionosphere disturbances on low frequency propagation, J. Geophys. Res., **56**, 403-408 (1951).
[3] T. R. Gilliland and A. S. Taylor, J. Res., Nation. Bur. Stan., Washington, **26**, 377-384 (1941).
[4] P. G. Sulzer, Ionosphere measuring equipment, Electronics, **19**, 137-141 (1946).

GEOMAGNETIC AND SOLAR DATA

INTERNATIONAL DATA ON MAGNETIC DISTURBANCES, THIRD QUARTER, 1952

Preliminary Report on Sudden Commencements

S.c.'s given by five or more stations are in italics. Times given are mean values, with special weight on data from quick-run records.

Sudden commencements followed by a magnetic storm or a period of storminess (s.s.c.)

1952 July *01d 20h 32m:* twenty-six.

1952 August *15d 20h 04m:* eighteen.—*17d 01h 22:* seven.

1952 September 07d 17h 55m: So Ci.—20d 19h 40: SM Ci.—*25d 15h 15:* twelve.—*28d 15h 25:* five.

Sudden commencements of polar or pulsational disturbances (p.s.c.)

1952 July 04d 04h 30m: SM Va.—06d 06h 54: Eb Te El Hr.—08d 01h 13: Tl Va.—09d 01h 57: CF Va.—14d 22h 00: Tr Le Wn.—14d 23h 35: CF Ci Eb.—15d 22h 00: Tr Wn CF.—15d 22h 32: El Hr SM.—17d 03h 40: CF SM Va.—18d 02h 34: CF Tl.—20d 00h 00: Wn CF Eb Tl.—20d 00h 40: CF SM.—20d 00h 59: Tl Hr Am SF.—22d 23h 08: CF Hr.—23d 21h 06: SM Tl.—*24d 00h 14:* six.—27d 21h 25: So CF.—*27d 22h 01:* seven.—31d 02h 38: Ni Tl El Hr.

1952 August 01d 02h 40m: SM Va.—*01d 19h 19:* five.—02d 18h 05: SM Ci.—*02d 22h 40:* twelve.—04d 01h 10: Wn SM SF Hr.—*07d 00h 12:* six.—*07d 23h 28:* eight.—*09d 18h 12:* five.—10d 00h 40: Wn Ci Va.—11d 01h 42: Wn CF Fu Ci.—*11d 21h 45:* six.—*12d 00h 44:* five.—12d 20h 03: Wn CF Fu Hr.—12d 20h 15: Tr Ci.—*15d 01h 05:* eight.—*18d 17h 43:* five.—18d 21h 20: Tr Fu.—20d 21h 38: Wn CF Fu.—21d 20h 17: So Wn.—23d 00h 57: Wn Fu SM.—23d 01h 32: Hr Le.—26d 20h 34: So Wn.—29d 20h 40: Tr Fu.—30d 20h 24: Tr So.—30d 20h 47: Wn CF.

1952 September 01d 11h 28m: Ka Am.—*01d 22h 36:* nine.—02d 07h 30: Am Ci.—02d 19h 12: So Wn.—*02d 21h 27:* six.—*03d 21h 33:* six.—04d 18h 33: Tr So Wn.—*07d 04h 00:* six.—*08d 19h 47:* five.—09d 19h 13: Tr Wn.—09d 21h 21: Le Wn Hr.—10d 23h 18: Wn CF.—10d 23h 55: SF Ta.—11d 20h 33: Tr Tl.—11d 21h 33: Eb Ci SM.—14d 03h 30: Ci SM Ta.—14d 15h 24: Ka Ta.—14d 22h 32: Ci Ta.—15d 23h 06: CF Ta.—16d 20h 38: Tr So.—16d 21h 14: Es SM.—17d 21h 54: Tr So Wn.—21d 00h 31: Hr Ta.—21d 23h 21: Wn Hr.—24d 22h 39: Wn Tl Hr Ta.—*24d 22h 52:* six.—27d 08h 33: Ka Am.—28d 22h 50: SM Hr.—29d 05h 28: SM Va.—29d 23h 29: Ci Hr.

Sudden impulses found in the magnetograms (s.i.)

1952 July 01d 21h 27m: four.—05d 10h 42: Ci El.—05d 18h 46: Ci Te Tn.—06d 10h 06: SM El.—13d 15h 00: Ka To.—16d 18h 44: So Wn.

1952 August *21d 09h 30m:* five.—26d 18h 42: Es Wn Ma.—30d 05h 34: SF El.

Geomagnetic planetary three-hour-range indices Kp, preliminary magnetic character-figures, C, and final selected days, July to September, 1952

July 1952									
E	1	2	3	4	5	6	7	8	Sum
1	1+	1+	1+	1+	1+	1−	5−	6o	18o
2	3−	2+	2−	3o	1+	1+	1o	2−	15o
3	2o	2o	2−	2−	3+	4−	3o	2+	20−
4	2o	3−	2+	2+	3−	3+	1o	2o	18+
5	3o	5o	5+	5o	6−	6−	6+	5−	41−
6	3o	5−	6+	4−	3o	2o	2o	2o	27−
7	3−	2o	3o	2+	2−	3−	2−	1−	17−
8	1−	2−	2+	2o	4o	3o	2o	3−	18+
9	3o	3−	4o	5o	3+	4o	3+	3o	28+
10	2+	4−	3+	4−	3+	5−	4o	3+	28+
11	4−	4o	4−	2−	2+	2o	2o	1−	20o
12	2+	2+	3−	3o	2o	1−	1o	2+	16+
13	1+	2o	1+	2o	3−	4−	3−	1+	17o
14	3o	3o	3−	3−	3o	4−	2o	3o	23o
15	3o	4o	3−	3+	3−	3o	2+	3+	24+
16	2+	3−	3−	2o	3−	2−	2o	1+	17+
17	1−	2+	2+	2−	2−	2+	2+	3−	16o
18	2−	3−	2−	2+	3−	2−	2−	2o	16+
19	1+	1−	1−	1+	2o	1o	2o	2o	11o
20	2+	2+	2+	6−	5+	4+	4+	5o	32−
21	4o	6−	5o	5o	6o	5o	4+	4+	39+
22	4+	3o	3o	3+	2o	2o	3+	4−	25−
23	3−	2+	3−	2o	2o	3−	2o	3+	20−
24	3o	2−	1o	2+	2o	3o	3−	3−	18+
25	1+	1+	2−	2+	3−	3+	3o	3o	19−
26	4−	3+	3o	2+	2+	2−	1o	1+	19−
27	2+	0+	1−	1o	2o	2o	2−	4+	14+
28	2o	2−	2−	1o	1−	1o	2o	0+	10+
29	0o	0+	0+	0+	1−	1−	1+	1o	5−
30	1o	0+	0+	1o	1−	0+	1−	1+	6−
31	2+	2−	4+	4o	4−	3+	3o	2o	24+

August 1952									
E	1	2	3	4	5	6	7	8	Sum
1	2+	3o	2+	2−	2o	1+	3o	2o	18−
2	3−	2o	2−	2−	2+	2−	3+	3o	18+
3	2−	4+	5−	4o	6−	5o	3−	2+	30+
4	3o	3+	3+	2o	2+	3−	4o	4o	25−
5	4−	3−	3−	3o	1+	3−	3−	2+	21o
6	5−	5−	4o	3o	2+	3−	2+	3−	26+
7	4o	3−	4o	2o	2+	1o	2o	3o	21o
8	3−	3−	3−	2+	2+	1+	2o	2o	18o
9	1o	1+	1+	1+	2−	1+	3o	3−	14−
10	4+	3−	2o	3−	4+	4−	3o	2+	25o
11	4−	2o	1+	3−	3+	2−	2+	4o	21o
12	5o	2+	3o	3+	3o	4o	4−	2+	27−
13	1+	2o	2+	2−	2−	2−	1−	1o	12+
14	1+	2o	1+	1+	1+	1−	1+	1−	10o
15	2o	1−	0+	1−	1−	1o	3o	3o	11+
16	3−	3−	1+	1o	0+	0+	0+	0+	9o
17	2+	3o	4+	5+	5−	4−	5+	4−	32+
18	5o	4+	3+	3−	4−	5−	4+	5o	33o
19	4o	4−	3−	3+	2+	3+	2o	2−	23o
20	3o	4+	4−	4−	3o	2+	2+	3+	26−
21	2o	1o	1o	3−	1+	2−	1+	1o	12o
22	1−	1−	2−	2−	1−	1+	1+	3−	11−
23	4o	2+	1+	2−	2−	2o	2o	1o	16o
24	1o	1+	3−	2o	1o	2−	1+	0+	11+
25	0o	1−	1+	2−	2o	1o	1o	1o	9−
26	1−	2−	1o	2o	1o	1o	2−	2o	11o
27	3o	3−	4o	3o	1+	2−	2−	1+	19−
28	2o	3−	1+	1−	0+	1o	1−	1−	9+
29	2−	1o	1+	2−	2+	4o	4o	4o	20o
30	5−	6−	5−	2−	2−	3−	3o	3−	27−
31	1+	3+	1+	2+	2+	1o	2o	4o	17+

September 1952									
E	1	2	3	4	5	6	7	8	Sum
1	6−	5+	6−	5+	4o	5−	4o	6−	40+
2	4+	5−	6o	5−	5o	4−	4−	4+	36+
3	4−	5−	4o	5−	3−	4−	3−	4o	30o
4	3−	3−	3o	3−	3o	2+	3−	1+	20+
5	3−	2−	3−	3o	3+	5−	4−	4−	25+
6	4−	4o	3+	2+	2o	3−	3−	3−	23+
7	1+	5−	4o	1+	2+	3o	5+	6+	28+
8	6o	6−	6−	5+	4+	5o	5+	6−	43o
9	5o	6−	5+	6o	4−	5+	4o	5o	40o
10	5−	4+	5−	4o	3+	1+	2o	3−	27o
11	3+	3−	2+	3o	3o	3−	2o	3+	22+
12	4−	4o	3+	3o	4o	3+	4o	3o	28+
13	1+	2−	1+	2−	1+	1o	1+	2o	12−
14	3+	5o	3+	4−	4o	5−	3+	3+	31−
15	3−	2−	2o	3o	3−	3−	3o	3+	21o
16	3−	2+	2−	3−	2+	1+	2−	3+	18o
17	2+	1+	2−	2o	3−	1o	1−	2−	13+
18	1+	1+	2−	1o	1−	1−	2−	1+	10−
19	1−	0o	1o	1−	1o	1+	1−	2−	7o
20	1+	1−	2−	1−	2−	2−	3+	4+	15+
21	6−	4−	2−	2o	1+	1+	2−	2o	19+
22	2+	3+	2o	1+	2−	1o	1+	1o	14o
23	1+	2−	1o	1o	2−	1+	1−	0+	9o
24	1o	2o	3−	2+	2+	4−	2+	3+	20−
25	2o	1−	1−	1−	1o	3−	3+	5+	16+
26	6−	6−	4o	2o	2−	1o	2o	1−	23−
27	2o	5o	5−	5−	4−	3+	2o	1+	27−
28	3−	4−	4+	5−	3+	4o	6o	5+	34o
29	5+	6o	6−	6o	5+	3+	6o	7o	45−
30	7+	5+	4−	6−	3+	4+	4−	2+	36−
31									

Preliminary *C*. 1952		
July	Aug.	Sep.
0.9	0.5	1.6
0.3	0.7	1.4
0.6	1.2	1.1
0.5	0.9	0.7
1.6	0.8	1.1
1.1	1.0	0.7
0.4	0.9	1.2
0.5	0.5	1.5
1.0	0.4	1.5
1.0	0.9	1.1
0.6	0.8	0.8
0.2	1.0	1.0
0.6	0.2	0.2
0.7	0.0	1.2
0.7	0.6	0.7
0.4	0.1	0.6
0.4	1.4	0.2
0.4	1.3	0.1
0.1	0.9	0.0
1.3	1.0	0.6
1.4	0.4	0.9
0.9	0.4	0.2
0.7	0.6	0.0
0.6	0.4	0.8
0.7	0.2	1.0
0.8	0.2	1.1
0.7	0.6	1.1
0.2	0.0	1.4
0.0	0.9	1.7
0.0	1.1	1.5
0.8	0.6	

Final selected days		
July	Aug.	Sep.
Five quiet		
2	14	13
19	16	17
28	25	18
29	26	19
30	28	23
Five disturbed		
5	3	1
6	12	8
9	17	9
20	18	29
21	30	30
Ten quiet		
2	9	4
7	13	13
12	14	15
16	16	16
17	21	17
18	22	18
19	24	19
28	25	20
29	26	22
30	28	23

1952 September 07d 07h 15m: SM Hr.—*12d 14h 20:* seven.—*20d 21h 47:* six.—24d 17h 42: Hr Ta.—*29d 20h 17:* fifteen.

Preliminary Report on Solar-flare Effects

Effects confirmed by ionospheric or solar observations are in italics.

1952 July 05d 18h 47m–19h 24m: Ch SJ.—11d 13h 16–13h 21: SM.—*12d 14h 50–15h 00:* CF.—13d 16h 29–17h 45: Tu.—*16d 09h 19–09h 40:* CF.—16d 14h 05: Hu.—17d 08h 15–08h 21: SM.—17d 20h 09: Tu.—18d 18h 07: Tu.—*23d 10h 54–11h 04:* CF.—28d 13h 30: Tu.

1952 August 04d 11h 20m–11h 30m: SM.—05d 11h 10: El.—13d 09h 50–09h 55: SM.—19d 16h 09–16h 15: SJ.—20d 15h 38–15h 46: SJ (s.i. after Es).—26d 18h 42: Ma (s.i. after Es and Wn).

1952 September *01d 12h 40m–12h 50m:* CF.—09d 10h 23: Ci.—10d 14h 42: Hu Va.—10d 21h 27–22h 54: Tn.—11d 12h 20–12h 30: SM.—12d 14h 20–14h 30: SJ.—13d 09h 09–09h 12: SM.—21d 09h 00-09h 09: SM.—*21d 12h 17–12h 35:* Wi CF Hr Wn.—*24d 12h 20–12h 30:* CF.

Ionospheric or solar disturbances without clear geomagnetic effect

1952 August 07d 06h 19m–06h 23m: CF.—07d 07h 44–08h 04: CF.—07d 08h 36–08h 44: CF.

Committee on Characterization of Magnetic Disturbances

J. Bartels, *Chairman*
University
Göttingen, Germany

J. Veldkamp
Kon. Nederlandsch Meteorologisch Instituut
De Bilt, Holland

CHELTENHAM THREE-HOUR-RANGE INDICES K FOR OCTOBER TO DECEMBER, 1952

[$K9$ = 500γ; scale-values of variometers in γ/mm: D = 5.4; H = 2.5; Z = 4.2]

Gr. day	October 1952		November 1952		December 1952	
	Values K	Sum	Values K	Sum	Values K	Sum
1	4432 2122	20	4322 3336	26	1233 3343	22
2	2322 3233	20	4432 3331	23	4422 5445	30
3	3431 2244	23	3233 1212	17	3443 2233	24
4	5554 3436	35	2131 1120	11	6333 3344	29
5	4465 5542	35	2212 1112	12	4434 3242	26
6	5454 3322	28	1333 2322	19	2321 2122	15
7	1233 2212	16	3322 2334	22	2122 1121	12
8	4212 3235	22	2332 2334	22	2121 1101	9
9	4212 1233	18	3321 2222	17	1010 0110	4
10	2322 1343	20	0011 0220	6	2221 2222	15
11	3323 2335	24	1111 0222	10	1333 2232	19
12	5442 2223	24	1011 1111	7	1133 3221	16
13	3211 2123	15	2000 0011	4	4455 4132	28
14	3431 1111	15	2221 2123	15	1201 1013	9
15	1100 1222	9	2333 1231	18	2223 2212	16
16	1322 2222	16	1132 3212	15	2312 2222	16
17	4431 2322	21	2122 2343	19	3332 0112	15
18	3453 2332	25	1222 2122	14	2321 1232	16
19	2134 1111	14	2211 2111	11	3000 2211	9
20	3222 2112	15	2112 2222	14	2211 1111	10
21	0013 4433	18	3354 3322	25	1221 1111	10
22	1212 1000	7	4333 2321	21	2112 2211	12
23	1011 1111	7	4442 2100	17	0011 0012	5
24	1010 0010	3	1123 2211	13	3324 4343	26
25	0113 2334	17	3113 2111	13	3534 3121	22
26	6435 4334	32	0133 1356	22	3322 2222	18
27	3332 1223	19	3355 5334	31	3332 1235	22
28	4322 2221	18	4343 3333	26	3322 3345	25
29	3212 3233	19	2122 2233	17	5434 3543	31
30	4522 3445	29	3132 2322	18	4434 3435	30
31	5465 4324	33			4243 3434	27

Ralph R. Bodle
Observer-in-Charge

Cheltenham Magnetic Observatory
Cheltenham, Maryland, U.S.A.

PROVISIONAL SUNSPOT-NUMBERS FOR OCTOBER TO DECEMBER, 1952

(Dependent on observations at Zurich Observatory and its stations at Locarno and Arosa)

Day	Oct.	Nov.	Dec.
1	20	14	13
2	23	12	12
3	22	7	14
4	42	0	16
5	33	9	22
6	37	13	32
7	37	32	38
8	23	30	50
9	26	30	38
10	24	26	28
11	16	23	34
12	15	16	40
13	15	18	47
14	14	22	63
15	11	23	71
16	10	15	67
17	0	28	67
18	0	35	66
19	8	43	66
20	15	47	50
21	25	42	40
22	27	39	35
23	35	35	35
24	33	30	29
25	37	28	18
26	40	17	36
27	34	14	15
28	33	8	0
29	32	0	7
30	26	7	9
31	22		16
Means.....	23.7	22.1	34.6
No. days.....	31	30	31

Mean for quarter: 26.9 (92 days)
Mean for year 1952: 31.1 (366 days)

M. Waldmeier

Swiss Federal Observatory
Zurich, Switzerland

PRINCIPAL MAGNETIC STORMS

(Advance knowledge of the character of the records at some observatories as regards disturbances)

servatory Observer- Charge)	Green-wich date	Storm-time GMT of begin.	Storm-time GMT of ending[1]	Sudden commencement Type[2]	Amplitudes[3] D	H	Z	C-figure, degree of activity[4]	Maximal activity on K-scale 0 to 9 Gr. day	Gr. 3-hr. period	K-index	Ranges D	H	Z
(1)	(2)	(3)	(4)	(5)	(6)	(7)	(8)	(9)	(10)	(11)	(12)	(13)	(14)	(15)
	1952	*h m*	*d h*		′	γ	γ					′	γ	γ
ege	Oct. 3	12 00	6 18	.....	....	....	....	s	5	3	8	320	2020	1390
L. Cleven)	Oct. 25	10 15	26 20	.....	....	....	....	ms	26	4,5,6	7	280	1920	980
	Oct. 28	08 30	31 21	.....	....	....	....	ms	30	6	7	310	1800	980
									31	4,6	7			
	Nov. 26	06 45	29 15	.....	....	....	....	s	27	4,5	8	270	2210	1400
	Dec. 1	06 40	5 14	.....	....	....	....	ms	2	5,6	7	190	1560	720
									4	4	7			
	Dec. 24	09 00	25 15	.....	....	....	....	ms	24	4,5,6	6	140	1280	770
	Dec. 28	12 00	3 05	.....	....	....	....	ms	29	6,7	6	170	1190	700
									30	6	6			
									31	5,6	6			
									1	4	6			
									2	4,5,6	6			
ka	Oct. 3	12 00	6 19	.....	....	....	....	s	5	3	9	129	1230	760
L. Skillman)	Oct. 21	08 25	22 06	.....	....	....	....	ms	21	5	6	20	281	236
	Oct. 25	10 18	26 18	s.c.*	−13	+21	−3	ms	26	1,4,5	6	70	832	810
	Oct. 29	08 30	31 21	.....	....	....	....	ms	31	5	7	76	888	224
	Nov. 26	06 00	29 00	.....	....	....	....	s	27	3,4	8	120	912	580
	Dec. 13	04 15	13 22	.....	....	....	....	s	13	5	8	119	931	630
	Dec. 24	09 25	25 15	.....	....	....	....	ms	24	5	6	48	400	420
ceveen	July 1	20 32	2 04	s.c.*	−3	+67	0	m	1	7,8	5	15	125	20
van	July 5	00 00	6 16	.....	....	....	....	ms	5	7	6	25	240	95
bben)									6	3	6			
	July 20	08 00	22 02	.....	....	....	....	ms	20	4	6	25	185	100
									21	5	6			
	Aug. 3	12 00	3 22	.....	....	....	....	ms	3	5	6	15	150	60
	Aug. 17	04 00	18 24	.....	....	....	....	m	17	4,5,7	5	30	160	65
									18	6,7,8	5			
	Sep. 1	00 00	3 24	.....	....	....	....	m	1	1,2,6,8	5	25	180	110
									2	1,3,5,8	5			
	Sep. 5	10 00	6 01	.....	....	....	....	m	5	6,8	5	25	130	80
	Sep. 7	17 00	10 15	.....	....	....	....	ms	7	8	6	35	225	105
									8	1,7	6			
									9	6	6			
	Sep. 14	00 00	14 24	.....	....	....	....	m	14	6	5	15	115	55
	Sep. 20	19 00	21 05	.....	....	....	....	m	21	1	5	20	100	60
	Sep. 25	15 16	26 07	s.c.	−1	+10	−2	m	25	8	5	45	120	75
									26	1,2	5			
	Sep. 28	14 00	30 24	.....	....	....	....	ms	28	7,8	6	45	230	180
									29	1,7,8	6			
									30	1	6			
ltenham	Oct. 3	18 ..	06 18	.....	....	....	....	ms	5	3	6	30	86	65
R. Bodle)	Oct. 25	22 ..	26 24	.....	....	....	....	ms	26	1	6	31	94	68
	Oct. 30	15 ..	1 03	.....	....	....	....	ms	31	3	6	25	80	59
	Nov. 21	00 ..	22 03	.....	....	....	....	m	21	3	5	18	86	38
	Nov. 26	06 ..	28 24	.....	....	....	....	ms	26	8	6	23	51	32
	Dec. 2	13 ..	5 01	.....	....	....	....	m	2	5	5	4	89	3
	Dec. 12	06 ..	13 13	.....	....	....	....	m	13	4	5	27	69	38
	Dec. 23	01 16	25 15	s.c.	1	16	1	m	25	2	5	14	58	13
	Dec. 27	21 ..	28 04	.....	....	....	....	m	27	8	5	14	99	81
	Dec. 28	14 ..	31 17	.....	....	....	....	m	30	8	5	15	53	9

[1]Approximate time of ending of storm construed as the time of cessation of reasonably marked disturbance movements in the es; more specifically, when the *K*-index measure diminished to 2 or less for a reasonable period.

[2]s.c. = sudden commencement; s.c.* = small initial impulse followed by main impulse (the amplitude in this case is that of the *impulse only*, neglecting the initial brief pulse); ... = gradual commencement.

[3]Signs of amplitudes of *D* and *Z* taken algebraically; *D* reckoned positive if towards the east and *Z* reckoned positive if vertically nwards.

[4]Storm described by three degrees of activity: *m* for moderate (when *K*-index as great as 5); *ms* for moderately severe (when = 6 or 7); *s* for severe (when *K* = 8 or 9).

PRINCIPAL MAGNETIC STORMS—Continued

Observatory (Observer-in-Charge)	Greenwich date	Storm-time GMT of begin.	Storm-time GMT of ending[1]	Sudden commencement Type[2]	Amplitudes[3] D	H	Z	C-figure, degree of activity[4]	Maximal activity on K-scale 0 to 9 Gr. day	Gr. 3-hr. period	K-index	Ranges D	H	Z
(1)	(2)	(3)	(4)	(5)	(6)	(7)	(8)	(9)	(10)	(11)	(12)	(13)	(14)	(15)
	1952	h m	d h		′	γ	γ					′	γ	γ
San Juan (P. G. Ledig)	*Note:* Observer-in-Charge reported that there were no important magnetic storms during October, November, and December, 1952.													
Honolulu (R. F. White)	Oct. 3	19 00	6 19	.....	....	....	....	ms	4	2	6	7	106	
	Oct. 21	08 17	22 08	s.c.*	....	....	....	m	21	5	4	6	50	
Instituto Geofisico de Huancayo (A. A. Giesecke M. Casaverde)	July 5	00 42	6 12	.....	....	....	....	m	5	7	5	7	175	
	July 20	00 41	22 05	.....	....	....	....	ms	20	6	6	5	241	
	Aug. 17	01 22	19 05	s.s.c.	0	+18	0	m	17	5,7	5	6	185	
	Aug. 31	23 58	3 08	.....	....	....	....	m	1	6	5	6	238	
	Sep. 7	03 47	10 07	.....	....	....	....	m	7	6	5	6	254	
	Sep. 25	15 15	1 05	s.s.c.*	+1	+33	0	m	29	7,8	5	8	384	
	Oct. 3	03 30	6 18	.....	....	....	....	m	3	8	5	6	294	
	Oct. 21	10 10	22 06	s.s.c.	0	+36	+5	ms	21	5	7	5	297	
	Oct. 25	10 18	26 19	.....	....	....	....	m	26	1,6	5	7	263	
	Oct. 29	12 57	31 19	.....	....	....	....	ms	30	6	7	6	272	
	(*Note:* Beginning time of storm of Oct. 29 obtained from *H* insensitive trace)													
	Nov. 26	01 36	28 21	s.s.c.	0	+8	0	ms	27	5	6	7	231	
	Dec. 24	10 00	25 05	.....	....	....	....	m	24	5,7	5	8	187	
	Dec. 27	15 00	28 04	.....	....	....	....	ms	27	8	6	5	198	
	Dec. 28	10 00	29 02	.....	....	....	....	m	28	6	5	3	202	
	Dec. 29	13 00	30 05	.....	....	....	....	m	29	6,7	5	5	296	
Vassouras (Lelio I. Gama)	Oct. 21	10 11	22 06	s.c.	+1	+45	+14	ms	21	5	7	8	98	
Apia (A. C. Stanbury)	July 5	00 42	6 16	.....	....	....	....	m	5	2	5	6	93	
	July 20	00 56	22 13	.....	....	....	....	m	20	4	5	3	90	
	July 31	01 ..	31 15	.....	....	....	....	m	31	3	5	2	68	
	Aug. 2	21 36	3 23	.....	....	....	....	m	3	2,3	5	5	115	
	Aug. 5	22 46	6 17	.....	....	....	....	m	6	1	5	3	98	
	Aug. 17	01 20	19 09	.....	....	....	....	m	17	3	5	5	72	
	Sep. 7	07 ..	10 15	.....	....	....	....	m	7	8	5	4	72	
									8	3	5			
									9	4	5			
	Sep. 20	18 51	21 14	.....	....	....	....	m	20	8	5	4	106	
	Sep. 25	15 18	26 15	.....	....	....	....	m	25	8	5	2	160	
									26	1	5			
	Sep. 26	19 41	28 14	.....	....	....	....	m	27	2	5	4	100	
	Sep. 28	15 28	1 12	.....	....	....	....	m	28	7	5	5	88	
									29	8	5			
									30	1	5			
Hermanus (A. M. van Wijk)	Oct. 3	12 ..	6 19	.....	....	....	....	ms	3	7	6	20	150	
									5	7	6			
	Oct. 8	(Sudden impulse at $23^h\ 05^m$; $K = 5$ in *H*)							8	8	5	....	....	....
	Oct. 10	16 ..	12 14	.....	....	....	....	m	11	4,7,8	5	15	78	
									12	1	5			
	Oct. 21	10 10	22 06	s.c.	+3	+31	+28	m	21	4,5,6,7	5	21	120	1
	Oct. 25	05 ..	27 11	.....	....	....	....	m	25	6	5	22	137	1
									26	1,4,5	5			
	Oct. 30	00 ..	1 03	.....	....	....	....	m	30	2,3,6,8	5	24	110	1
									31	3,5,6	5			
	Nov. 8	.. ..	.. ..	.....	....	....	....	m	8	8	5			
	Nov. 16	.. ..	.. ..	.....	....	....	....	m	16	5	5	Minor dis-		
	Nov. 17	.. ..	.. ..	.....	....	....	....	m	17	7	5	turbances		
	Nov. 26	.. ..	.. ..	.....	....	....	....	m	26	7	5			
	Nov. 27	04 ..	28 21	.....	....	....	....	m	27	4,7	5	16	87	
	Dec. 1	08 ..	5 21	.....	....	....	....	m	1	4,5,7	5	23	131	1
									2	4,5,6	5			
									4	1	5			
									5	3	5			
	Dec. 12	21 ..	13 22	.....	....	....	....	m	13	3,4	5	16	125	
	Dec. 24	01 15	25 21	s.c.	−1	−14	−11	ms	24	5	6	16	108	
	Dec. 27	16 ..	28 04	.....	....	....	....	m	27	8	5	16	57	
	Dec. 28	07 ..	3 05	.....	....	....	....	ms	29	7	6	21	91	

PRINCIPAL MAGNETIC STORMS—Concluded

bservatory Observer- n-Charge)	Green-wich date	Storm-time		Sudden commencement				C-figure, degree of activity[4]	Maximal activity on K-scale 0 to 9			Ranges		
		GMT of begin.	GMT of ending[1]	Type[2]	Amplitudes[3]				Gr. day	Gr. 3-hr. period	K-index	D	H	Z
					D	H	Z							
(1)	(2)	(3)	(4)	(5)	(6)	(7)	(8)	(9)	(10)	(11)	(12)	(13)	(14)	(15)
	1952	*h m*	*d h*		′	γ	γ					′	γ	γ
heroo E. Webb)	Oct. 3	20 50	6 18	.....	....	....	....	m	3	7	5	17	134	113
									4	5,7,8	5			
									5	3,7	5			
	Oct. 8	23 06	.. ..	s.c.	8	10	35	(No appreciable activity followed)						
	Oct. 21	10 11	22 09	s.c.	2	23	5	m	21	4,5,7	5	12	82	103
	Oct. 25	17 00	26 23	.....	....	....	....	m	26	1,4,5	5	19	120	120
	Oct. 30	14 10	31 23	.....	....	....	....	m	30	8	5	19	86	123
									31	1,5,6				
	Nov. 21	01 00	22 18	.....	....	....	....	ms	21	3	6	16	108	125
	Nov. 26	06 00	28 18	.....	....	....	....	m	27	4,5	5	18	97	....
	(*Note: Z*-spot shifted during storm of Nov. 26)								28	5	5			
	Dec. 1	14 30	5 14	.....	....	....	....	m	2	1,5	5	14	85	99
									3	1,5	5			
									4	1	5			
									5	1	5			
	Dec. 13	00 00	13 15	.....	....	....	....	m	13	3,4,5	5	18	138	139
	Dec. 27	18 00	1 21	.....	....	....	....	ms	27	8	6	15	98	79
langi E. Ervin)	Oct. 3	12 00	6 19	.....	....	....	....	ms	5	3	6	27	164	79
	Oct. 21	10 11	22 08	s.c.*	−2	42	0	m	21	4,5	5	23	98	25
	Oct. 25	03 25	27 12	.....	....	....	....	m	26	4,5	5	22	121	37
	Oct. 29	12 00	2 01	.....	....	....	....	m	30	6	5	21	124	50
									31	1,4,5,6	5			
	Nov. 21	02 15	21 19	.....	....	....	....	m	21	2,3,4	5	20	140	61
	Nov. 26	04 00	29 19	.....	....	....	....	m	27	4,5	5	25	113	55
									28	5	5			
	Dec. 1	03 50	5 14	.....	....	....	....	ms	4	1	6	21	186	53
	Dec. 13	01 50	13 19	.....	....	....	....	ms	13	4	6	27	155	56
	Dec. 24	05 15	25 16	.....	....	....	....	m	24	5	5	18	104	20
	Dec. 27	16 00	(Storm still in progress Dec. 31, 1952)						....	...	.....	.....	.....	
berley F. Baird)	Oct. 3	20 ..	6 19	.....	....	....	....	m	4	2,3,4	5	20	139	80
									5	3,5	5			
	Oct. 26	00 ..	27 12	.....	....	....	....	m	26	4,5	5	25	85	52
	Oct. 30	14 ..	1 09	.....	....	....	....	m	31	4,5	5	26	131	58
	Nov. 16	00 ..	18 12	.....	....	....	....	m	16	5	5	18	113	37
	Nov. 20	17 31	21 14	.....	....	....	....	m	21	2,3	5	22	142	34
	Nov. 26	01 30	29 01	.....	....	....	....	m	27	4,5	5	16	141	57
	Dec. 1	12 ..	5 14	.....	....	....	....	m	4	1	5	14	153	62
	Dec. 13	00 ..	14 03	.....	....	....	....	m	13	3,4,5	5	21	140	66
	Dec. 27	18 ..	1 15	.....	....	....	....	m	27	8	5	19	119	53

LETTERS TO EDITOR

THE MEASUREMENT OF THE DENSITY OF THE ATMOSPHERE BY THE SEARCHLIGHT TECHNIQUE

Recently, Elterman[1] published the results of a determination of the density of the atmosphere at altitudes up to 62 km by the searchlight technique. Following a suggestion made by Tuve, *et al.*,[2] in 1935, Elterman modulated the searchlight beam by means of a rotating Venetian-blind type of shutter and used a tuned receiver to measure the intensity of the light scattered from the beam by the atmosphere. The searchlight beam was modulated to reduce the effect of the night skylight. The modulation of the beam from a 60-inch searchlight presented a serious problem. There are some advantages in using a high-intensity flash-lamp instead of a modulated carbon-arc searchlight beam, but the difficulties encountered by Elterman can be overcome more easily if Tuve's original suggestion is extended to cover the polarization of the light scattered from the searchlight beam.

According to Rayleigh's law of molecular scattering, the polarization of the light scattered from the searchlight is given by the term $1 + \cos^2 \beta$, where β is the angle between the direction of the searchlight beam and the direction of the scattered ray. If the searchlight beam is observed from a direction which is normal to the searchlight beam, the scattered light is plane polarized. The degree of polarization of the night skylight is small.[3] Hence, the light scattered from the searchlight beam can easily be distinguished from the background skylight without modulating or pulsing the searchlight beam. A rotating polarizing device can be placed in front of the photomultiplier in the receiver. The output of the photomultiplier can then be considered to be made up of a d-c component and an a-c component. The a-c component will be a measure of the polarized light and the d-c component will give the background light.

The background light can be kept to a minimum if a dark area of the sky is selected and by the appropriate choice of a filter. The proper filter is selected by the following considerations: According to the Rayleigh scattering law, the amount of light scattered out of the beam is approximately proportional to the inverse fourth power of the wavelength of the light. The extinction coefficient for clear air is known or can be measured with adequate precision. (The extinction coefficients given by Elterman[1] are in error by as much as a factor of 5.) When proper account is made of the spectral energy distribution of the carbon arc and the spectral sensitivity of the 1P21 photomultiplier, it is seen that the effective energy distribution of the scattered light shows a peak at approximately 3800 Å and a half intensity width of about 500 Å. Corning filter 7-59 will transmit this light and reduce the background light to a low value.

[1]L. Elterman, J. Geophys. Res., **56**, 509-520 (1951).

[2]M. A. Tuve, E. A. Johnson, and O. R. Wulf, Terr., Mag., **40**, 452-454 (1935).

[3]S. K. Mitra, The upper atmosphere, Calcutta, Royal Asiatic Society of Bengal (1948).

In summary, the advantages of using the polarization of the light scattered from a searchlight beam as a means of separating the scattered light from the background light are as follows:

(1) No modulating or pulsing device is necessary on the searchlight. In the case of the modulated beam, the shutter reduces the amount of light in the beam significantly and the shutter is cumbersome to use and build.

(2) A relatively simple receiver system can be used.

The disadvantage is as follows:

(1) A relatively large distance between the receiver and searchlight station is required, whereas with the modulated beam it is desirable but not necessary to have a large distance between the two stations.

Edward V. Ashburn

Michelson Laboratory,
U.S. Naval Ordnance Test Station, Inyokern,
China Lake, California, October 29, 1952
(Received November 3, 1952)

DISCUSSION OF THE KELSO PAPER ON "A PROCEDURE FOR THE DETERMINATION OF THE VERTICAL DISTRIBUTION OF THE ELECTRON DENSITY IN THE IONOSPHERE"[1]

In his paper, Kelso points out that the distribution of electron density in the ionosphere can be rather simply estimated from virtual height *versus* frequency data by a numerical procedure. His method involves averaging the virtual heights corresponding to a number of frequencies, selected in accordance with a rule whose derivation was made to depend upon the application of the Gauss-Christoffel quadrature formula. It is perhaps not immediately apparent upon inspection of Kelso's paper that his rule corresponds to nothing more complex than integration of the true-height integrand obtained by previous workers, merely by averaging with equal weight a finite number of equi-spaced ordinates. Indeed, it may be recalled that the Japanese scientist Yoshika Nakata, made use of this technique of true-height analysis while at the Physical Institute for Radio Waves, during the Second World War, and prepared extensive tables from which as many as 45 selected frequencies could be quickly determined for use in scaling the virtual heights. It may be noted, as well, that application of the Gauss-Christoffel formula to the derivation of this rule is not especially well-founded.

As has been shown by earlier workers, the true height of reflection of a wave of frequency f_v can be expressed by either of the following integrals:

$$h_T(f_v) = \frac{2}{\pi}\int_0^{f_v} \frac{h'(f)\,df}{\sqrt{f_v^2 - f^2}} = \frac{2}{\pi}\int_0^{\pi/2} h'(f_v \sin\theta)\,d\theta \quad \ldots\ldots\ldots(1)$$

[1]J. M. Kelso, A procedure for the determination of the vertical distribution of the electron density in the ionosphere, J. Geophys. Res., 57, 357-367 (1952).

The first integral is my[2] equation (13), Kelso's (9), while the second integral is my (14), and is basically the same as Kelso's (17). As is evident from the right-hand member of (1) above, the true height can be determined by finding the area under the curve of virtual height plotted to an altered frequency scale. The curve formed by plotting virtual height $h'(f)$ *versus* θ, with $f = f_v \sin \theta$, is called the "derived curve." The area under the derived curve can be found by several means, one of which is the computation of the average ordinate for a number of equally-spaced values of the abscissa θ. Instead of plotting the derived curve, one may immediately compute the frequencies $f = f_v \sin \theta$ which corresponds to the number n of equally-spaced θ values, and then average the virtual heights corresponding to these frequencies. If Kelso's equations (26), (25), (24), and (19) are examined in correct order, it can be discovered that his procedure is nothing more than the averaging process indicated above.

In arriving at the foregoing elementary result, Kelso has made use of the esoteric Gauss-Christoffel quadrature formula. In using this device, he has attempted to show that the preceding method of calculation (actually a crude way of integrating the derived curve) is possessed of unique merits. His procedure is to find the best distribution of ordinates to evaluate the first integral of (1), based upon achieving the best polynomial fit to the virtual height *versus* frequency function. However, the result so obtained clearly does not give an accurate estimate of the second integral (1), since it is well known that averaging equally-spaced ordinates with equal weight is a very rough form of integration, in error even for second-degree polynomials. The basic futility of Kelso's argument is that since the virtual-height curve is an empirical function, it can hardly be expected to have polynomial form. The derived curve, a warping of the empirical virtual-height curve, is still of indeterminate functional form. It is, however, an equally logical starting point for efforts at numerical integration. It is doubtful that integration of the derived curve by the elementary averaged ordinate method possesses any intrinsic merits beyond those apparent from its simplest derivation.

The above remarks should by no means be taken to disparage the utility of the Nakata-Kelso technique for determining true height. Numerical methods have the great advantage of eliminating the plotting of graphs, and are especially adaptable to automatic machine computation.

L. A. Manning

Radio Propagation Laboratory,
Department of Electrical Engineering,
Stanford University,
Stanford, California, October 30, 1952
(Received November 3, 1952)

[2]L. A. Manning, The determination of ionospheric electron distribution, Proc. Inst. Radio Eng., 37, 599-603 (1949).

NOTES

(1) *Spring meeting of USA National Committee of URSI-IRE Professional Group on Antennas and Propagation*—A meeting of the USA National Committee of the International Scientific Radio Union (URSI) and the Institute of Radio Engineers Professional Group on Antennas and Propagation will be held at the National Bureau of Standards, Washington, D.C., on April 27, 28, 29, and 30, 1953. The sessions will concern the following topics: Radio measurement methods and standards, tropospheric radio propagation, ionospheric radio propagation, terrestrial radio noise, radio astronomy, and radio waves and circuits, including general theory. A preliminary program and advance registration forms will be available after March 16, 1953. These and further information concerning the meetings may be obtained from Dr. A. H. Waynick, Secretary, USA National Committee of URSI, Pennsylvania State College, State College, Pennsylvania.

(2) *Meetings of the American Geophysical Union*—The thirty-fourth annual meeting of the American Geophysical Union and of its eight sections will be held in Washington, D.C., May 4-6, 1953.

(3) *Eighth Pacific Science Congress, Philippines, 1953*—The Eighth Pacific Science Congress will be held in Manila on the campus of the University of the Philippines, from November 16 to 28, 1953, under the auspices of the Republic of the Philippines and the National Research Council of the Philippines. The National Research Council of the Philippines is inviting the National Research Councils of the various countries and other representative institutions, and, through them, scientists and delegates to participate in this Congress. In planning the scientific program, the organizing committee has kept in mind the objectives of the Pacific Science Association; namely, "to initiate and promote cooperation in the study of scientific problems that affect the prosperity of the Pacific Peoples."

(4) *Recent seminars at the Geophysics Research Directorate, Air Force Cambridge Research Center*—The following seminars were held at the Geophysics Research Directorate in South Boston, Massachusetts: January 21, 1953, "Excitation of nitrogen bands in the aurora," by Dr. Lewis Branscomb, National Bureau of Standards; January 30, 1953, "Developments in asymptotic solution of differential equations," by Prof. Morris Kline, New York University; February 6, 1953, "Observations of the pinch effect and magneto-hydrodynamic waves," by Prof. Winston H. Bostick, Tufts College; February 13, 1953, "Weather and flight safety," by Jerome Lederer, Flight Safety Foundation; and February 18, 1953, "Solar variations and the earth's atmosphere," by Dr. Donald H. Menzel, Harvard College Observatory.

(5) *Magnetic disturbance*—The United States *Hydrographic Bulletin* (No. 48 of November 29, 1952) contained the following account of a magnetic disturbance off the south coast of Australia:

Third Officer C. H. Chandler, of the British S.S. *Muncaster Castle*, Captain

A. G. Gorham, Master, reported that on a voyage from Aden to Adelaide at $05^h\ 15^m$ GMT, September 29, 1952, in Investigator Strait, a magnetic disturbance was observed which caused a deviation of 32° west. At this time, Cape Borda bore 221° true, 10.5 miles distant. The vessel was on course 70° by gyro. At $06^h\ 00^m$ GMT the deviation dropped to 22° west, and at $06^h\ 30^m$ GMT increased to 26° west. Mr. Chandler further stated that on previous voyages in this position and on the same course the deviation was 2° east, and no magnetic disturbances were observed. Weather was overcast, with good visibility; wind north, force 2; slight sea and swell; barometer 29.85 inches; air temperature 61°F.

(6) *Geomagnetic activities of the United States Coast and Geodetic Survey*—Mr. Richard G. Green completed observations at magnetic repeat stations in the New England area in October 1952.

Mr. C. J. Husum, of the Inter-American Geodetic Survey, visited Washington and the Cheltenham Magnetic Observatory, where he made observations to standardize three field magnetometers and three earth inductors being used for field work in Central and South America.

Mr. James H. Baden was assigned to the Honolulu Magnetic Observatory in October 1952.

Four volumes of the HV series of publications were issued, giving magnetic hourly values for 1949 at Sitka, Tucson, San Juan, and Honolulu.

(7) *Personalia*—Father *E. Gherzi*, the former director of the Zi-Ka-Wei Observatory, has joined the staff of the National Service for Meteorology and Geophysics at Macao (Portuguese territory in China). Although still in the experimental stage, measurements of the intensity of cosmic radiation are being carried out at Macao with a pulse counter, type 82 *C*, made by Italelectronics Commerciale.

NOTICE

Established in 1898, the Journal of Geophysical Research, the continuation of "Terrestrial Magnetism and Atmospheric Electricity," commences with this issue its fifty-sixth consecutive year of publication. Beginning with January 1953, all correspondence connected with the Journal, including manuscripts for publication, subscriptions and remittances, changes of address, orders for back issues, and inquiries relating thereto, should be sent direct to The Editor, Journal of Geophysical Research, 5241 Broad Branch Road, N.W., Washington 15, D. C., U.S.A.

LIST OF RECENT PUBLICATIONS

By W. E. Scott

Department of Terrestrial Magnetism,
Carnegie Institution of Washington,
Washington 15, D. C.

(Received January 15, 1953)

A—*Terrestrial Magnetism*

Alldredge, L. R. Keeping track of the earth's magnetic field. Physics Today, **5**, No. 11, 8-12 (1952).

Amberley Observatory. Magnetic results for 1949. Wellington, R. E. Owen, Govt. Printer, 50 pp. (1952). [Issued under the authority of the Hon. R. M. Algie, Minister of Scientific and Industrial Research.]

Amberley Observatory. Magnetic results for 1950. Wellington, R. E. Owen, Govt. Printer, 52 pp. (1952). [Issued under the authority of the Hon. R. M. Algie, Minister of Scientific and Industrial Research.]

Apia Observatory. Annual report for 1943. Wellington, R. E. Owen, Govt. Printer, 164 pp. (1950). [Issued under the authority of the Hon. K. J. Holyoake, Minister of Scientific and Industrial Research; contains magnetic results for 1943.]

Apia Observatory. Magnetic and meteorological results for 1949. Wellington, R. E. Owen, Govt. Printer, 146 pp. (1951). [Issued under the authority of the Hon. R. M. Algie, Minister of Scientific and Industrial Research.]

Baird, H. F., and A. L. Cullington. Magnetic resurvey of New Zealand at epoch 1st July, 1945. Wellington, R. E. Owen, Govt. Printer, Geophys. Mem. 1, 54 pp. + 7 isomagnetic charts (1952). 28 cm. [Issued under the authority of the Hon. R. M. Algie, Minister of Scientific and Industrial Research.]

Barnett, S. J. Method for determining magnetic moments and for measuring susceptibilities and permeabilities. J. App. Phys., **23**, No. 9, 975-976 (1952).

Bartels, J., and J. Veldkamp. International data on magnetic disturbances, second quarter, 1952. J. Geophys. Res., **57**, No. 4, 531-533 (1952).

Bates, L. F. Some post-war developments in magnetism. Proc. Phys. Soc., A, **65**, No. 392, 577-594 (1952). [Presidential address delivered May 20, 1952.]

Bernard, P. Isolement de la variation undécennale de la composante horizontale du champ magnétique terrestre par combinaisons linéaires d'ordonnées. Ann. Géophys., 8, No. 2, 248-252 (1952).

Bock, R. Der mitteleuropäische Anteil am paneuropäischen Normalfeld der erdmagnetischen Vertikalintensität. Geol. Jahrb., Hannover, **66**, 671-684 (Juli 1952).

Bodle, R. R. Cheltenham three-hour-range indices *K* for July to September, 1952. J. Geophys. Res., **57**, No. 4, 534 (1952).

Chamberlain, N. G. Observations of terrestrial magnetism at Heard, Kerguelen and Macquarie Islands (carried out in co-operation with the Australian National Antarctic Research Expedition, 1947-1948). Melbourne, Commonwealth of Australia, 10 + 5 pls. (Feb. 12, 1952). [Issued under the authority of the Hon. W. H. Spooner, Minister for National Development.]

Copenhagen, Det Danske Meteorologiske Institut. Magnetisk aarbog. 2^{den} del: Grönland—Annuaire magnétique, 2eme partie: le Groenland, 1943, 1944, and 1945. Köbenhavn, G. E. C. Gad, 27 pp. each (1951 and 1952). 32 cm.

Copenhagen, Det Danske Meteorologiske Institut. Magnetisk aarbog. 1ste del: Danmark (undtagen Groenland)—Annuaire magnétique, 1ere partie: Le Danemark (exceptè le Groenland). 1951. Köbenhavn, G. E. C. Gad, 27 pp. (1952). 32 cm.

Deutsches Hydrographisches Institut. Jahresbericht 1951. Hamburg, No. 6, 72 pp. with 12 pls. (1952). [Contains report on terrestrial magnetism.]

Fanselau, G. Ergebnisse der Beobachtungen am Adolf Schmidt-Observatorium für Erdmagnetismus in Niemegk in den Jahren 1939-1944. II. Teil: Aktivitätszahlen, Kennziffern, tägliche Gänge usw. Berlin, Akad.-Verlag, 107 pp. (1952). [Published under the auspices of the Meteorologischer Dienst der Deutschen Demokratischen Republik, Erdmagn. Jahr. 1939-1944.]

Gama, L. I. Recherches théoriques et pratiques sur les variomètres unifilaires. Observatório Magnético de Vassouras, No. 1, 125 pp. (1951).

Helwan, Royal Observatory. Annual report for the year 1941. Published under the direction of M. R. Madwar, Director. Cairo, Government Press, 81 pp. (1951). 32 cm. [Contains values of the magnetic elements at Helwan Observatory for 1941.]

Helwan, Royal Observatory. Seismological, magnetic and meteorological report for the year 1942. Published under the direction of M. R. Madwar, Director. Cairo, Government Press, 44 pp. (1951). 34 cm. [Contains values of the magnetic elements at Helwan Observatory for 1942.]

Holm. G. R. Gravitation and gyromagnetism. J. Geophys. Res., 57, No. 4, 527-530 (1952).

Kato, Y. On the characteristics of SC* of magnetic storm. Sci. Rep. Tôhoku Univ., Ser. 5, Geophysics, 4, No. 1, 5-8 (1952).

Kirkpatrick, C. B. On current systems proposed for S_D in the theory of magnetic storms. J. Geophys. Res., 57, No. 4, 511-526 (1952).

Nagata, T. On the position of the auroral zone. Rep. Ionosphere Res. Japan, 6, No. 3, 159-161 (1952).

Nagata, T., and N. Fukushima. Constitution of polar magnetic storms. Geophys. Notes, Tokyo, 5, No. 1, 85-97 (1952).

Thailand. Report on the operations of the Royal Survey Department, Ministry of Defence, for the year 1947-1948. Printing Office, Royal Survey Dept., 22 pp. (rec'd Nov. 7, 1952). [Contains some results of magnetic observations.]

Tino, Y. A new exposition of the Fe-Ni phase diagram. J. Sci. Res. Inst., Tokyo, 46, 47-52 (June 1952).

Toperczer, M. Der Verlauf der erdmagnetischen Elemente in Wien, 1851 bis 1950. Arch. Met. Geophys. Biokl., A, 5, Heft 2, 231-249 (1952).

United States Coast and Geodetic Survey. Magnetic hourly values, Honolulu, T. H., 1949. Washington, D.C., U.S. Coast Geod. Surv., No. HV-Ho49, 45 pp. (1952).

United States Coast and Geodetic Survey. Magnetic hourly values, San Juan, Puerto Rico, 1949. Washington, D.C., U.S. Coast Geod. Surv., No. HV-SJ49, 44 pp. (1952).

United States Coast and Geodetic Survey. Magnetic hourly values, Sitka, Alaska, 1949. Washington, D.C., U.S. Coast Geod. Surv., No. HV-Si49, 45 pp. (1952).

United States Coast and Geodetic Survey. Magnetic hourly values, Tucson, Arizona, 1949. Washington, D.C., U.S. Coast Geod. Surv., No. HV-Tu49, 44 pp. (1952).

Williams, H. J. Magnetic domains. Bell Lab. Record, 30, No. 10, 385-396 (1952).

B—*Terrestrial Electricity*

Barbier, D., and H. Pettit. Photometric observations of the airglow and of the aurora borealis at College, Alaska. Ann. Géophys., 8, No. 2, 232-247 (1952).

Blifford, I. H., L. B. Lockhart, Jr., and H. B. Rosenstock. On the natural radioactivity in the air. J. Geophys. Res., 57, No. 4, 499-509 (1952).

Chalmers, J. A. Point discharge currents. J. Atmos. Terr. Phys., 2, No. 3, 301-305 (1952).

Chapman, S. Theories of the aurora polaris. Ann. Géophys., 8, No. 2, 205-225 (1952).

Dauvillier, A. Observation du champ électrique atmosphérique à Khartoum durant l'éclipse totale de Soleil du 25 février 1952. Paris, C.-R. Acad. sci., 235, No. 16, 852-854 (1952).

Gill, E. W. B., and G. F. Alfrey. The electrification of liquid drops. Proc. Phys. Soc., B, **65**, No. 391, 546-551 (1952).

Hosler, C. L., M. D. Burkhart, and H. Neuberger. On the effect of time lapse between sampling and expansion in the Aitken nuclei counter. Bull. Amer. Met. Soc., **33**, No. 6, 251-254 (1952).

Ishikawa, G., M. Kadena, and M. Kitamura. An effect of the atmospheric electric field upon the observation of ions in the atmosphere. Kyoto, J. Geomag. Geoelectr., **4**, No. 1, 1-6 (1952).

Israël, H. Die Höhe der luftelektrischen Ausgleichsschicht. Ann. Géophys., **8**, No. 2, 253-257 (1952).

Israël, H. The diurnal variation of atmospheric electricity as a meteorological-aerological phenomenon. J. Met., **9**, No. 5, 328-332 (1952).

Israël, H. Zum Tagesgang des luftelektrischen Potentialgefälles. II—Potentialgefälle und Dampfdruck. Ber. D. Wetterdienst US-Zone, No. 38, 409-411 (1952).

Kakioka Magnetic Observatory. Report of the Kakioka Magnetic Observatory, Geoelectricity, 1936-1940. Kakioka, No. 15, 257 pp. (1952). 30 cm. [Contains atmospheric electric potential gradient and earth-current potential gradient results, years 1936-1940.]

Moore, D. J. Measurements of condensation nuclei over the North Atlantic. Q.J.R. Met. Soc., **78**, No. 338, 596-602 (1952).

Mühleisen, R. Positive und negative elektrische Raumladungen in atmosphärischer Luft bei Schönwetter. Naturwiss., **39**, Heft 16, 376-377 (1952).

Osterbrock, D. E. The electrical conductivity in the solar atmosphere. Phys. Rev., **87**, No. 3, 468-470 (1952).

Petrie, W. Forbidden line of N II in the aurora. Phys. Rev., **87**, No. 6, 1002 (1952).

Vegard, L. Great intensity variations of $H\alpha$ and effects in auroral spectrograms taken in rapid succession. Nature, **170**, 536-537 (Sept. 27, 1952).

Wichmann, H. Zur Theorie des Gewitters. Arch. Met. Geophys. Biokl., A, **5**, Heft 2, 187-230 (1952).

C—*Cosmic Rays*

Barrett, P. H., L. M. Bollinger, G. Cocconi, Y. Eisenberg, and K. Greisen. Interpretation of cosmic-ray measurements far underground. Rev. Mod. Phys., **24**, No. 3, 133-178 (1952).

Green, H. S., and H. Messel. On the theory of the angular and lateral spread of the nucleon component of the cosmic radiation. Proc. Phys. Soc., A, **65**, No. 393, 689-701 (1952).

Hodson, A. L. The altitude variation of penetrating showers. Proc. Phys. Soc., A, **65**, No. 393, 702-708 (1952).

Hutchinson, G. W. On the possible relation of galactic radio noise to cosmic rays. Phil. Mag., **43**, No. 343, 847-852 (1952).

Mills, B. Y. The distribution of the discrete sources of cosmic radio radiation. Aust. J. Sci. Res., A, **5**, No. 2, 266-287 (1952).

Morand, M., et S. Desprez-Rebaud. Sur la répartition de l'intensité des traces isolées produites par le rayonnement cosmique dans des émulsions nucléaires tournantes, axées sur l'étoile polaire et conservant une orientation fixe par rapport au Soleil. Paris, C.-R. Acad. sci., **235**, No. 4, 294-296 (1952).

Neher, H. V., and S. E. Forbush. Correlation of cosmic-ray ionization measurements at high altitudes, at sea level, and neutron intensities at mountain tops. Phys. Rev., **87**, No 5, 889-890 (1952).

Wilson, J. G. (Editor). Progress in cosmic ray physics. Interscience Publishers, Inc., New York (or North-Holland Publishing Co., Amsterdam), xvi + 557 (1952).

D—*Upper Air Research*

Aono, Y. On world-wide distribution of f_0F2. Rep. Ionosphere Res. Japan, **6**, No. 2, 69-78 (1952).

Banerjee, S. S., and R. R. Mehrotra. Equivalent paths of the ordinary waves for oblique incidence at the ionosphere. J. Sci. Industr. Res., New Delhi, **11**, No. 6, 216-218 (1952).

Baral, S. S. Studies on sporadic *E*. J. Sci. Industr. Res., New Delhi, A, **11**, No. 7, 290-296 (1952).

Bates, D. R. Some reactions occurring in the earth's upper atmosphere. Ann. Géophys., 8, No. 2, 194-204 (1952).

Bhargava, B. N. A new early-morning ionospheric phenomenon. Nature, **170**, 983-984 (Dec. 6, 1952).

Brown, R. H. Radio-frequency radiation from Tycho Brahe's supernova (A.D. 1572). Nature, **170**, 364-365 (Aug. 30, 1952).

Budden, K. G. The theory of the limiting polarization of radio waves reflected from the ionosphere. Proc. R. Soc., **215**, No. 1121, 215-233 (1952).

Budden, K. G., and G. G. Yates. A search for radio echoes of long delay. J. Atmos. Terr. Phys., **2**, No. 3, 272-281 (1952).

Choudhury, D. C. Production of the *E*-layer in the oxygen dissociation region in the upper atmosphere. Phys. Rev., 88, No. 2, 405-408 (1952).

Defence Research Board, Canada. The earth's exterior atmosphere and the counterglow. Defence Scientific Information Service, D.R.B., Canada, No. T65R (July 8, 1952). [A collection of recent Russian papers translated by E. Hope.]

Denisse, J. F., and J.-L. Steinberg. Radio observations of the solar eclipses of September 1, 1951, and February 25, 1952. Nature, **170**, 191-192 (Aug. 2, 1952).

Feinstein, J. On the nature of the decay of a meteor trail. Proc. Phys. Soc., B, 65, No. 393, 741 (1952). [Letter to Editor.]

Fukushima, N., and T. Hayasi. A relation between *F*2-layer disturbance and geomagnetic condition. Rep. Ionosphere Res. Japan, 6, No. 3, 133-136 (1952).

Gauzit, J. Relations entre la température et les phénomènes de dissociation ou d'ionisation photochimique dans la haute atmosphère. Examen particulier de la région *E*. Ann. Géophys., 8, No. 2, 226-231 (1952).

Greenhow, J. S. A radio echo method for the investigation of atmospheric winds at altitudes of 80 to 100 km. J. Atmos. Terr. Phys., **2**, No. 3, 282-291 (1952).

Greenhow, J. S., and G. S. Hawkins. Ionizing and luminous efficiencies of meteors. Nature, **170**, 355-357 (Aug. 30, 1952).

Hawkins, G. S., and M. Almond. Radio echo observations of the major night-time meteor streams. Mon. Not. R. Astr. Soc., **112**, No. 2, 219-233 (1952).

Hawkins, G. S., and M. Almond. Radio echo observations of the daytime meteor streams in 1951. Astr. Contrib., Univ. Manchester, Ser. 1, Jodrell Bank Annals, **1**, No. 1, 2-12 (April 1952).

Hewish, A. The diffraction of galactic radio waves as a method of investigating the irregular structure of the ionosphere. Proc. R. Soc., A, **214**, No. 1119, 494-514 (1952).

International Scientific Radio Union. Tidal phenomena in the ionosphere. Brussels, General Secretariat, U.R.S.I., Special Report No. 2, 72 pp. (rec'd Oct. 17, 1952).

Lindquist, R. An investigation of the ionizing effect in the *E*-layer near sunrise. J. Geophys. Res., 57, No. 4, 439-458 (1952).

Lüst, R. Linienemission der interstellaren Materie im Radiofrequenzbereich. Naturwiss., **39**, Heft 16, 372-374 (1952).

Matsushita, S. Semi-diurnal lunar variations in the sporadic-*E*. Kyoto, J. Geomag. Geoelectr., **4**, No. 1, 39-40 (1952). [Letter to Editor.]

Minnis, C. M. The graphical representation of the longtitude effect in F_2-region. J. Atmos. Terr. Phys., **2**, No. 3, 261-265 (1952).

Miya, K., and N. Wakai. Characteristics of ionospheric disturbances during severe magnetic storms. Rep. Ionosphere Res. Japan, 6, No. 3, 137-146 (1952).

Neužil, L. Influences météoriques sur la couche sporadique *E*. Prague, Central Astron. Inst. Czechosl., 3, No. 3, 40-43 (1952).

Nicolet, M. Actions du rayonnement solaire dans la haute atmosphère. Ann. Géophys., 8, No. 2, 141-193 (1952).

Obayashi, T. Some characteristics of ionospheric storms. Rep. Ionosphere Res. Japan, 6, No. 2, 79-84 (1952).

Ostrow, S. M., and M. PoKempner. The differences in the relationship between ionospheric

critical frequencies and sunspot number for different sunspot cycles. J. Geophys. Res., **57**, No. 4, 473-480 (1952).

RENSE, W. A. The origin of zodiacal light. Astroph. J., **115**, No. 3, 501-505 (1952).

SATYANARAYANA, R., AND S. R. KHASTGIR. Polarization of down-coming wireless waves of medium wave lengths. J. Sci. Industr. Res., New Delhi, **11**, No. 6, 211-215 (1952).

SUGIURA, M., M. TAZIMA, AND T. NAGATA. Anomalous ionization in the upper atmosphere over the auroral zone during magnetic storms. Rep. Ionosphere Res. Japan, **6**, No. 3, 147-154 (1952).

UYEDA, H. AND Y. ARIMA. Classification of *F*2-layer storms with respect to their world-wide distribution and characteristics of them. Rep. Ionosphere Res. Japan, **6**, No. 1, 1-12 (1952).

VILLARD, O. G., JR., AND A. M. PETERSON. Scatter-sounding: A new technique in ionospheric research. Science, **116**, 221-224 (Aug. 29, 1952).

WATTS, J. M. Oblique incidence propagation at 300 kc using the pulse technique. J. Geophys. Res., **57**, No. 4, 487-498 (1952).

E—*Earth's Crust and Interior*

BULLEN, K. E. Cores of terrestrial planets. Nature, **170**, 363-364 (Aug. 30, 1952).

COTTON, C. A. Fourmarier's suction theory of geosynclines, and the "vertical push" explanation of geanticlinal orogeny. Science, **116**, 261 (Sept. 5, 1952).

GUTENBERG, B. Wave velocities in the outer part of the earth's mantle. Nature, **170**, 289 (Aug. 16, 1952).

HAVEMANN, H. The earth's face determined by the core. Trans. Amer. Geophys. Union, **33**, No. 5, 749-754 (1952).

LARSEN, E. S., JR., N. B. KEEVIL, AND H. C. HARRISON. Method for determining the age of igneous rocks using the accessory minerals. Bull. Geol. Soc. Amer., **63**, No. 10, 1045-1052 (1952).

LIBBY, W. F. Chicago radio carbon dates, III. Science, **116**, No. 3025, 673-681 (1952).

LUSKIN, B., M. LANDISMAN, G. B. TIREY, AND G. R. HAMILTON. Submarine topographic echoes from explosive sound. Bull. Geol. Soc. Amer., **63**, No. 10, 1053-1068 (1952).

OFFICER, C. B., M. EWING, AND P. C. WUENSCHEL. Seismic refraction measurements in the Atlantic Ocean. Part IV: Bermuda, Bermuda Rise, and Nares Basin. Bull. Geol. Soc. Amer., **63**, No. 8, 777-808 (1952).

REVELLE, R., AND A. E. MAXWELL. Heat flow through the floor of the eastern North Pacific Ocean. Nature, **170**, 199-200 (Aug. 2, 1952).

RIKITAKE, T. On the electrical conductivity in the earth's core. Bull. Earthquake Res. Inst., Tokyo Univ., **30**, pt. 3, 191-205 (1952).

SLICHTER, L. B. An electromagnetic interpretation problem for the sphere. Proc. R. Soc., A, **214**, No. 1118, 356-370 (1952).

UFFEN, R. J., AND A. D. MISENER. On the thermal properties of the earth's interior. Proc. Phys. Soc., B, **65**, No. 393, 742 (1952). [Letter to Editor.]

UREY, H. C. The origin of the earth. Sci. Amer., **187**, No. 4, 53-60 (1952).

VÄYRYNEN, H. Maan kuoren muodostumisesta (On the genesis of the earth's crust). Terra, No. 4, 128-137 (1951). [English summary accompanies.]

WAIT, J. R. The electric fields of a long current-carrying wire on a stratified earth. J. Geophys. Res., **57**, No. 4, 481-485 (1952).

F—*Miscellaneous*

BLAHA, M. Solar corona and the corpuscular emission of the sun. Prague, Bull. Central Astron. Inst. Czechosl., **3**, No. 3, 29-34 (1952).

DOAK, P. E. The reflexion of a spherical acoustic pulse by an absorbent infinite plane and related problems. Proc. R. Soc., **215**, No. 1121, 233-254 (1952).

JEFFREYS, H. The origin of the solar system. Proc. R. Soc., A, **214**, No. 1118, 281-291 (1952). [Bakerian lecture.]

KAMIYAMA, H. Variation of the effectiveness of the solar flare according to its location. Sci. Rep. Tôhoku Univ., Ser. 5, Geophysics, **4**, No. 1, 1-4 (1952).

SAN MIGUEL (ARGENTINA), OBSERVATORIO DE FISICA COSMICA DE. Memorias del Observatorio de San Miguel, No. 1, Seccion Geoelectrica (prepared by Arturo J. Yriberry, S. J.). Typis privatis Spec. Phys. cosm. sanet. Michaelis, 54 pp. (1952). 30 cm.

SCOTT, W. E. List of recent publications. J. Geophys. Res., **57**, No. 4, 543-546 (1952).

WALDMEIER, M. Provisional sunspot-numbers for July to September, 1952. J. Geophys. Res., **57**, No. 4, 534 (1952).

WHYBREW, W. E., G. D. KINZER, AND R. GUNN. Electrification of small air bubbles in water. J. Geophys. Res., **57**, No. 4, 459-471 (1952).

WILLETT, H. C. Atmospheric reactions to solar corpuscular emissions. Bull. Amer. Met. Soc., **33**, No. 6, 255-258 (1952).

NOTICE

When available, single unbound volumes can be supplied at $3.50 each and single numbers at $1 each, postpaid.

Charges for reprints and covers

Reprints can be supplied, but prices have increased considerably and costs depend on the number of articles per issue for which reprints are requested. It is no longer possible to publish a schedule of reprint charges, but if reprints are requested approximate estimates will be given when galley proofs are sent to authors. Reprints without covers are least expensive; standard covers (with title and author) can be supplied at an additional charge. Special printing on covers can also be supplied at further additional charge.

Fifty reprints, without covers, will be given to institutions paying the publication charge of $4.00 per page.

Alterations

Major alterations made by authors in proof will be charged at cost. Authors are requested, therefore, to make final revisions on their typewritten manuscripts.

Orders for back issues and reprints should be sent to Editorial Office, 5241 Broad Branch Road, N.W., Washington 15, D.C., U.S.A.

Subscriptions are handled by The Editorial Office, 5241 Broad Branch Road, N.W., Washington 15, D.C., U.S.A.

CONTENTS—Concluded

JOURNAL OF GEOPHYSICAL RESEARCH